Dendronized Amphiphilic Copolymers Synthesized from Methacrylate Derivatives as Potential Topical Microbicides

By

Shauntrece Nicole Hardrict

Thesis submitted to the Faculty of the Virginia Polytechnic Institute and State University in partial fulfillment of the requirements for the degree of

DOCTOR OF PHILOSOPHY

in

CHEMISTRY

Approved by:

Richard D. Gandour

S. Richard Turner

James E. McGrath

Judy S. Riffle

Richey M. Davis

November 5, 2009
Blacksburg, VA

Keywords: amphiphile, dendronized polymer, ionomer, topical microbicide

Dendronized Amphiphilic Copolymers Synthesized from Methacrylate Derivatives as Potential Topical Microbicides

Shauntrece N. Hardrict

ABSTRACT

The need for a preventative agent to curtail the rampant spread of HIV, other STDs and mucosal pathogens is urgent. Topical microbicides based on amphiphilic compounds have been identified as an attractive means toward this goal.

Novel dendritic methacrylate macromonomers—di-*tert*-butyl 4-(2-*tert*-butoxycarbonyl-ethyl)-4-[3-(2-methacryoloxyethyl)ureido]heptandioate (**MI**) and di-*tert*-butyl 4-(2-*tert*-butoxycarbonylethyl)-4-[3-methyl-3-(2-methacryoloxyethyl)ureido]heptanedioate (**MIII**)—were synthesized, characterized, and subsequently polymerized via conventional free radical polymerization in acetonitrile employing AIBN as an initiator.

Methyl 3-mercaptopropionate (MMP), a chain transfer agent, was employed to target low molecular weight (<10,000 g/mol) polymers. Dendronized homopolymers were prepared from **MIII** with varying MMP concentrations (0–10 mol%). MALDI-TOF MS characterized the homopolymer prepared with 10 mol% MMP (M_n = 2,481 g/mol).

In the presence of MMP, **MIII** (5 to 25 mol%) was copolymerized with alkyl (methyl, ethyl, and *n*-butyl) methacrylates. Copolymer composition correlated well with monomer feed; M_ns of 3–10K g/mol were observed.

Ionizable polymers were achieved via acidolysis with trifluoroacetic acid; significant increases in T_g were observed. For the copolymers, the T_gs of the acids increased as the copolymer composition increased in **MIII**. For the homopolymers, T_gs decreased with increasing MMP concentration.

The solubilities of carboxylic acid functional polymers were studied in 5 w/v % aqueous triethanolamine (aq TEA) at a concentration of 12.5 mg/mL. Clear, homogeneous solutions of the deprotected macromonomer, **MIII**(OH), homopolymer, P**MIII**(OH), and **MIII**(OH)/MMA copolymer series were observed; copolymer solubility decreased as the aliphatic chain length of the alkyl methacrylate increased.

The amphiphilic dendronized polymer series incorporates many features shown beneficial in the pursuit of effective antimicrobial agents: amphiphilicity, multiple anionic functional groups, a polymer backbone, and aqueous solubility. Additionally, biological selectivity (e.g. cytotoxicity) is expected to be tunable through the control of molecular weight, alkyl chain length (n*), copolymer composition, and molecular architecture.

To my loving grandmother (Odessa Koonce Hardrict) whose strength, leadership, and will I have admired all the days of my life — I am who I am because of you; thank you for being the one and only constant in my life. You are my rock!

To my nieces and nephews: the potential your life holds inspires me daily; allow neither man nor woman to put boundaries on your dreams.

In memory of:

Solomon "Stevie" Rooks (1985–2008) thank you for sharing twenty-three years of life with us and teaching us to live by your motto: "That's life, get over it!"

Reginald "Reggie" Hardrict (1959–2004), a loving uncle and a victim of the AIDS epidemic, the loss of your life inspired my interest in this work; thank you for being my light during this journey. I miss you, dearly.

ACKNOWLEDGEMENTS

I would like to extend heartfelt thanks to those who have assisted me in my matriculation at Virginia Tech. Sincere gratitude is extended to Dr. Richard Gandour for accepting me into his research group, allowing me to prove myself without prejudgment, and for his constant academic and moral support. It is because of his emphasis on education that I have grown significantly as a scientist and mentor. To Dr. S. Richard Turner, thank you for accepting me into your research group and agreeing to take on this collaborative project; I appreciate your 'open-door' policy and willingness to help. I would also like to thank Dr. James McGrath, Dr. Judy Riffle, and Dr. Richey Davis for serving on my research committee; you were always willing to be of assistance and for that I am thankful. I would like to extend a special thank you to Dr. Riffle for several lengthy SEC discussions.

Several other faculty members contributed on this journey: I would like to thank Dr. Harry Gibson and Dr. Alan Esker for always being open for discussion; I would also like to thank Dr. Timothy Long for discussions, instrument use, and for allowing me to present my research to his group. Many thanks to Dr. Joseph O. Falkinham for trying to make a microbiologist out of me and always being willing to answer my many questions. I am very thankful for our graduate program director, Dr. Paul Deck; on many occasions he went above and beyond on my behalf. Thank you for not taking your title lightly and doing your job so well; you are appreciated! I am also very grateful for the support and encouragement of Dr. Patricia Amateis.

I would like thank the analytical services (Geno Iannacone, Hugo Azurmendi, and William Bebout) and stockroom (Jan McGinty, Patrick McGinty, and Sharelle Dillon) staffs for keeping us 'going'. I would be up a creek if not for IT support—thank you, Mr. Larry Jackson.

I am grateful to Mark Flynn, who ran many SEC samples on my behalf; thank you for your hard work. Many thanks to Ms. Myra Williams for her help in the microbiology lab; it was pleasure to work with you. I would also like to thank Justin Tanner for helping me get through those very long days in the microbiology lab; I will forever remember to "Embrace the Micro"! To Dr. Rebecca Huyck-Brown, thank you for being my 'go-to' person for SEC analysis; you were always pleasant, prompt, and extremely helpful!

To those I affectionately call "the office ladies" (Mary Jane Smith, Tammy Jo Hiner, Esther Brann, Laurie Good, and Millie Ryan): I sincerely thank you for your administrative support but I thank you more for your moral support. You may never know just how much it meant to me!

I would like to thank both of my research groups in general for their willingness to help on a daily basis. A special thank you goes to Dr. Eko Sugandhi for helping me get acclimated in the lab and for being a friend. Thank you to Dr. André Williams, Dr. Richard Macri, and Marcelo Actis for keeping the work environment fun! I will always remember 'snack time'; I hope to implement this into my next work environment. Thank you to Nick Stambach, my first undergraduate research mentee, for being the best undergraduate researcher; I enjoyed working with you. Thank you, LaShonda Cureton and Dr. Keiichi Osano, for your assistance with SEC analysis and data retrieval.

The list of friends I've made on this journey is much too long to list here but please know that I am thankful for each and every one! A special thank you to Dr. Andrew Duncan, Dr. Natalie Arnett, Drs. Rachael and Desmond VanHouten, Dr. Astrid Rosario, Dr. Phil Huffstetler, Dr. Michael Shane Thompson, Dr. Michael Zalich, John Boyd, Dr. Yin-Nian Lin, and Dr. William Harrison—you were supportive, you made me laugh, and you listened to my gripes—

THANK YOU! To my best girlfriends (Kesha Forrest, Dr. Maisha Smith, LaTanya Martin, Maro Mitchell, and Donyelle Granderson), thank you for always calling to "check-in"; I look forward to our lives together, now that I can have a life. Ladies, I love and appreciate you; thank you so much for your friendship!

I would like to thank my Sorors of the Tau Mu Omega and Theta Chi Chapters of Alpha Kappa Alpha Sorority, Incorporated for their love and support over the years. I am very grateful for the experiences we've shared.

I would like to thank the members of Asbury United Methodist Church for being a loving and supportive family. A special thank you to one member in particular, Carol Crawford-Smith. Carol, thank you for providing a dance home for me at The Center of Dance; it was an essential key to happiness. With that, I would also like to thank each and every person who supported the FUSiON Dance Company. Love, blessings, and sincere gratitude to Dr. Barbara Pendergrass for recognizing FUSiON for what it was— a ***F***unky, ***U***nfeigned, ***S***ophisticated, ***i***nnovative, ***O***mnibus, ***N***ecropolis of cultural barriers. To ALL who attended workshops and served on the performing company: thank you for sharing your passion for dance with me.

To my family, thank you for being patient! It was your love and support that sustained me on this journey! To my mother, Karen Merkson, thank you for being the best example of discipline and hard work; I owe my work ethic to you. To my younger brothers, Michael Monroe and Eric Merkson, thank you for being my biggest fans; your love means the world to me. To my Aunt Gloria Hardrict Ewing, thank you for all the little things that meant so much! To my uncle and aunt, Drs. Ronald and June Hardrict, thank you for ALL that you've done for me. You are truly role models for successful living with a communal spirit—lifting as we climb!

I thank GOD for each and every proponent and adversary I have encountered on this journey; I am wiser, stronger, and so much better!

TABLE OF CONTENTS

LIST OF FIGURES

LIST OF TABLES

LIST OF EQUATIONS

Chapter 1: Introduction

1.1 AIDS: A Health and Economic Pandemic

The spread of sexually transmitted diseases (STDs) is a global challenge. In 2004, approximately 40 million people were reportedly living with the human immunodeficiency virus (HIV), 4.9 million people were newly infected, and 3.1 million died of acquired immune deficiency syndrome (AIDS)-related diseases.[1] Females are 4–17 times[2, 3] more susceptible to infection than their male partners, represent more than half of the infected population; and, as a result, bear a disproportionate burden in this crisis.[4] There is an urgent need to develop new strategies to reduce HIV-transmission that can be controlled by women themselves.[5-8]

HIV is a retrovirus, a single stranded RNA virus, that can infect a number of different cells including CD4 bearing macrophages and T-helper lymphocytes in the host cell. The HIV life cycle (**Figure 1**) consists of multiple steps that may be targeted to achieve effective inhibition. Many of the current HIV therapies are combinations of reverse transcriptase and protease inhibitors. However, drug resistant HIV-1 strains emerged after treatment with these drugs. Drug resistance has prompted a search for antivirals that function through other mechanisms of action. An alternative approach to antiviral therapy involves the inhibition of virus attachment to and fusion with the host cell—the first step of the HIV life cycle. Microbicides that function via this mechanism are referred to as entry/fusion inhibitors.

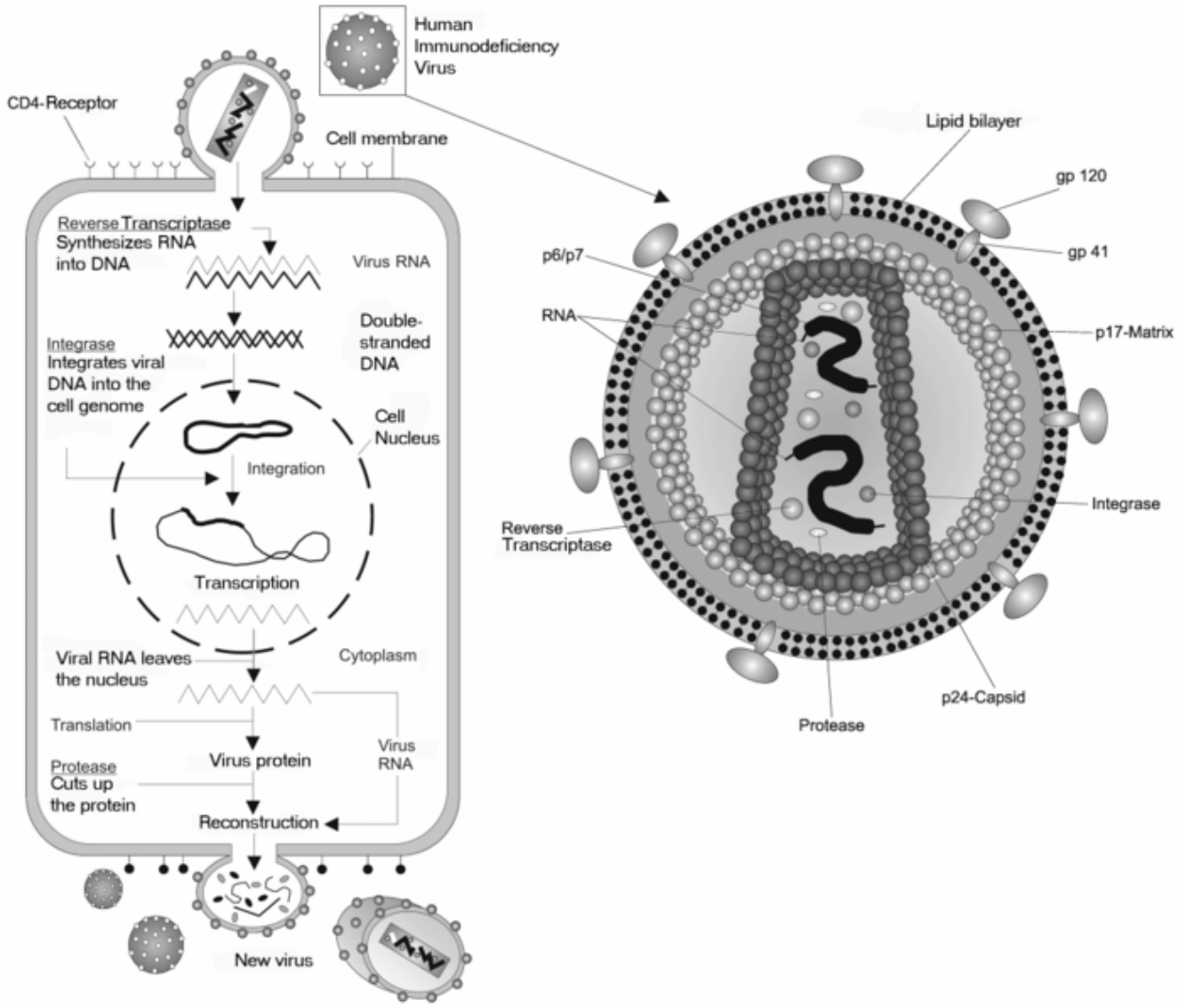

Figure 1. HIV life cycle.[9]

1.2 Topical Microbicides

The development of vaginally applied antimicrobial compounds (topical microbicides) with broad-spectrum activity against sexually transmitted pathogens has been identified as a high-priority approach to control the spread of STDs.[10, 11] By definition, a microbe is a tiny organism that cannot be seen with the unaided eye and is generally classified in one of four categories: bacteria, viruses, fungi or protozoa. A topical microbicide is a chemical agent that may be applied to mucosal surfaces, such as the nose or vagina, and functions as a chemical barrier to microbes. Ideally, topical microbicides should be (1) highly active against pathogenic microorganisms, (2) efficacious and fast-acting *in vivo*, (3) safe, (4) non-absorbable, (5) stable, (6) easy to formulate, (7) bio-adhesive, (8) acceptable and appealing to users, and (9) inexpensive.[12] To date, efforts toward the development of topical microbicides with antiviral activity include products that: (1) maintain or enhance normal vaginal defense mechanisms (e.g., antimicrobial peptides), (2) disrupt or inactivate the pathogen (e.g., N-9, cellulose acetate phthalate [CAP]), (3) block virus-cell binding and fusion of pathogens (e.g., carrageenan, CAP, naphthalene sulfonate polymers, dendrimers), or (4) adversely affect the pathogen life cycle (e.g., dendrimers and reverse transcriptase inhibitors).[13] In addition to the multiple modes of action available for these compounds, multiple intravaginal drug delivery systems are being explored for the delivery of these compounds including creams and gels, tablets and suppositories, vaginal films, and vaginal rings.[14]

Amphiphiles represent one group of fast-acting, chemical agents proposed as microbicides.[15] Nonoxynol-9, the most widely used spermicide in the U.S., is a nonionic detergent that functions through the disruption of cell membranes. However, its detergency

adversely affects epithelial cells and normal vaginal flora, which may increase the risk of urinary tract infections[16, 17], vulvovaginal candidiasis[18], genital ulcers[19] and the transmission of HIV[20]. Amphiphilic synthetic polymers have been utilized as chemical disinfectants and biocides.[21] Polymeric disinfectants have been prepared from many conventional synthetic polymers, including poly(vinyl pyridine)s[22], poly(vinyl alcohol)s[23], polyacrylates[24], polymethacrylates[25], and polystyrenes[26]. Medicinal use of polymer disinfectants is limited due to their lack selectivity for bacterial over human cells. However, certain anionic polymers—Ushercell™ (sodium cellulose sulfate)[27], polystyrene sulfonate[28], and Emmelle™ (dextrin-2-sulfate)[29] — effectively inhibit the entry of HIV into vaginal or cervical cells by binding to pathogens without disrupting cellular membranes (i.e. entry/fusion inhibitors). Ushercell™ and polystyrene sulfonate, two polymers evaluated in clinical trials as non-irritating topical microbicides, also possess contraceptive properties.

1.3 Proposed Research

Antimicrobial and anti-HIV activities of a homologous series of amphiphiles, as triethanolammonium salts, with hydrophobic tail lengths of 12–22 carbons and tri-functional hydrophilic headgroups have been investigated by Gandour et al.[30, 31] The research presented herein involves the synthesis of amphiphilic dendronized polymer analogues based on these compounds. Amphiphilic copolymers prepared from novel dendritic methacrylate macromonomers with pendant tri-functional hydrophilic headgroups and alkyl methacrylate monomers were targeted. This design incorporates several features shown beneficial in the pursuit of effective antiviral agents: amphiphilicity, multiple anionic functional groups, and a polymer backbone. By varying the comonomer feed, the hydrophilic/hydrophobic composition was varied.

Chapter 2: Literature Review of Anionic Polymeric Microbicides as anti-HIV Agents

2.1 Anionic Polymeric Microbicides as anti-HIV agents

2.1.1 Introduction

The inhibitory effect of polyanionic substances on the replication of the herpes simplex virus (HSV) and other viruses was first reported nearly five decades ago.[32] However, these observations did not generate much interest because the antiviral action of the compounds was considered nonspecific.[32] The polysulfonate, suramin, a hexasodium salt of naphthalenetrisulfonic acid, (**Figure 2**) was reported to exhibit potent anti-AIDS activity in 1984.[33] This result combined with the increasing number of HIV/AIDS diagnoses in the early 1980s fueled research interest in polyanions as anti-HIV/AIDS agents. Polyanionic molecules are now well established as potent *in vitro* inhibitors of HIV replication.[29] Their activity spectrum has been shown to encompass a variety of enveloped viruses, including herpes simplex virus (HSV), human cytomegalovirus (HCMV), vesicular stomatis virus (VSV), influenza A virus, and respiratory syncytical virus (RSV).

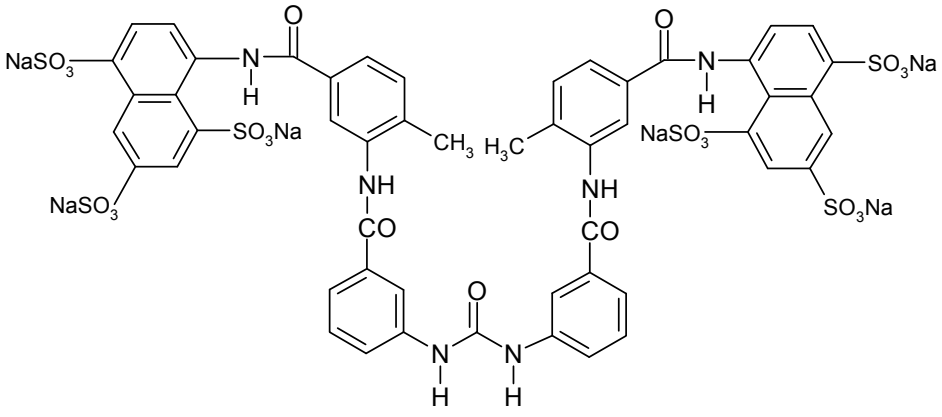

Figure 2. Suramin.

Both synthetic and natural anionic polymers have been evaluated as potential vaginal topical microbicides for prevention of the sexual transmission of HIV. *In vitro* studies have revealed several characteristic properties: i) broad-spectrum antiviral activity against HIV and a number of enveloped viruses, ii) inhibition of syncytium formation between HIV-infected and normal CD4 T cells, iii) low induction of viral resistance in cell culture, and iv) low cytotoxicity.[34]

The mechanism of action attributed to the antiviral activity of polyanions has been probed with various experimental techniques: radiolabelled HIV particles [35], a radioimmunoassay [36], flow cytometry [37], and a p24 ELISA assay [38]. From these and similar studies, *in vitro* polyanion anti-HIV activity was attributed to their ability to shield the positively charged sites in the V3 loop of the viral envelope glycoproteins (gp120).[39-41] The V3 loop is necessary for virus attachment to the host cell's surface heparan sulfate, a primary binding site. Polyanions also inhibit the viral fusion process, a vital step in the virus replication cycle during which the viral DNA is injected into the host cell cytoplasm. Unfortunately, the use of anionic polymers as topical microbicides has been limited by their pharmacological properties (short plasma half-life, toxic side effects, partial inactivation by plasma components, and a poor ability to penetrate infected tissues and cells), which result in a low bioavailability and hence poor antiviral activity *in vivo*.[42]

In spite of these drawbacks, anionic polymers are still being pursued in the development of topical anti-HIV microbicides. Formulations of low concentrations of an effective polyanion may prove therapeutic as topical microbicides despite their pharmacological properties *in vivo*. Several anionic polymers have been investigated in clinical trials – 1) sulfate esters of polysaccharides [dextrin/dextran sulfates, cellulose sulfate, and carrageenans], 2) aryl sulfonates

[poly(styrene-4-sulfonate and poly(naphthalene sulfonate)/PRO 2000], and 3) aliphatic [Carbomer974P/BufferGel ™] and aromatic carboxylates [cellulose acetate phthalate (CAP)][29] (**Figure 3**).

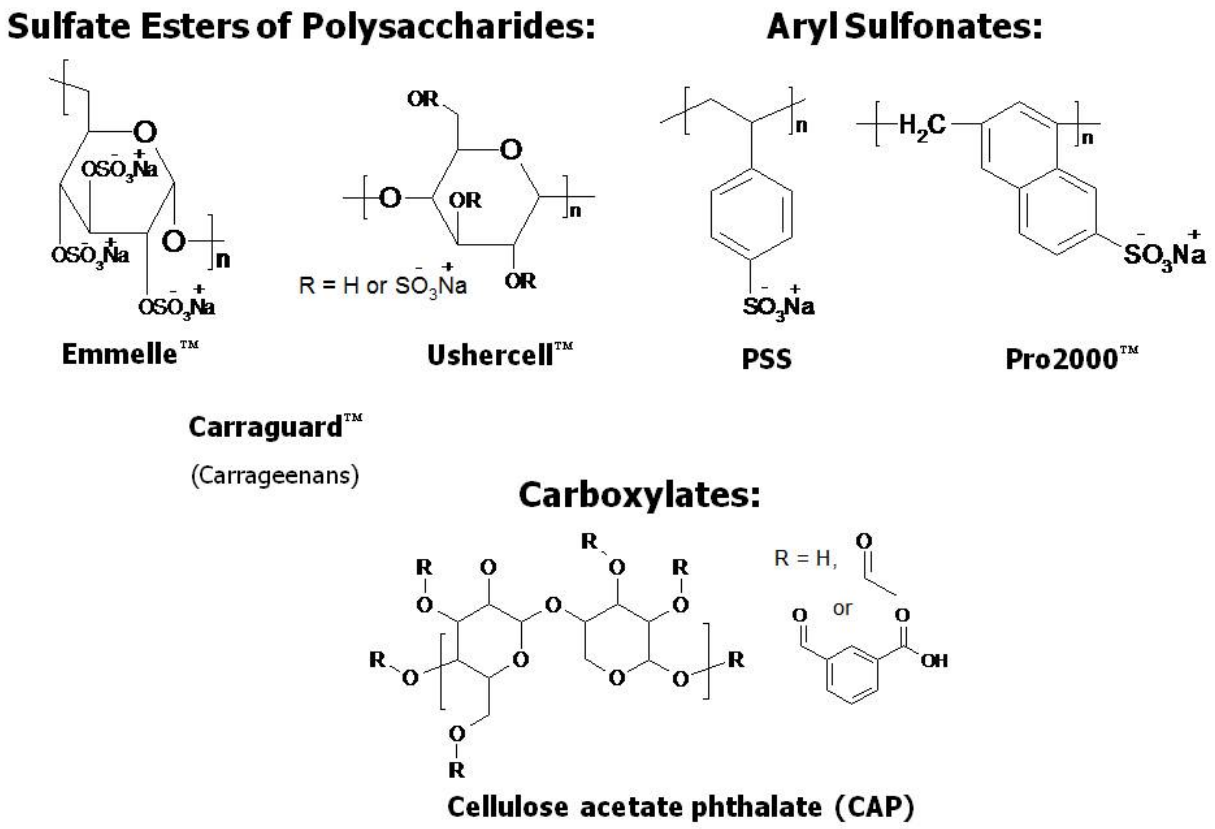

Figure 3. Anionic Microbicides Investigated in Clinical Trials.

2.1.2 Sulfated polysaccharides

Dextran sulfate was the first sulfated polysaccharide discovered to possess anti-AIDS activity.[43, 44] At present, sulfated polysaccharides are well established as potent *in vitro* inhibitors of HIV replication; examples include heparin[35, 45], dextran sulfate[35, 43-45], pentosan polysulfate[46], cellulose sulfate, and lentinan sulfate[47]. The antiviral activity of these compounds

is dependent on the density and distribution of the sulfate groups; anti-HIV activity increased with increasing molecular weight. Comparative studies of different sulfated polysaccharides have shown that, in order to achieve anti-HIV-1 activity, these compounds should have a minimum molecular weight of 3,000 and an average of at least two sulfate groups per monosaccharide unit.[48] Sulfated polysaccharides have been shown effective at concentrations as low as 0.01 μg/mL and noncytotoxic up to 2.5 mg/mL.[32] However, high blood anticoagulant activities characteristic of many sulfated polysaccharides is an undesirable side effect and has limited their use as antiviral agents.[42]

2.1.3 Synthetic Polysaccharide derivatives

Synthetic, polyanionic polysaccharide derivatives have proven highly effective as *in vitro* HIV inhibitors. These synthetic mimics are designed to exploit the antiviral activity exhibited by natural polysaccharides while minimizing the undesirable anticoagulant side effects.

Dextran sulfate and derivatives thereof have received much attention in this regard. Derivatized dextrans with varying percentages of carboxymethyl, sulfonate, benzylamide, and benzylamide sulfonate substituents were synthesized and investigated for antiviral activity.[49] These heparin mimics demonstrated antiviral activity against a host of envelope viruses (HCMV, RSV, HIV-1, HIV-2, HSV-1 and HSV-2) with 50% inhibitory concentrations (IC_{50}) ranging from 6 to 30 μg/mL; the compounds were not active against non-envelope viruses. Activity was only observed when the compounds were present during virus adsorption—confirming the mechanism of action as inhibition of virus-cell binding. Although molecular weight and the nature of the substituents played an important role in the antiviral activity of the compounds tested, conformational factors related to the distribution and sequence of the substituents on the sugar backbone were identified as influential factors. Similar observations were made in the

comparison of dextran sulfate, a copolymer of acrylic acid and vinyl alcohol sulfate (PAVAS), and sulfated cyclodextrins of comparable molecular weight and degree of sulfation screened for activity against HCMV.[50] PAVAS was 10-fold more potent than dextran sulfate, which was in turn 20-fold more active than sulfated cyclodextrin.

Dextrin 2-sulfate (D2S) (Emmelle™), a sulfated polysaccharide, showed promise as a potential topical microbicide in Phase I and II clinical trials. D2S exhibits *in vitro* broad-spectrum activity against several laboratory strains of HIV-1 in a variety of human cell lines, lymphocytes and macrophages with an IC_{50} of 0.5 μg/mL.[44] However, inhibition is significantly lessened in the case of R5 HIV-1 viruses.

Other synthetic polysaccharide derivatives were investigated as anti-HIV microbicides and reached advanced clinical trials; examples include sodium cellulose sulfate (Ushercell™, Polydex Pharmaceuticals, Toronto, Canada), cellulose acetate phthalate (CAP), and carrageenans (Carraguard™, Population Council, New York, USA).[29] Sodium cellulose sulfate (NaCS) is a long chain sulfated polysaccharide (1900 kDa). Due to its nonspecific binding properties to cells and HIV-1, NaCS was investigated as a vaginal microbicide and spermicide. Formulations containing up to 6% NaCS proved relatively safe in short-term studies, however, its detergency and marked anticoagulation activity are of potential concern in the case of long-term, repeated usage at high concentrations. Carraguard™ is a microbial gel containing 3% carrageenan–a sulfated polysaccharide derived from seaweed. Carrageenan is commonly used in cosmetics, toothpastes and food products, and therefore, was expected to be safe and nontoxic in microbial applications. Advanced Phase III effectiveness trials performed for NaCS, Carraguard™, and Ushercell™. The United States Food and Drug Administration (US FDA) approved an Investigational New Drug application for Ushercell™; however, clinical trials were halted when

the Contraceptive Research and Development (CONRAD) Program reported interim data that revealed Ushercell™ less effective than a placebo administered during testing.

More recently, sulfated derivatives of the *Escherichia coli* K5 polysaccharide emerged as potential HIV inhibitors.[51-53] The structure of the capsular K5 polysaccharide is similar to *N*-acetyl heparosan, a heparin biosynthetic precursor, but lacks anticoagulant activity. K5 polysaccharide derivatives exhibited IC_{50} values between 0.07 and 0.46 μM, and cytotoxicity was not observed within the concentration range evaluated (≤ 9 μM). In contrast to heparin, K5 derivatives potently inhibit infection and replication of a broad spectrum of R5, X4, TCLA and primary HIV-1 isolates in different CD4 target cells. Notably, most polyanions have been shown effective inhibitors of infection by X4 viruses but prove ineffective against infection by R5 viruses.[54-56]

2.1.4 Anionic microbicides from conventional polymers

Sulfated polymers, such as sulfated polyvinyl alcohol (PVAS) and sulfated copolymers of acrylic acid and vinyl alcohol (PAVAS), are potent inhibitors of both HIV-1 replication and HIV-1 induced giant cell formation (syncytium) *in vitro*.[57] PAVAS (10K and 20K) and PVAS proved effective against HIV-1 in MT-4 cells with 50% antiviral effective concentrations (EC_{50}) of 0.15, 0.11, and 0.18 μg/mL, respectively. Dextran sulfate exhibited an EC_{50} of 0.39 μg/mL in the same assay. In addition, complete inhibition of syncytium formation was achieved at 4 μg/mL, whereas much higher and potentially toxic concentrations (100 μg/mL) of dextran sulfate were required to achieve the same result. The mechanism of action was attributed to inhibition of virus adsorption to the cells. These sulfated synthetic polymers demonstrated anticoagulant activities two- to threefold lower than that of heparin. This study demonstrated

that the polysaccharide backbone of the pioneer compounds is not essential in the design of anti-HIV-1 agents.

Sodium polystyrene sulfonate (PSS), a long chain sulfonated anionic polymer (751 kDa), exhibited broad-spectrum *in vitro* activity against a host of viruses and STDs including, HIV, human papillomavirus (HPV), HSV-1, HSV-2, *Chlamydia trachomatis*, and *Neisseria gonorrhoeae*.[58-60] Its mechanism of inhibition has been attributed to both the direct interaction of the compound with infectious virions and a blocking effect at the cell surface.[59] However, the potential use of PSS in vaginal microbicide formulations is likely to be limited by the high concentrations necessary to achieve anti-HIV activity in cultured cells, their well known property to bind serum proteins, and marked anticoagulating activity.[29]

Pro 2000/5, a synthetic naphthalene sulfonic acid-formaldehyde copolymer (~5 kDa), can bind to CD4 with nanomolar affinity and block the binding interactions between CD4 and HIV gp120.[61] PRO 2000/5 functions to inhibit HIV infection by irreversible binding to and/or denaturation of the critical V3 region of the HIV envelope.[62] PRO 2000^{TM} Gel (Indevus Pharmaceuticals, Inc. Lexington, MA USA), a gel comprising a synthetic carbomer, a lactate buffer system and a synthetic naphthalene sulfonate, proved safe and effective in Phase III clinical trials.

2.1.5 Polycarboxylates

Polymer analogues of Aurintricarboxylic acid (ATA) (**Figure 4**) were among the first polyanionic compounds to exhibit anti-HIV activity.[63] After this initial discovery, De Clercq et al. reported anti-HIV activity of various aurintricarboxylic acid fractions and analogues.[64] Fractionation of ATA polymers revealed a direct correlation between molecular weight and antiviral activity but not cytotoxicity. These studies also suggested that an increase in selectivity

index was possible by increasing the molecular weights of the ATA fractions. Analogues of ATA polymers in which the carboxylic acid moiety was replaced with a sulfonic acid or phosphonic acid group were also found to prevent the cytopathic effect of HIV-1 and HIV-2 in MT-4 cells and HIV-1 in CEM cells.

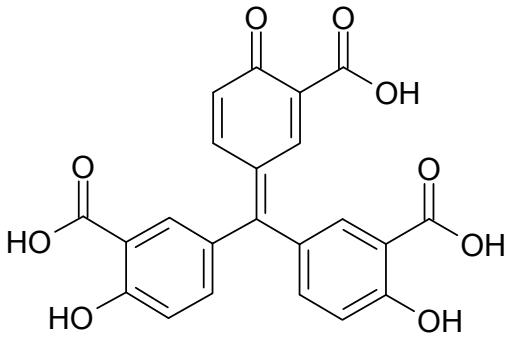

Figure 4. Aurintricarboxylic acid (ATA).

Leydet et al. reported the synthesis and anti-HIV activity of a series of unsaturated micelle-forming surfactants with a vinyl group at one end and a polar anionic headgroup.[65] Although the monomers did not exhibit activity, several of the polymerized anionic surfactant compounds proved active against HIV-1 (IC_{50}: 0.1 –3 μg/mL), while nontoxic to the host cells (CEM and MT-4) (≤100 μg/mL). Increasing the charge number on each hydrocarbon chain to 2–4 anionic groups did not markedly affect the HIV-1 inhibition.[66]

Polyanions based on a disaccharide core exhibited antiviral activity against HIV-1 provided that the number of anionic groups per molecule was sufficiently high.[67] In this case, 16 anionic groups per molecule resulted in IC_{50} values in the range of 0.4 –1.85 μM for HIV-1, whereas activity was not observed for molecules consisting of 8 or 10 anionic groups. The results of this study prompted further investigation of the effect of increasing the number of anionic groups per molecule on anti-HIV activity. A series of polyanions, bearing 18–48 carboxylate

groups, was prepared through the radical addition of thiomalic acid and mercaptopropionic acid onto perallyated cyclodextrins (CDs).[68] Compounds with a greater number of anionic groups per molecule (36–48) exhibited a 2-fold increase in inhibitory effect against HIV-1 (III_B) in MT-4 cells compared to compounds with fewer (18–24) anionic groups: IC_{50} ranging from 0.1 to 0.3 μM versus 0.7 to 1.4 μM. Cytotoxicity was not observed at the concentrations studied (≤ 36–62 μM). One notable observation of this study was the difference in the inhibitory effect of cyclodextrin carboxylate derivates compared to cyclodextrin sulfate derivatives[69] for HIV-2. At comparable concentrations, cyclodextrin sulfate derivatives demonstrate broad-spectrum activity through inhibition of both HIV-1 and HIV-2, whereas the carboxylate derivatives did not exhibit an inhibitory effect on HIV-2.

Negatively charged proteins offer antiviral activity without anticoagulant activity. In a study of glycoproteins designed as drug carriers for other anti-HIV agents, it was found that the carriers themselves exhibited intrinsic anti-HIV activity.[70] Their activity was attributed to an increased negative charge of a particular glycoprotein. Human serum albumin (HSA), a globular protein, was modified by reaction of its protein-lysine groups with succinic[70, 71] and aconitiic acid [72] to incorporate one or two carboxylic acid groups, respectively. Antiviral activity against HIV-1 was observed but anticoagulant properties were not. These compounds only partially inhibit the binding of free virus particles to the cell; they mainly inhibit the virus-cell fusion process.[48]

Cellulose acetate phthalate (CAP) and Carbomer 974P/BufferGel™ represent two polycarboxylates investigated in advanced clinical trials as potential topical microbicides.[29] BufferGel™ (ReProtect, LLC; Baltimore, MD USA) or Carbopol polymer 974P is a negatively charged buffering polymer (polyacrylic acid) gel that is both spermicidal and microbicidal.

BufferGel™ (pH 3.9) maintains the natural acidity of the vagina to ensure the survival of lactobacilli that are able to produce lactic acid and hydrogen peroxide which inactivate many pathogens that cause STIs.[73, 74] Acidform™ gel, a similar system, is an anti-HIV gel investigated in Phase III clinical trials.[75]

2.1.6 Polyphosphates

Inorganic polyphosphates, linear polymers of orthophosphate, are found widely in nature.[76-78] They are present in human pathogens including *Neisseria meningitides*[79], *Neisseria gonorrhoeae*[80], and *Mycobacterium tuberculosis* H37Ra [81] and have been shown to possess antibacterial[82, 83]and anti-HIV activity [84].

Double-stranded, synthetic polynucleotides poly(A)-poly(U) [85] and poly(I)-poly(C)[86] represent a second class of polyphosphates shown to possess *in vitro* anti-HIV activity [34].

2.1.7 Combination Therapies

Combination microbicides have been proposed as a means to afford inhibition by interrupting the transmission of HIV at different stages of the infectious process.[13, 87] The combination of two candidate microbicides, cellulose acetate 1,2-benzenedicarboxylate (CAP), a HIV-1 entry inhibitor, and UC781, a HIV-1 reverse transcriptase inhibitor (RTI), resulted in effective synergy for inhibition of MT-2 cell infection by HIV-1IIIB, a laboratory-adapted virus strain.[88] The 95% effective concentration values for the combination were reduced approximately 15- to 20-fold compared with those corresponding to the single compounds. Combination strategies (of oral therapies) have revolutionized HIV treatment and might offer promise in the pursuit of effective topical prevention as well.[89] MIV-150, a non-nucleoside reverse transcriptase inhibitor, exhibited significant activity against HIV-1 primary isolates and

no toxicity in pre-clinical trials, however, low oral bioavailability was also observed.[90] By changing the mode of delivery from oral to intravaginal delivery in a combination therapy, an effective anti-HIV agent with diminished systemic side effects was achieved—PC-815 gel. *In vivo* pharmacological studies of PC-815 gel, a combination therapy consisting of carrageenan and MIV-150, revealed activity for HIV superior to that of Carraguard™ system (carrageenan).[90]

2.2 Dendrimers as Anionic Microbicides

2.2.1 Introduction

Polyvalent interactions, characterized by the simultaneous binding of multiple ligands on one biological entity to multiple receptors on another, occur broadly in nature and possess uniquely different characteristics compared to the corresponding monovalent interaction.[91] For instance, polyvalent interactions can be collectively much stronger. It has also been demonstrated that intermolecular, as well as intramolecular interactions, are enhanced in polymeric systems.[92] As a result, increasing attention has been devoted to highly branched structures, which may be designed as polyvalent ligands, for biomedical applications with the hope that their architecture leads to interesting effects on biological properties.

Traditionally, synthetic polymers are divided into three major classes based on macromolecular architecture: linear, cross-linked or branched. Dendritic polymers represent the fourth and the most recently discovered class of macromolecular architecture.[93] This class of polymers includes dendrimers, hyperbranched polymers, dendrigrafts, hybrid dendritic-linear macromolecules, and dendronized polymers. Due to their branched nature and potential for polyvalent interactions, dendritic polymers have received much attention in biomedical applications.

Dendrimers present a novel class of polyanionic macromolecules with broad-spectrum antiviral activity and minimal toxicities. The first dendrimer reports were published by Vogtle[94], Denkewalter[95, 96], Tomalia[97], and Newkome[98, 99] in the late 1970s and early 1980s. Since their discovery, dendrimer molecules have been employed in a number of biological applications—chiefly as drug delivery agents. More recently, dendrimers were investigated as effective drugs in their own right.[100, 101]

Dendrimers are monodisperse polymers composed of multiple perfectly branched monomers that emanate radially from a central core; dendrimer synthesis is achieved via either divergent[97] or convergent[102] growth strategies. The identical fragments attached to the central core are called dendrons, and the number of branch points encountered upon moving outward from the core to the periphery defines the dendrimer generation—level of branching. The three dimensional branched architecture of a dendrimer consists of three distinct regions: multivalent surface, branching repeat, and encapsulated core. **Figure 5** illustrates the chemical composition of commonly used dendrons.

Dendrimers have a number of unique properties as a consequence of their branched architecture. For instance, dendritic branching affords respectable molar masses and quite densely filled volumes on a cubic nanometer scale. In addition, the supramolecular organization of dendrons can lead to columnar or spherical superstructures.[103] Such structures have been confirmed in diffraction studies performed by Percec et al., which reveal the formation of spherical or cylindrical (columnar) superstructures that pack into cubic or hexagonal columnar phases.[104, 105]

In contrast to linear polymers, the number of peripheral end-groups increases as dendrimer molecular weight and generation increase. The multivalent nature of dendrimers

affords the opportunity for multiple interactions with large surfaces, such as those found on biomolecules or in biological systems.[91, 106]

2.2.2 Dendrimers as Antivirals

Dendrimer multivalency has been exploited in a variety biological applications including the prevention of tumor cell adhesion and metastasis (*in vivo*)[107] and the inhibition of a multitude of viruses, including influenza virus, respiratory syncytial virus (RSV) [108], measles virus, and HIV [109, 110].

By altering the nature of the core and repeating units, the number of layers (generation) and the chemistry of the terminal groups, it is possible to synthesize a single polymeric molecule of defined three-dimensional structure and size.[111] This is a highly beneficial feature due to the fact that a direct structure-property relationship may be achieved with only subtle changes in the dendrimer design parameters.[112] As a result of these unique properties, dendrimers are considered new molecular tools in the fields of medicine and biotechnology.[113]

Witrouw et al. studied polyamidoamine (PAMAM) dendrimers as potential anti-HIV microbicides.[114] In this study, two derivatives were synthesized: a naphthyl disulfonic acid dendrimer (BRI2923), a fourth generation PAMAM dendrimer prepared from an ammonia core, with 24 naphthyl disulfonic acid terminal groups; and a phenyldicarboxylic acid dendrimer (BR6195), a fourth generation PAMAM dendrimer prepared from ethylene diamine core with 32 phenyl dicarboxylic acid terminal groups (**Figure 6**). In each case, a thiourea linker and sodium counterions were used for consistency. Antiviral activity was observed for both BRI6195 and BRI2923 against HIV-1(III_B) in MT-4 and C8186 cells, with EC_{50} values of 0.1 μg/mL and 0.3 μg/mL, respectively. BRI6195 and BRI2923 were also shown to inhibit different strains of HIV-1 (NL4.3 and RF), clinical HIV isolates (HE and L1), various HIV-2 strains (ROD and EHO)

and simian immunodeficiency virus (SIV, strain MAC_{251}), and HIV strains resistant to reverse transcriptase (RT) inhibitors, in different cell lines at EC_{50} values ranging from 0.01 to 3.5 μg/mL. The sulfated polysaccharide, DS, control exhibited comparable activity for these viruses (EC_{50} values, 0.04 to 10.6 μg/mL). Toxicity was not observed for the PAMAM dendrimers up to the highest concentration measured (250 μg/mL) and high selectivity indices (up to 25, 000) resulted.

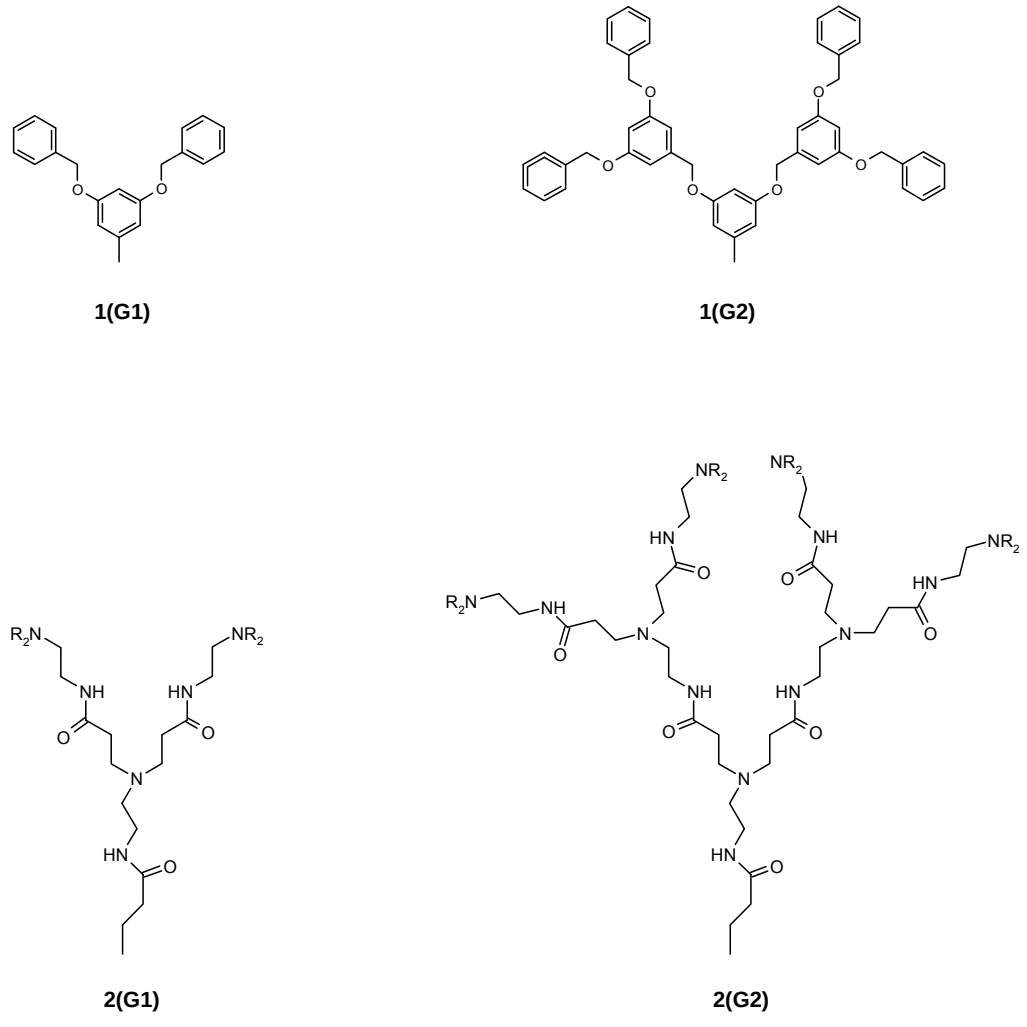

Figure 5. Frechet-type dendrons (1) and polyamidoamine (PAMAM) dendrons (2).

In virus adsorption assays in which cells were infected with HIV-1 (NL4.3), DS, BRI2923 and BRI6195 inhibited virus-cell binding at IC_{50} values of 0.4, 0.9, and 0.3 μg/mL, respectively. These studies confirmed the mode of action of BRI6195 and BRI2923 as virus attachment/entry inhibitors. Cellular uptake and confocal microscopy studies revealed that BRI2923 was capable of penetrating the cell, whereas BRI6195 was not. This result was further confirmed in 'time of addition' experiments in which BRI2923 exhibited activity at multiple stages of viral infection, namely virus attachment/entry, reverse transcriptase and integrase. According to these studies, BRI2923 is a multi-target antiviral agent. This work suggested that cell penetration, and thus mode of action vary with the nature of the initiator and anionic termini and proposes the concept of a dual action antiviral, which may function as both a preventative (virus attachment/entry inhibitor) and therapeutic (reverse transcriptase and integrase inhibitor) agent.

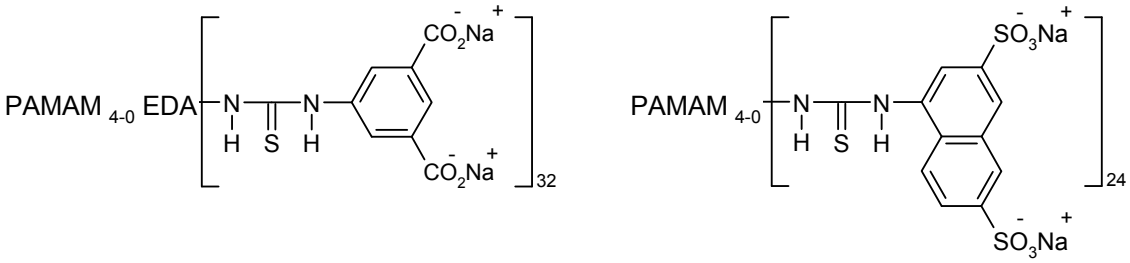

BRI6195 **BRI2923**

Figure 6. Antiviral dendrimers: BRI6193 and BRI2923. [110]

Dual action antiviral activity has been observed in dendrimer microbicides investigated for activity against HSV[115, 116] and HIV[110]. Among these is SPL7013 (**Figure 7**), a new generation dendrimer microbicide active against both HSV and HIV. SPL7013 was prepared from benzhydrylamine; four successive additions of L-Lysine to the divalent core produce a dendrimer with 32 terminal amine groups. The last step in the synthesis involves a reaction between the amine terminal groups and sodium 1-(carboxymethoxy)naphthalene-3,6-disulfonate

to achieve 32 sodium disulfonate terminal groups attached via amide linkers. In non-human primate efficacy studies, a single intravaginal dose of a clinical formulation containing 5% w/w SPL7013 protected all pig-tailed macaques (i.e. monkeys) from a single intravaginal infection by a strain of SHIV.[109] Additional studies of 5% w/w SPL7013 formulations report efficacy against HIV-1 infection of primary peripheral blood mononuclear cells (PBMC) and macrophages (MΦ) and against the transfer of virus infection from epithelial cell lines to activated PBMCs.[13] Unformulated SPL7013 also proved effective as an anti-HSV agent at concentrations as low as 1 mg/mL.[117] VivaGel, the clinical drug product of SPL7013, is a water-based carbopol gel buffered to a physiologically compatible pH. In 2003, an investigational new drug application was submitted to the United States Food and Drug Administration (US FDA); initial phase I clinical trials showed that the safety profile of VivaGel formulations containing 0.5 to 3.0% w/w SPL7013 was comparable to that of the placebo gel following once daily intravaginal dosing for seven consecutive days.[112]

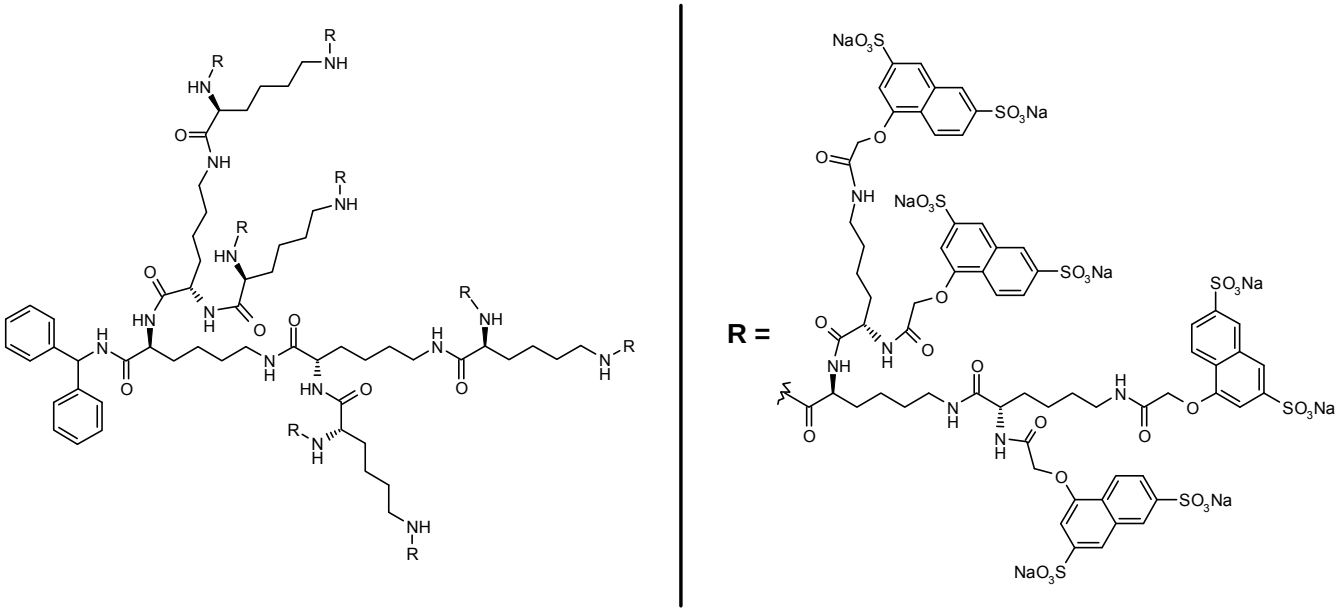

Figure 7. Chemical Structure of SPL7013, the dendrimer antiviral in VivaGel. [112]

The main strategy in the design of effective antiviral dendrimer microbicides has been primarily based on the binding of the dendrimer to the viral surface. One alternative, but complementary approach toward antiviral therapy involves the inhibition of virus/host cell binding through blockage of the viral receptor on the host cell surface.[118-120] The multivalency of dendrimers is further exploited in the design, synthesis, and antiviral application of glycodendrimers, carbohydrate functional dendrimers, which may present a feasible means toward this approach.[121]

Oligo- and polysaccharides cover the surface of all mammalian cells. Through their recognition by carbohydrate-binding proteins on other mammalian cells, viruses, bacteria, and bacterial toxins, surface carbohydrates are the first lines of interaction with the extracellular world. Studies of lectin binding indicate a significant increase in binding affinity to ligands with multiple carbohydrate binding sites.[122, 123] Given this and the fact that the first step of infection involves attachment of the virus to specific oligosaccharide epitopes on the host cell surface, efforts to identify effective multivalent carbohydrate ligands for pathogens expressing multiple carbohydrate-binding sites have been pursued.[124] Since the work of Toyokuni et al.[125] with commercially available lysyl-lysine, many research groups have taken interest in the potential use of dendrimers as scaffolds for multivalent carbohydrate ligands.

Glycodendrimers present a promising class of multivalent ligands, with the potential to block carbohydrate-mediated microbial adhesion. This concept has been successfully demonstrated with the influenza A virus. One application of these molecules involves their interaction with *Fimbrae* protein to inhibit infection by *Escherichia coli*.[126]

Sialic acid is the most prevalent sugar of the glycolipids and glycoproteins on the mammalian cell surface and is the key epitope recognized as essential for a number of pathogenic infections. *N*- and *O*- substituted derivatives of neuraminic acid are generally referred to as sialic acid; *N*-Acetylneuraminic acid (**Figure 8**) is the predominant derivative. Moreover, sialic acid-containing polymers are potent inhibitors of hemagglutination of human erythrocytes by influenza viruses. Sialic acid functional, fourth generation (G4) PAMAM dendrimers interact with haemagglutin, the major surface protein of influenza A, to prevent viral adhesion to cells exhibiting sialic acid at their surfaces.[127-129]

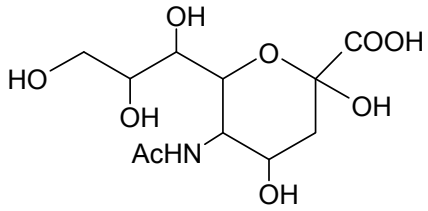

Figure 8. N-Acetylneuraminic Acid.

2.3 Dendronized Polymers

2.3.1 Introduction

The quest for larger size, well-defined molecular objects has led to various extensions of the dendrimer concept, including the use of a polymer as a polyfunctional, polydisperse core.[130] By replacing the small molecule core of traditional dendrimers with a polymer, the steric repulsion of the pendant dendrons may be exploited as a means to stretch the polymer backbone (**Figure 9**). Depending upon the stiffness of the polymer backbone, the degree of dendron coverage, the dendron size and structure, and dendron/solvent interactions, a flexible polymer may be converted into a rigid rod or a "filled molecular cylinder". This approach is referred to

as shape control by the implementation of steric strain[131], and the resulting polymers are referred to as 'dendronized polymers'. Dendronized polymers are also, but less commonly, referred to as polymers with dendritic side chains, dendrimers with polymeric cores, rod-shaped dendrimers, cylindrical dendrimers or denpols. Tomalia and Kirchhoff first reported rod-shaped dendrimers in a US patent.[132] In a later report[133], the synthesis of polyethyleneimine via the living cationic polymerization of 2-ethyl-2-oxazoline and its subsequent deprotection for the synthesis of rod-shaped poly(amidoamine) structures was described in detail.

Dendronized polymers represent a special class of graft copolymers or, in the case of complete coverage, comb polymers with dendron side chains. These dendron side chains strongly influence polymer conformation. Percec et al. performed extensive studies of the chain conformation and supramolecular structure of dendron-substituted polystyrene and poly(methyl methacrylate) that revealed the effects of the degree of polymerization and dendron geometry.[131] Schluter et al. recognized the significance of dendron decoration on polymer conformation and overall shape of the dendronized macromolecules rendering them shape persistent, cylindrical nanoscopic objects.[134]

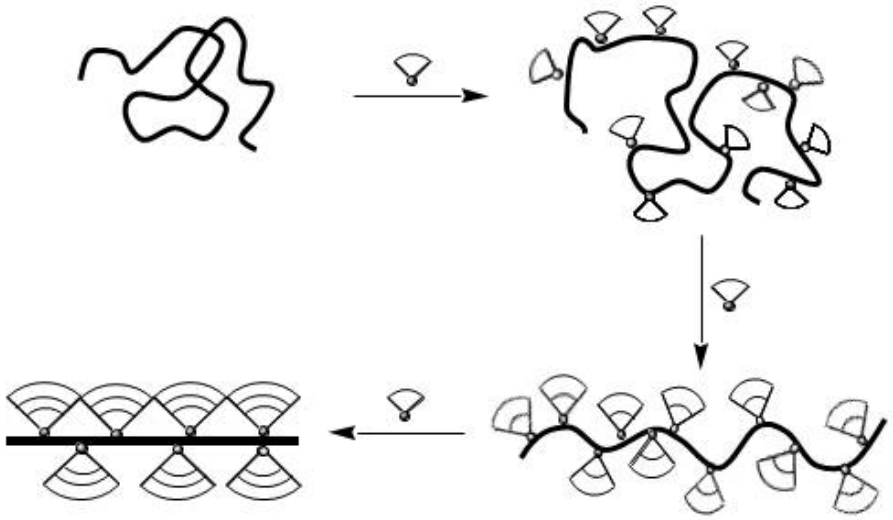

Figure 9. The steric induced effect of dendritic side chains on polymer backbone.

2.3.2 Synthesis of Dendronized Polymers

Dendronized polymers may be synthesized by one of two synthetic methods: macromonomer method or "coupling-to" method (**Figure 10**). The classification of these synthetic methods differs only in what comes first—the polymer or the dendron.

The "coupling-to" method starts with a linear polymer to which a dendritic layer is attached. The "coupling-to" method may be divided into subcategories based upon whether the dendrons are attached via convergent or divergent growth. In the case of convergent growth, preformed, high-generation dendrons are attached to anchor groups along the backbone of a linear polymer. Conversely, the divergent route involves the attachment of first generation (G1) dendrons to polymer anchor groups and the successive addition of G1 dendrons to achieve higher generation dendrons. The "coupling to" approach via convergent growth has been studied intensively by Schluter et al. with Frechet-type polybenzyl ether dendrons and hydroxy-functional poly(*p*-phenylene)s. Limited conversion of polymer analogous reactions and

incomplete dendron coverage was observed as a function of increasing dendron generation. Incomplete dendron coverage is common to and the major disadvantage of the "coupling to" method. To date, much of the success in the synthesis of dendronized polymers has been achieved employing the macromonomer method.[135]

Synthesis via the macromonomer approach involves the attachment of a polymerizable group to the focal point of a preformed dendron, and the polymerization of the resulting 'macromonomer' via radical polymerization, polycondensation, or living polymerization techniques.[136] The advantage of this approach lies in the guarantee of well-defined side chains and complete coverage—one dendron per repeat unit. On the other hand, the bulky dendron substituent sterically hinders the polymerization site and consequently decreases polymerization kinetics making it difficult to achieve a high degree of polymerization (DP), and therefore high molecular weight polymers.[137-139] However, a high degree of polymerization was achieved when a spacer was inserted between the polymerizable group and the bulky dendron and long reaction times were employed. Conversely, in the study of the polymerization kinetics of spacer less G2 dendronized styrene and methacrylate derivatives, a strong increase in the rate of free radical polymerization was observed above a certain critical monomer concentration.[140] This result was attributed to the self-organization of the growing polymer chain into a spherical or columnar superstructure in solution, which was dependent upon the degree of polymerization.

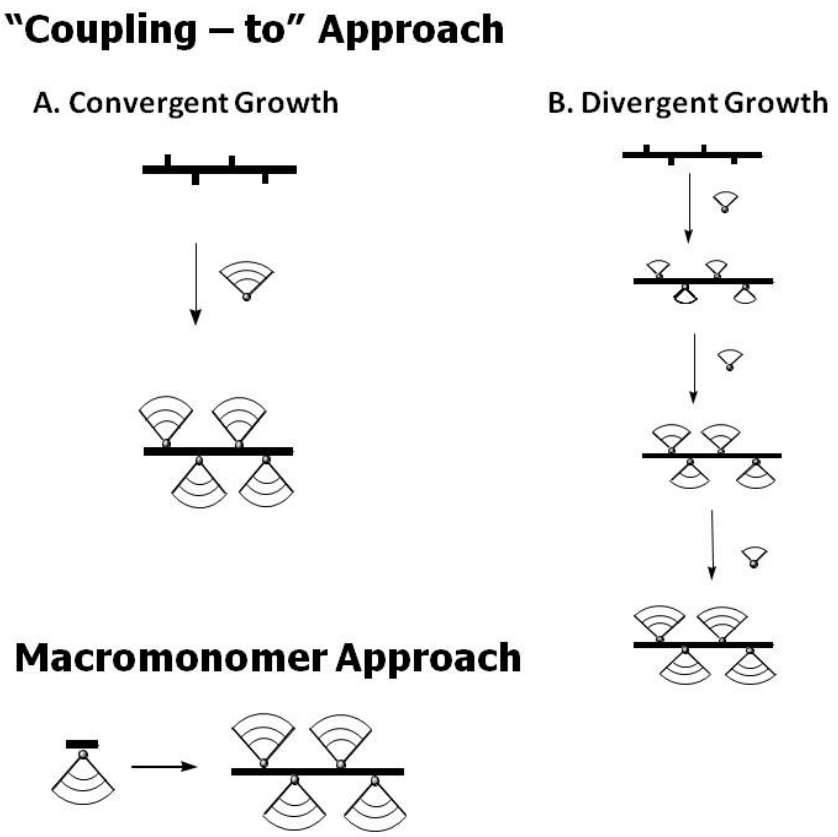

Figure 10. Synthetic methods towards dendronized polymers.

Frechet and Hawker studied the synthesis of dendrimers via convergent growth and were the first to report the synthesis of a dendronized polymer via the macromonomer approach.[141, 142]

Several detailed reviews discuss the synthesis and characterization of dendronized polymers and the advantages and disadvantages of each synthetic method.[130, 136, 143]

2.3.3 Amphiphilic Dendronized Polymers

Hybrid linear dendritic block copolymers have been employed to achieve various self-assembly effects. For example, block copolymers that form large micellar structures in solution have been prepared.[144-146]

Amphiphilic block copolymers have been prepared and shown to form large spherical and cylindrical micelles in solution, which were described as superamphiphiles and hydraamphiphiles, respectively.[147-149]

The ability to synthesize linear polymers with dendritic side groups broadens the scope of potential efforts toward defined nanostructures for supramolecular chemistry. Due to their lateral dimensions, form-anisotropy, and shape persistence, amphiphilic dendronized polymers afford a number of different architectures e.g. blockwise, lengthwise, and radially segregated amphiphiles[130] which result in a variety of morphologies (**Figure 11**). Novel amphiphilic dendronized polymers have been prepared from a variety of different combinations of linear polymers and dendrons.

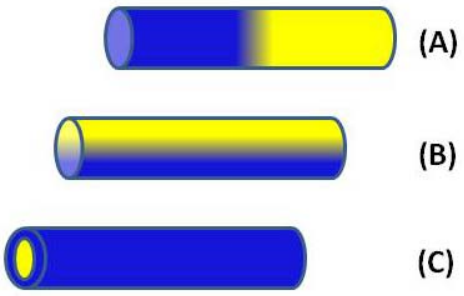

Figure 11. Architectures derived from amphiphilic dendronized polymers: a) block; b) lengthwise; and c) radially segregated cylindrical nanoscopic objects.

Dendronized polymers with a methacrylate backbone, aliphatic polyester dendrons, and a hydroxy-functional periphery were synthesized by a combination of techniques—atom transfer radical polymerization (ATRP) and the "coupling to" approach through the divergent growth method—to achieve a polymer with a hydrophobic backbone and hydrophilic dendron

substitutents (**Figure 12**).[150] Four generations (G1-G4) of dendronized polymers were prepared, and the effect of increased hydrophilicity and molecular size on their solution properties was studied. Dynamic light scattering and turbidity measurements in aqueous solution revealed aggregation upon heating for the first generation (G1) dendronized polymers, whereas, aggregation was not observed for the higher generation polymers. The aggregation of the G1 polymers was attributed the contribution of the hydrophobic methacrylate backbone. Although the dimensions of the polymers were shown to increase with increasing generation, low viscosities and Newtonian flow behavior in both aqueous and dimethyl sulfoxide solutions were observed for the polymers studied, behavior characteristic of dendrimers.[151] These molecules represent novel amphiphiles in which the hydrophobic core of a stiff polymer is masked by a hydrophilic shell.[150]

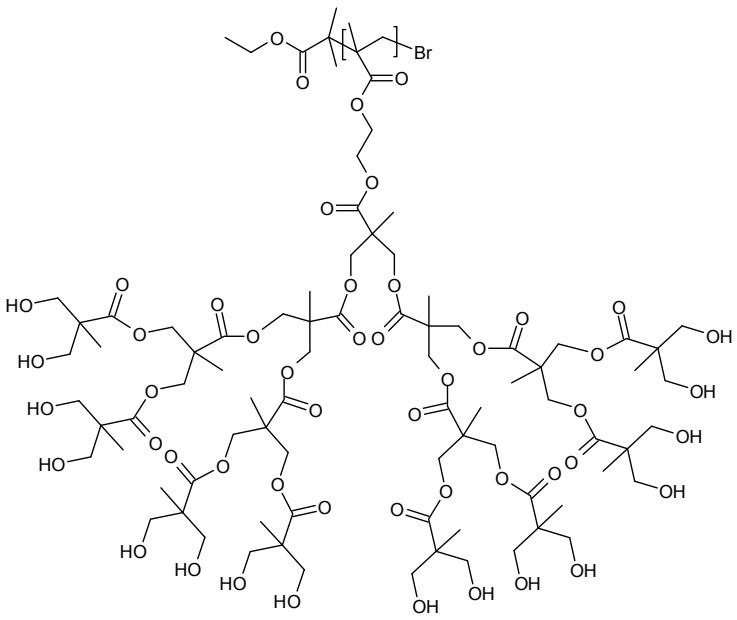

Figure 12. Amphiphilic dendronized polymers: hydrophobic core masked by a hydrophilic shell.

Unimolecular dendronized polymeric amphiphiles have been proposed as potential nanocontainers.[152] Dendronized polymers of linear polyethyleneimine and PAMAM-type dendrons (G0-G5) functionalized with hexyl acrylate were prepared and their ability to encapsulate water-soluble Rhodamine 6G dye molecules was studied as a function of dendron generation. Encapsulation was monitored through ^{1}H NMR; R6G exhibits a singlet at 2.30 ppm due to the two methyl groups attached to the unsaturated rings, upon encapsulation the signal shifts and splits (1.90 and 1.94 ppm) as a result of steric or non-covalent interactions resulting from the close packing inside the nanoamphiphiles. Loading capacity was shown to increase with molecular weight (i.e. increasing volume of the cavity). However, capacity density factor (loading capacity divided by the weight-average molecular weight of the repeat unit) decreased with increasing generation. Analysis via UV-VIS, photoluminescence, and ^{1}H NMR spectroscopies confirmed that less dye molecules per molecular weight were encapsulated at high generation (G3–G5). Novel unimolecular nanocomposites with the potential for selective encapsulation were demonstrated.

Amphiphilic polymer brushes with alternating hydrophilic linear and hydrophobic dendritic side chains have been synthesized (**Figure 13**).[153] Styryl macromonomers possessing Frechet-type dendrons[154] and *N*-[2-(2-bromoisobutyryloxy)ethyl] maleimide[155] were prepared according to their respective literature procedures, and subsequently copolymerized via conventional free radical polymerization to achieve a dendronized (G1–G3) alternating copolymer. To incorporate the hydrophilic linear side chains, *tert*-butyl acrylate, initiated by the maleimide derivative of the dendronized copolymer, was polymerized via ATRP. Hydrolysis of the *tert*-butyl branches under acidic conditions produced amphiphilic dendronized polymer brushes with linear hydrophilic poly(acrylic acid) (PAA) and hydrophobic dendritic side chains.

Amphiphilic polymer brushes with novel architecture and multiple "tunable" features—the brush conformation and properties may be tailored by varying the dendron generation and length of linear polymer side chains; well-defined, hydrophobic dendrons render the backbone rigid; and potential functionalization through the PAA side chains—were achieved.

Fréchet-type dendrons were also employed in the design of rod-coil amphiphilic block copolymers. Yi et al. prepared poly(acrylic acid)-*b*-dendronized polystyrene (PAA-*b*-DPS) copolymers[156] to achieve the rod-coil block copolymers. Macroinitiators (PMA-Br) were prepared from poly(methyl acrylate) and polymerized via ATRP employing 2-bromo-2-methyl propionic acid phenyl ester as an initiator. The PMA-Br macroinitator initiated the polymerization of Fréchet-type dendritic styrene macromonomers of increasing generation (G1–G3). The resulting PMA-*b*-DPS copolymers were hydrolyzed and acidified to achieve the targeted ionic amphiphilic block copolymer PAA-*b*-DPS (G1–G3).

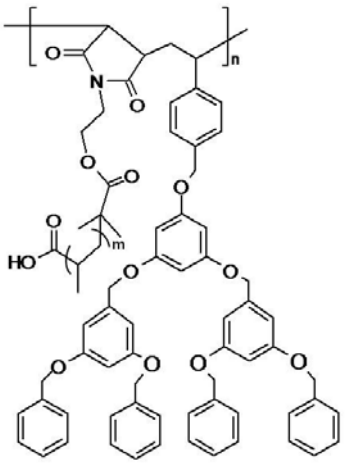

Figure 13. Amphiphilic dendronized copolymers: alternating hydrophilic aliphatic chains and hydrophobic dendrons.

The self-assembly of two copolymer systems, PAA_{25}-*b*-$DPS(G2)_{22}$ and PAA_{25}-*b*-$DPS(G2)_{65}$, were studied at room temperature in DMF, a common solvent for both blocks, and H_2O, a selective solvent, mixtures at an initial copolymer concentration of 2 mg mL^{-1}. In a binary solvent mixture (H_2O, 50 wt%), PAA_{25}-*b*-$DPS(G2)_{22}$ formed large compound micelles (LCMs) with a mean diameter of approximately 50 nm—a morphology typical of PS-*b*-PAA systems with very short hydrophilic blocks.[157, 158] Under the same conditions, PAA_{25}-*b*-$DPS(G2)_{65}$ formed vesicles in which the coil-like PAA blocks were located at the periphery of the membrane and the rod-like DPS blocks were arranged to form the bilayer wall. The vesicles were not uniform in size but ranged in diameter size from 60 to 150 nm; however, uniform wall thickness (28 nm) was observed. The wall thickness proved to be smaller than twice the contour length of the $DPS(G2)_{65}$ block (32.5 nm). This observation demonstrated the influence of the 'rod' block length on self-assembly behavior. Additionally, it is believed that the π-π aromatic stacking of the Fréchet-type dendrons functions to increase the stability of the bilayer vesicle structure.[159] Yi et al. also observed a host of interesting morphologies with amphiphilic comb-dendronized diblock copolymers consisting of hydrophobic Percec-type dendronized polystyrene (DPS) blocks and hydrophilic comb-like poly(ethylene oxide) grafted polymethacrylate [P(PEOMA)]blocks. The aggregation behavior of $P(PEOMA\text{-}300)_{55}$-b-DPS_{105} was studied in a binary solvent system of THF (common solvent) and CH_3OH (selective solvent) at an initial copolymer concentration of 3 mg/mL. With increasing CH_3OH content morphological changes were observed. Solutions became turbid at 30 wt% CH_3OH. At 70 wt % CH_3OH, twisted string aggregates (250 nm in diameter) were formed. Increasing the CH_3OH content to 85 wt% resulted in clear vesicle-like aggregates with relatively compact structures ranging in diameter size from 100 to 300 nm. Vesicle wall thickness was estimated from TEM images to be approximately 60

nm, which is thicker than that of vesicles from conventional block copolymers and attributed to the stretching cylindrical molecular morphology unique to the dendronized polymer. At 95 wt% CH_3OH, large compound micelles were observed.

In addition to the solution properties, the bulk properties were also studied for these systems using differential scanning calorimetry (DSC), polarized optical microscopy (POM) and wide angle X-ray diffraction (WAXD). Percec-type dendronized homopolymers (homo-DPS) are known to exhibit typical hexagonal columnar thermotropic liquid crystalline (LC) phase (Φh). DSC curves of the comb-dendronized block copolymers revealed a first order transition from isotropic phase to hexagonal columnar phase which was further confirmed by POM and WAXD studies. One drawback of the block copolymers compared to the homo-DPS system is that only weak birefringence is observed under POM after cooling to 110 °C and prolonging annealing times at that temperature showed no improvement. This result was attributed to the possibility of that the PEOMA block might prevent the dendronized block from stacking into a dense liquid crystalline phase. However, microphase separation was also evident in the appearance of two glass transition temperatures (T_gs) in the DSC curve for P(PEOMA-475)$_{74}$-b-DPS$_{181}$: -64 °C for P(PEOMA-475)$_{74}$ block and 48 °C for the DPS$_{181}$. The P(PEOMA) T_g was not observed in the DSC curves for P(PEOMA-300)$_{55}$-*b*-DPS$_{105}$ or P(PEOMA-300)$_{55}$-*b*-DPS$_{153}$; its absence was attributed to low P(PEOMA) content.

Dendronized methacrylate monomers with Frechet-type dendrons were copolymerized with poly(ethylene oxide) macroinitiators via ATRP to achieve dendronized poly(methacrylate)-*b*-poly(ethylene oxide), a novel amphiphilic block copolymer (**Figure 14**).[160] Micellar aggregation, characterized by transmission electron microscopy (TEM) and scanning electron microscopy (SEM) was studied as a function of polymer concentration, common solvent, and

increased water content in a binary solvent mixture of THF and water. The unique copolymer architecture led to morphological variety. At a polymer concentration of 0.4 mg/mL, the aggregates observed ranged from a combination of spherical and dendritic morphologies to large compound micelles (LCMs) to bowl-shaped aggregates with increasing water content (10 to 50 wt%). Doubling the polymer concentration (0.8 mg/mL) resulted in aggregates ranging from vesicles to LCMs to porous spheres. It was noted that as the polymer concentration increased relatively low water content was required to form vesicles. Large and collapsed vesicles were formed when the selective solvent was changed from water to methanol (0.4 mg/mL polymer concentration and 20 wt% MeOH). Changing the common solvent from THF to DMF resulted in a significant change in morphology—from spheres to rods (0.4 mg/mL polymer concentration and 20 wt% MeOH). The morphology change was attributed to an increased degree of solubilization in the core. In general, spherical aggregates are characteristic in cases in which the soluble block is longer than the insoluble block (e.g. star micelles). However, in the case of the amphiphilic dendronized block copolymers in which the soluble block (DP = 113) was longer than the insoluble block (DP = 40) multiple morphologies were observed and a simple core-shell structure was not easily obtained. The rigidity and unique structure of the dendronized core-forming block resulted in large compound aggregates, which could be attributed to the effective packing of the bulky side chains. These amphiphilic dendronized block copolymers have been employed in the fabrication of microporous honeycomb films, and their film formation was studied systematically as a function of polymer concentration, relative humidity, substrate, and spreading method.[161]

Amphiphilic nanoscopic cylinders with the propensity to segregate lengthwise are of great interest as potential mimics of ion channel membrane proteins.[162] The concept of

lengthwise segregation differs significantly from that observed in traditional amphiphilic block copolymers whose homophilic domains are oriented perpendicular to the backbone.

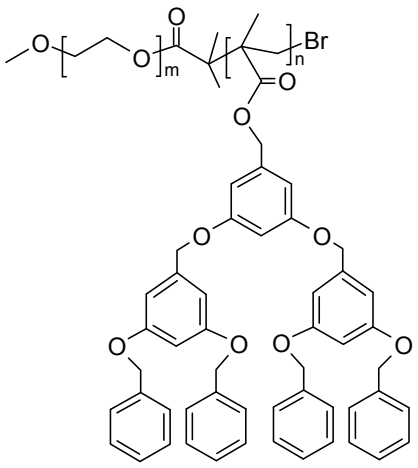

Figure 14. Amphiphilic dendronized polymers: block copolymers.

Schluter et al. set out to achieve this goal with the synthesis of dendronized poly(*p*-phenylene)s. They synthesized poly(*p*-phenylene)s with a hydrophilic dendron and a hydrophobic dendron on each repeat unit[163] and poly(*p*-phenylene)s carrying both a pendant dendron and a flexible chain at each repeat unit[164] (**Figure 15**). In each case, novel macromonomers with the desired combination of dendron and linear substituents were prepared and polymerized via Suzuki polycondensation. Langmuir-Blodgett experiments provided evidence of lengthwise segregation of the dendritic substituents into hydrophilic and hydrophobic domains.

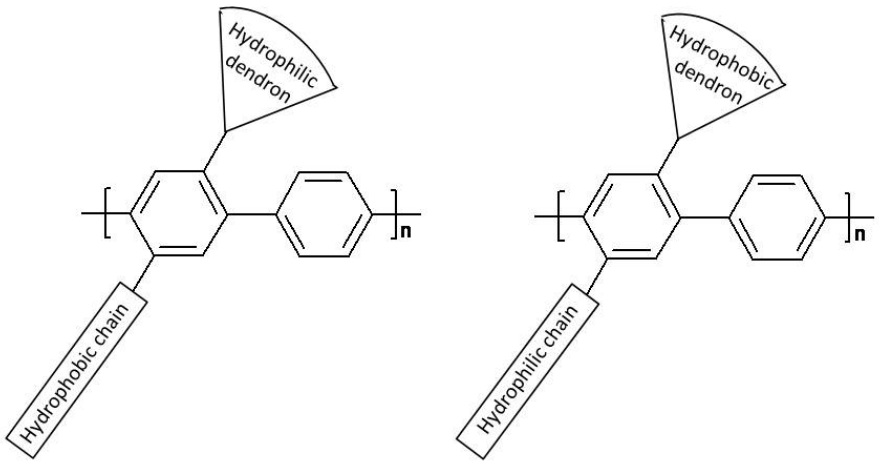

Figure 15. Amphiphilic dendronized polymers with propensity toward lengthwise segregation.

2.3.4 Dendronized Polymers – Potential Antivirals?

Dendronized polymers were initially proposed for use in the production of molecular composites and as crystallinity modifiers for polymeric materials.[133] Since such time, the field of dendronized polymers has developed substantially and thrives at the interface of organic chemistry, polymer synthesis, and materials science. To date, dendronized polymers have been investigated as a) catalyst supports in nanodimensions [165-167], b) polyinitiators for the synthesis of "hairy" functional derivatives[168], c) energy transfer, light harvesting and/or electrically conducting materials[169-174], d) objects for covalent attachment by the move-connect-prove strategy between individualized molecules on solid surfaces[175], e) surface coatings for patterning and to induce periodicity changes from Angstrom to nanometer scale[176, 177], and f) lengthwise segregated polar/nonpolar constituents of novel "supercylinders"[163].

Effect of Branched Architecture on Antiviral Activity

Increasing attention has been devoted to highly branched structures such as dendrimers and star polymers for biomedical applications with the hope that their architecture leads to interesting effects on biological properties. As with dendrimers, dendronized polymers possess multivalency, nanoscale size, and unique conformations. The use of dendronized polymers in biomedical applications is promising; one application of major focus has been their use as ultrahighly charged polyelectrolytes for DNA wrapping and subsequent gene transfer.[178] However, in contrast to dendrimers, few biological studies of dendronized linear polymers have been reported to date.

As mentioned previously, glycodendrimers have proven effective virus/host cell binding inhibitors through the blockage of viral receptors. Roy et al.[179] synthesized sialic acid functional polylysine dendrimers and tested them as influenza virus agglutination inhibitors. Increased inhibition with generation and potency comparable to that of polyacrylamide-based sialic acid inhibitors[180] was observed. This result suggested that the branched architecture, exhibiting increased polyvalent binding with reduced toxicity, might be more effective compared to linear polymer inhibitors and prompted a study of the effect of architecture on antiviral activity.

Variations in dendritic architecture were shown to have a profound effect on the potency of sialate-based polymeric viral inhibitors. The antiviral activity against influenza A virus was evaluated for sialic acid functional polymers of varying architecture including linear polyacrylamide (**I**), comb-branch (**II**), dendrigraft (**III**), spheroidal polyamidoamine dendrimers (**IV**), and dendronized polymer architectures (**V**) (**Figure 16**).[128] Although linear polyacrylamide polymers were capable of inhibiting influenza-induced agglutination of chicken red blood cells (cRBC), they were extremely toxic to Madin Darby Canine Kidney (MDCK)

cells. A significant reduction in cell toxicity was observed for inhibitors based on dendritic architectures.

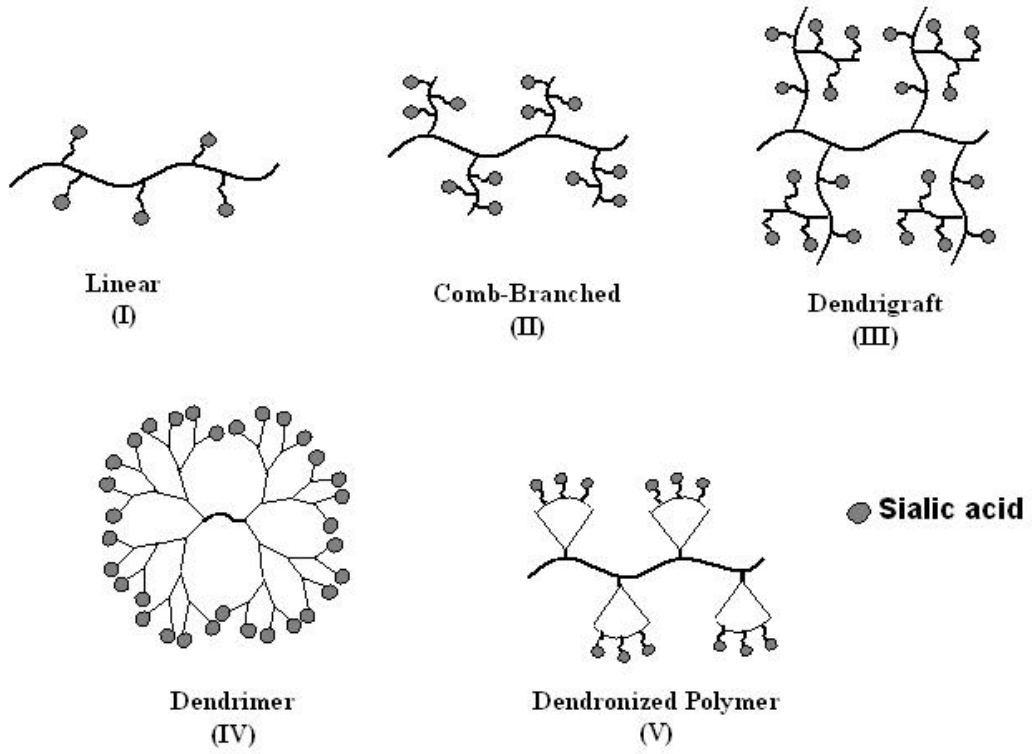

Figure 16. Macromolecular architectures investigated for antiviral activity.[128]

In regard to antiviral activity, spheroidal PAMAM dendrimers did not exhibit a significant increase in activity compared to monomeric sialic acid (SA) (**Figure 8**). The lack of activity in this case was attributed the fixed, rigid size and shape of this architecture, which may limit its ability to interact with the virus and the fact that these polymers are relatively small (1–10 nm) compared to influenza virus (~120 nm)—more dendrimers per virion may be necessary to effectively block adhesion. However, the larger, more flexible polyethyleneimine dendronized polymers were 1000 times more effective than monomeric SA. Dendrigraft polymers were 50,000 times stronger inhibitors than monomeric SA. Both the dendronized and dendrigraft

polymers were approximately 500 times stronger than other polymer inhibitors. The degree of sialic acid substitution (i.e. dendron generation) and polymer size seemed to influence the ability of dendritic polymers to inhibit influenza A via polyvalent binding forces and steric hindrance resulting for the ability of the polymers to conform and wrap around receptor sites.

Dendritic polymers offer a nontoxic alternative as adhesion inhibitors for the influenza virus and may provide a variety of potential synthetic inhibitors due to the wide range of available polymer structures.

Dendronized Polysaccharides – Toward Antivirals

Chitosan is a nontoxic, biodegradable, bioactive polymer that has proven useful as a carrier in drug delivery systems, as an antibacterial agent, and in other medical applications. The use of chitosan is limited by its poor solubility in both organic solvents and aqueous solutions. Chitosan-dendrimer hybrids (CDHs) have been prepared in an effort to increase chitosan solubility and processability. Employing sialic acid dendrons (G1 and G2) with triethylene glycol spacers and reductive amination as coupling chemistry, Roy et al. synthesized dendronized chitosan sialic acid hybrids.[181] The authors did not target complete dendron coverage. With only 0.15 equivalents added per repeat unit, the 87% coverage (0.13 equivalents) and 40% coverage (0.06 equivalents) was achieved for the G1 and G2 polymers, respectively. A variety of CDHs with carboxyl, ester, and poly(ethylene glycol) functional termini were synthesized and evaluated for biodegradation properties.[182] These CDHs may be useful in applications as biomedical or supermolecular polysaccharides, including use as antiviral agents. Biological studies were reportedly underway.[183]

Cellulose is a polydisperse, linear homopolymer consisting of regio- and enantio-selective β-1,4-glycosidic linked D-glucose units; it has three reactive hydroxyl groups—at the

C2, C3, and C6 positions. The properties of cellulose derivatives depend on the nature of the substitution, the substituent position, and substituent distribution along the cellulose chain. Regioselective functionalization of cellulose has attracted increasing attention because of its potential toward precisely modified cellulose materials that possess new properties. Dendritic side chains effectively increase the functionality of cellulose derivatives, producing new derivatives that would most likely be biocompatible and useful in biomedical applications.

Newkome et al. reported the preparation and characterization of dendronized cellulose derivatives through reaction with dendrons possessing isocyanate functional focal moieties.[184] A preliminary report showed that cellulose regioselectively reacted with isocyanate-functional dendrons (G1–G3) at the C6, primary hydroxyl group to produce dendronized cellulose polycarbamates.[185] These reactions were performed in a *N,N*-dimethylacetamide/LiCl solvent system using dibutyltin dilaurate (DBDL) as a catalyst. Nitrogen content, obtained from elemental analysis, served as evidence of monosubstitution (DS = 1) in spite of the excess of the isocyanate dendrons used in reaction. Spectroscopy (^{13}C NMR and FTIR) was used to further confirm chemical structure. Cellulose has moderate thermal stability exhibiting a two-stage degradation profile with a characteristic rapid decomposition between 250 and 350 °C and low residual char yields. Thermogravimetric analysis of the dendritic derivatives revealed lower onset of degradation temperatures but higher char yields compared to cellulose alone. In a second report, Newkome et al. repeated this synthesis with isocyanate dendrons of varying surface functionality including ester, cyano, and silyoxy. Homogeneous- and heterogeneous-modified polymers were prepared using these dendrons; the dendronized cellulose derivatives exhibited solubility in several organic solvents ranging from DMAc to MeOH. The nitrogen content of these carbamates revealed DS = 1 for the ester and cyano functional derivative and DS

= 0.5 for the silyoxyl derivative; the decreased substitution was attributed to the instability of the silyoxyl dendron under the reaction conditions employed. Evidence of the carbamate functionality via ^{13}C NMR and FT-IR served as confirmation of chemical structure. Combinatorial-type reaction of the three different dendrons with cellulose resulted in heterogeneous-surface derivatives. The degree of substitution was comparable to that observed for the homogeneous-modified cellulose derivatives.

Zhang et al. prepared a dendronized cellulose derivative with pendant amphiphilic side chains.[186] Beharas' amine, a hydrophobic first generation dendron, was coupled directly to (carboxymethyl)cellulose (CMC), and the resulting *tert*-butyl ester peripheral groups were converted to aminoamide substituents with use of *N,N*-dimethyl-1,3-propanediamine (DMPDA). The polymers were fully characterized via NMR, FTIR, IV, SEC, and TGA. Novel dendronized cellulose derivatives were achieved; however, the synthetic route presented proved more complex than that proposed by Newkome et al.[184]

Cytotoxicity of Dendronized Polymers

The cytotoxicity, biodistribution, and pharmacokinetics of synthetic, water-soluble, rigid-rod dendronized linear polymers consisting of a poly(4-hydroxystyrene) backbone and fourth-generation polyester dendrons were evaluated in normal and tumored mice.[187] Toxicity experiments were performed *in vitro* with MDA-MB-231 human breast cancer cells to determine biocompatibility, and cell viability was evaluated using the MTT assay. The polymers did not exhibit high levels of toxicity over the concentration range investigated with 85% cell viability observed at 0.25 mg/mL and 70% at 3.00 mg/mL, the highest concentration tested. After determining that the polymers were biocompatible, *in vivo* experiments were performed in mice to determine time-dependent biodistribution profiles. As with linear polymers, a positive

correlation was observed between the molecular weight of the dendronized polymers and their blood circulation time. Increased blood circulation half-lives promoted increased access to tumor vasculature, resulting in higher concentrations in excised tumors. Low molecular weight polymers showed little tissue specific accumulation, however, elevated polymer levels were discovered in the kidneys accompanied with high renal clearance. The high molecular weight polymers exhibited significantly decreased renal excretion and accumulation in the liver and spleen, which is not uncommon as revealed in previous studies of PEO.[188] The dendronized polymers proved relatively nontoxic and applicable for biomedical applications.

2.4 Summary and Motivation for Research

The need for a preventative agent to curtail the rampant spread of HIV and other STDs and mucosal pathogens is urgent. Topical microbicides have been identified as an attractive means toward this goal. Polyanionic molecules are potent *in vitro* inhibitors of HIV replication and show promise as effective microbicides.[29] However, the need for sufficient anionic character per molecule proves an important factor in the design of antiviral agents. To date, polyanionic antiviral agents have evolved from polysaccharides and their derivatives to conventional polymers to dendrimers. As synthetic and characterization methods for dendronized polymers progress, their application as antiviral agents is anticipated. The synthesis of a second generation macromonomer with peripheral *tert*-butyl protected carboxylates and a methacrylate polymerizing unit, as well as its free radical polymerization, and subsequent deprotection to produce anionic dendronized polymers has been reported.[189]

2.5 Research Objectives

The objective of this research was to synthesize a potent topical microbicide to curtail the rampant spread of HIV and other STDs and mucosal pathogens. Antimicrobial and anti-HIV activities of a homologous series of amphiphiles, as triethanolammonium salts, with hydrophobic tail lengths of 12–22 carbons and tri-functional hydrophilic headgroups have been reported (**Figure 17**).[30, 31] This research involves the preparation of polymer analogues of these materials. The copolymerization of novel dendritic methacrylate macromonomers and alkyl methacrylates via conventional free radical polymerization and subsequent deprotection was proposed to achieve amphiphilic dendronized copolymers; the proposed synthetic design is illustrated in **Figure 18**.

Novel methacrylate macromonomers (**5**) were synthesized and polymerized via conventional free radical polymerization using AIBN as an initiator. To begin, Weisocyanate™ (**2**) was prepared according to literature procedure.[30] Chain-extended alcohol derivatives (**3**) of Weisocyanate™ (**2**) were prepared with treatment of aminoethanol, **1**. Through a reaction of the alcohol derivative (**3**) and methacryloyl chloride (**4**) novel methacrylate macromonomers with pendant tri-functional hydrophilic headgroups (**5**) were obtained. Dendronized copolymers (**7**) were achieved via conventional free radical polymerization of the novel methacrylate macromonomers (**5**) and alkyl methacrylate monomers (**6**) with pendant aliphatic chains of varying length. To achieve ionizable polymers (**8**), the *tert*-butyl groups of (**7**) were removed with trifluoroacetic acid (TFA). By varying the feed ratio and the length of the pendant chain of **6**, the hydrophilic/hydrophobic copolymer composition was varied.

The dendronized polymers are expected to show enhanced anti-HIV activity compared to the small molecule amphiphiles given the significant increase in functionality imparted by the dendritic side chains. Additionally, selectivity (e.g. cytotoxicity) may be tunable through the control of molecular weight and the hydrophilic/hydrophobic composition.

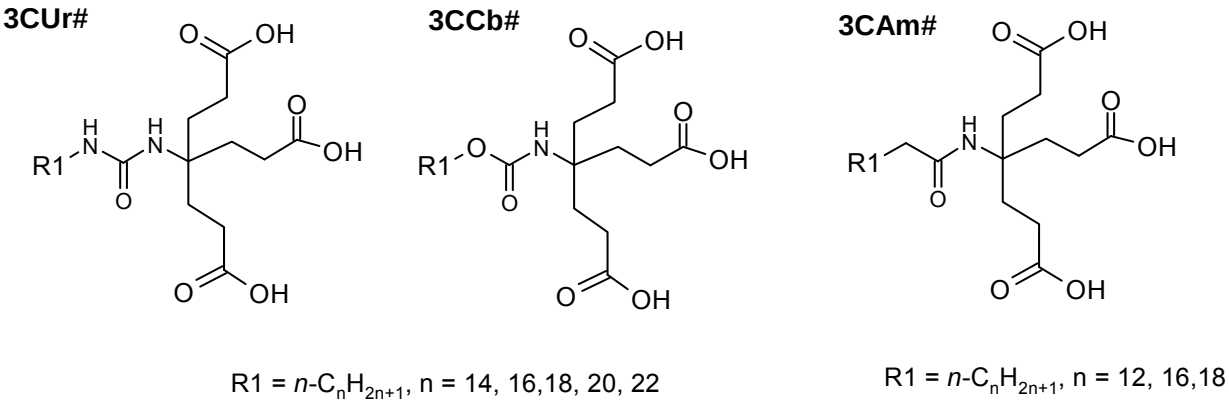

Figure 17. Tri-functional Amphiphiles. Nomenclature: 3C (three —CH_2CH_2COOH); Ur (ureido, —NHCONH—) Cb (carbamido, —OCONH—); Am (amido, —CONH—); and # (number of carbon atoms in tail).

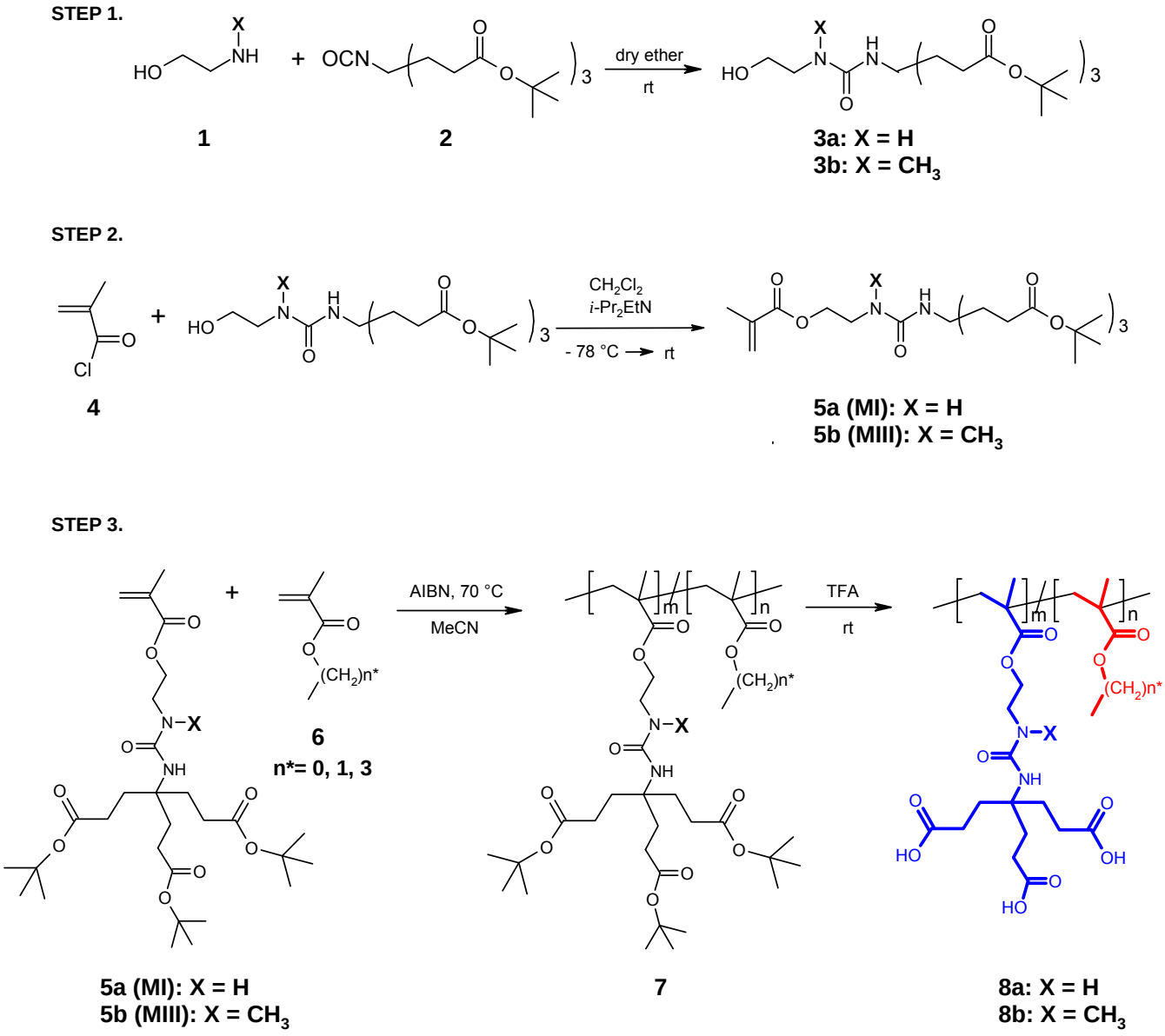

Figure 18. Synthetic scheme for amphiphilic dendronized copolymers.

Chapter 3: Experimental

3.1 Materials

In the synthesis and characterization of dendronized amphiphilic copolymers, the following reagents and solvents were employed. 2-Aminoethanol (Aldrich, 99%) and *N*-methyl-2-aminoethanol (Aldrich, 99%) were distilled under reduced pressure. Methyl methacrylate (Aldrich, 99% 10–100 ppm MEHQ) was passed through a column of basic aluminum oxide, stirred over CaH_2 for 24 h, and distilled under nitrogen. Ethyl methacrylate (Alfa Aesar, 98+%; 100 ppm 4-methoxy phenol), butyl methacrylate (Aldrich, 99%; 10 ppm MEHQ), and *tert*-butyl methacrylate were passed through a column of basic aluminum oxide. Methacryloyl chloride (Fluka, ≥97%; ~0.02 % 2,6-di-*tert*-butyl-*p*-cresol) was distilled under nitrogen. Methyl 3-mercaptopropionate (Aldrich, 98%) was used as received. Dichloromethane (Fisher Scientific, HPLC Grade) was passed through a column of basic aluminum oxide and distilled under nitrogen. Acetonitrile (Fisher Scientific, HPLC Grade) was stirred over CaH_2 for 24 h, distilled under nitrogen, and stored over molecular sieves (4Å). Diethyl ether (EMD) was dried over $MgSO_4$ and stored over molecular sieves (4Å). Weisocyanate™ was prepared according to literature procedure[30]. Unless otherwise specified, all remaining solvents and reagents were used as received.

3.2 Measurements

3.2.1 Nuclear Magnetic Resonance (NMR)

Proton nuclear magnetic resonance spectroscopy (^{1}H NMR) was employed to confirm the chemical composition and purity of all solvents, monomers, oligomers and polymers utilized in

this research. Samples were dissolved in the appropriate deuterated solvents, ($CDCl_3$ or CD_3OD), at a typical concentration of 10% (0.1g/1 mL). The spectra were obtained with a Varian INOVA spectrometer operating at 400 MHz with a 22.1° pulse angle, acquisition time of 3.7s and a 1s relaxation delay. The chemical composition of compounds **3** and **5** were also characterized with ^{13}C NMR. The spectra were obtained in $CDCl_3$ on a Varian INOVA spectrometer operating at 100 MHz with a 45° pulse angle, acquisition time of 1.2 s and a 1s relaxation delay. Resonances were reported in ppm relative to the known solvent residual peak in order of chemical shift (δ), followed by the splitting pattern and number of protons, where applicable. Abbreviations used in the splitting pattern were as follows: s = singlet, d = doublet, t = triplet, q = quartet, quin = quintet, m = multiplet, and br = broad.

3.2.2 Fourier Transform Infrared Spectroscopy (FTIR)

Fourier transform infrared spectroscopy (FTIR) was utilized to confirm the structure of compounds **3** and **5**. Measurements were conducted on a Nicolet Impact 400 FTIR spectrometer. IR spectra were recorded on neat samples with an FTIR equipped with a diamond attenuated total reflectance system, and reported in cm^{-1}.

3.2.3 Melting Point Determination

Melting point determination served as a measure of purity for the compounds synthesized. Melting points were determined in open capillary tubes and uncorrected. Melting point data were reported as a range: the temperature at onset of melting and the temperature at which the sample was completely liquid and a meniscus was evident.

3.2.4 Elemental Analysis

Elemental Analysis (EA) was employed as a measure of chemical composition and purity of the novel compounds synthesized in this research. Elemental analyses were performed by Atlantic Microlab; Atlanta, GA.

3.2.5 High Resolution Mass Spectrometry (HRMS)

Compounds **3** and **5** were analyzed via high resolution mass spectrometry (HRMS) to determine chemical composition and purity. HRMS data were obtained on a dual-sector mass spectrometer in FAB mode with 2-nitrobenzylalcohol as the proton donor.

3.2.6 X-ray crystallography

X-ray crystallography was employed as measure of chemical composition for compound **3**. The chosen crystal was mounted on a nylon CryoLoop™ (Hampton Research) with Krytox® Oil (DuPont) and centered on the goniometer of an Oxford Diffraction Gemini diffracometer or an Oxford Diffraction Xcalibur™ diffracometer operating at 100 K with Mo radiation and a Sapphire 3 detector. The data collection routine, unit cell refinement, and data processing were carried out with the program CrysAlis.[190] After identifying the space group, the structure was solved by direct methods and refined using SHELXTL NT.[191] SHELXTL NT was used for molecular graphics generation[191]. Measurements and analysis was performed by Dr. Carla Slebodnick.

3.2.7 Thin Layer and Column Chromatography

Analytical thin layer chromatography was performed on silica gel-coated (60 Å) polyester plates. Compounds were detected by UV light or by treatment with a solution of phosphomolybdic acid (10 wt%) in ethanol followed by drying with a heat gun. Flash column chromatography was carried out on silica gel (60 Å, Silicycle) in a 4″ diameter column; a

gradient solvent system was employed as the mobile phase. A slurry of silica gel in hexanes was poured into the column and compressed with air pressure to achieve a six-inch layer of silica gel. The flow rate of the mobile phase was adjusted to approximately 1 inch/min. The crude product, dissolved in $CHCl_3$, was loaded on the column. The polarity of the mobile phase was gradually increased by adding EtOAc (hexanes/EtOAc): 90/10 (50 mL), 80/20 (50 mL), 70/30 (mL), 60/40 (50 mL), 50/50 (100 mL), 0/100 (mL). The column was flushed with $CHCl_3$ (100 mL). Twenty-two ~25 mL fractions were collected. Common fractions were identified with TLC, combined, concentrated, and dried under vacuum. Typically, the macromonomers were identified in fractions 18–22.

3.2.8 Size Exclusion Chromatography (SEC)

Molecular characterization of the dendronized homo- and copolymers was performed in multiple solvents on three different size exclusion chromatography (SEC) instruments.

Analyses in tetrahydrofuran (THF) were performed by Rebecca Huyck Brown and Keiichi Osano in the laboratory of Professor Timothy Long. Samples (15–20 mg) were analyzed with three in-line 5μ PL-gel MIXED-C columns and a Waters SEC 410 Refractive Index (RI) detector (operating at 880 nm) with an autosampler inline with a MiniDAWN multi-angle laser light scattering (MALLS) detector (operating at 690 nm). The analyses were performed at 40 °C with a flow rate of 1.000 mL/min; the system was calibrated with narrow polydispersity polystyrene standards. The results were reported as number average molecular weight (M_n) and polydispersity (M_n/M_w) with absolute molecular weights obtained from the MALLS detector.

Analyses in *N*-methylpyrrolidone with 0.05 M lithium bromide (NMP/LiBr) were performed by Mark Flynn in the laboratory of Professors Judy S. Riffle and James E. McGrath.

Samples (15–20 mg) were analyzed with three in-line 5μ PL-gel MIXED-C columns and a Waters 2414 refractive index detector with an autosampler inline with a Viscotek 270 dual detector. The analyses were performed at 60 °C with a flow rate of 1.000 mL/min; the column temperature was maintained at 60 °C due to the viscous nature of NMP. The system was calibrated with narrow polydispersity polystyrene standards. Both the mobile phase solvent and sample solution were filtered.

Analyses in chloroform ($CHCl_3$) were performed by Mark Flynn in the laboratory of Professors Judy S. Riffle and James E. McGrath.

3.2.9 Matrix-Assisted Laser Desorption/Ionization – Time of Flight (MALDI-TOF)

Analysis performed by Dr. Anthony P. Gies in the Department of Chemistry at Vanderbilt University, 7330 Stevenson Center, Nashville, TN 37235. Samples were analyzed using an Applied Biosystems 4700 Proteomics Analyzer MALDI-TOF/TOF MS (Applied Biosystems, Framingham, MA) equipped with 355-nm Nd:YAG lasers. All spectra were obtained in the positive ion mode using an accelerating voltage of 8 kV for the first source, 15 kV for the second source, and a laser intensity of ~ 10% greater than threshold. The grid voltage, guide wire voltage, and delay time were optimized for each spectrum to achieve the best signal-to-noise ratio. The collision energy is defined by the potential difference between the source acceleration voltage and the floating collision cell; in our experiments this voltage difference was set to 1 kV. Air was used as a collision gas at pressures of 1.5×10^{-6} and 5×10^{-6} Torr (which will be referred to as “low” and “high” pressure, respectively). All spectra were acquired in the reflectron mode with a mass resolution greater than 3000 fwhm; isotopic resolution was observed throughout the entire mass range detected. External mass calibration was performed using protein standards from a Sequazyme Peptide Mass Standard Kit (Applied

Biosystems) and a three-point calibration method using Angiotensin I (m = 1296.69 Da), ACTH (clip 1-17) (m = 2093.09 Da), and ACTH (clip 18-39) (m = 2465.20 Da). Internal mass calibration was subsequently performed using a PEG standard (M_n = 2000; Polymer Source, Inc.) to yield monoisotopic mass accuracy better than $\Delta m = \pm 0.05$ Da. The instrument was calibrated before every measurement to ensure constant experimental conditions.

All samples were run in a dithranol matrix (Aldrich) doped with sodium trifluoroacetate (NaTFA, Aldrich). Samples were prepared using the dried-droplet method with weight (mg) ratios of 50:10:1 (Dithranol:polymer:NaTFA) in tetrahydrofuran (THF, Fisher). After vortexing the mixture for 30 sec, 1 μL of the mixture was pipetted on the MALDI sample plate and allowed to air dry at room temperature. MS and MS/MS data were processed using the Data Explorer 4.9 software (Applied Biosystems).

3.2.10 Differential Scanning Calorimetry (DSC)

Differential scanning calorimetry (DSC) was conducted with a TA Instruments Model Q1000. The samples (3–8 mg) were heated at a rate of 10 °C/min in a nitrogen atmosphere. The midpoints of the specific heat increases in the transition region during the second heating scan were reported as the glass transition temperatures.

3.2.11 Thermogravimetric Analysis

Thermogravimetric analysis (TGA) on a TA Instruments Model Q500 was employed as a first approximation of thermal degradation prior to DSC analysis as well as to investigate the thermal stability of the homo- and copolymers synthesized. The samples were heated at 10°C/min from 25 to 600 °C in either Nitrogen or air. The weight loss of the sample was

measured as a function of temperature. The temperature at which the sample exhibited a 5 % weight loss, $T_{5\%}$, was reported.

3.3 Synthesis and Characterization of Novel Methacrylate Macromonomers

*3.3.1 Synthesis of Di-tert-butyl 4-(2-(tert-Butoxycarbonylethyl)-4-[3-(hydroxyethyl)ureido]heptanedioate (**3a**)*

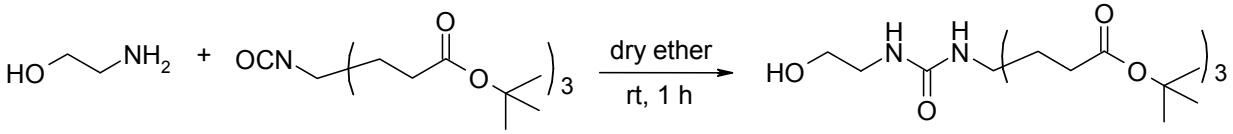

3a

In a typical reaction, Weisocyanate™ (4.01 g, 9.20 mmol) was stirred in dry Et_2O (22 mL) at rt and 2-aminoethanol (0.55 mL, 9.1 mmol) was added via syringe. Within 30 min, a white solid precipitated from solution. The solution was concentrated and the crude product was dried under vacuum overnight. The resulting white solid (4.580 g, 99%) was recrystallized from a mixture of EtOAc and hexane and dried under vacuum to give colorless crystals; yields ranged from 74 to 80%; mp 145.0–145.5 °C; ^{1}H NMR (400 MHz, $CDCl_3$): δ 1.44 (s, 27H), 1.93 (m, 6H), 2.24 (m, 6H), 3.27 (q, 2H), 3.45 (t, 1H), 3.67 (q, 2H), 4.98 (t, 1H), 5.09 (s, 1H); ^{13}C NMR (100 MHz, $CDCl_3$): δ 28.0, 29.8, 30.4, 43.1, 56.3, 63.1, 80.5, 158.0, 173.2; FTIR: 3334, 2950, 1713, 1143; HRMS (m/z): $[M+H]^+$ calcd for $C_{25}H_{47}N_2O_8$, 503.3332; found, 503.3357; analysis for $C_{25}H_{46}N_2O_8$: % calcd, C, 59.74; H, 9.22; N, 5.57; % found, C, 59.90; H, 9.35; N, 5.59. X-ray crystallography: Colorless rods (0.08 x 0.17 x 0.41 mm^3) were crystallized from ethyl acetate/hexanes at room temperature. The Laue symmetry was consistent with the triclinic crystal system and the space group $P\bar{1}$ was chosen. The asymmetric unit of the structure comprises two crystallographically independent molecules. The final refinement model involved

anisotropic displacement parameters for non-hydrogen atoms and a riding model for all hydrogen atoms. Two-site disorder was modeled at one of the alcohol groups, with relative occupancies 0.732(3) and 0.268(3).

*3.3.2 Synthesis of Di-tert-butyl 4-(2-tert-Butoxycarbonylethyl)-4-[3-(2-hydroxyethyl)-3-methylureido]heptanedioate (**3b**)*

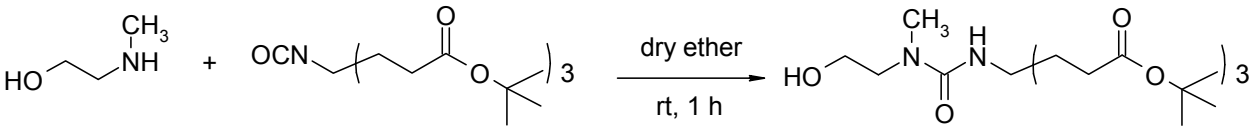

3b

Employing *N*-methyl-2-aminoethanol, compound **3b** was prepared in a similar fashion: Weisocyanate™ (1.01 g, 2.29 mmol) was stirred in dry Et_2O (7 mL) at rt and *N*-methyl-2-aminoethanol (0.20 mL, 2.5 mmol) was added via syringe. The reaction solution was stirred at rt for an hour. The solution was concentrated resulting in a yellow, viscous liquid, which was dried under vacuum overnight. The resulting pale yellow solid was recrystallized from a mixture of EtOAc and hexane and dried under vacuum to give colorless, transparent crystals with yields ranging from 73 to 80%; mp 95.9–96.5 °C; ^{1}H NMR (400 MHz, $CDCl_3$): δ 1.38 (s, 27H), 1.91 (m, 6H), 2.17 (m, 6H), 2.83 (s, 3H), 3.32 (t, 2H), 3.50 (t, 1H), 3.67 (q, 2H), 5.25 (s, 1H); ^{13}C NMR (100 MHz, $CDCl_3$): δ 28.0, 30.0, 30.6, 35.3, 52.1, 56.7, 61.7, 80.5, 158.5, 173.2; FTIR: 3305, 2950, 1718, 1148; HRMS (m/z): $[M+H]^+$ calcd for $C_{26}H_{49}N_2O_8$, 517.3489; found 517.3485; analysis for $C_{26}H_{48}N_2O_8$: % calcd C, 60.44; H, 9.36; N, 5.42; % found C, 60.50; H, 9.31; N, 5.36. X-ray crystallography: Colorless rods (0.19 x 0.25 x 0.39 mm^3) were crystallized from ethyl acetate/hexanes. The Laue symmetry was consistent with the triclinic space groups P1 and $P\bar{1}$. Centric space group $P\bar{1}$ was chosen based on the $|E^2-1|$ value (0.992) and the Z value. The asymmetric unit of the structure comprises one crystallographically independent molecule.

The final refinement model involved anisotropic displacement parameters for non-hydrogen atoms and a riding model for the alkyl hydrogen atoms. Hydrogen atom positions and isotropic thermal parameters were refined independently for the hydroxyl hydrogen that is potentially involved in hydrogen bonding.

*3.3.3 Synthesis of Di-tert-butyl 4-(2-tert-Butoxycarbonyl-ethyl)-4-[3-(2-methacryoloxyethyl)ureido]heptandioate (**5a, MI**)*

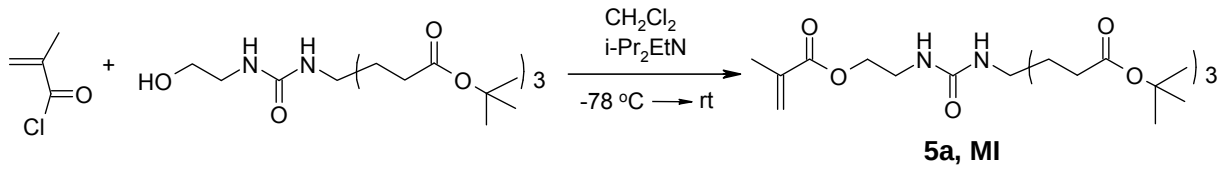

5a, MI

To prepare the methacrylate macromonomer, **5a (MI)**, alcohol **3a** (5.01 g, 9.98 mmol) was placed in a round-bottom flask, which was sealed with a septum and purged with argon. Dichloromethane (15 mL) and diisopropylethylamine (Aldrich, ≥99%) (*i*-Pr_2EtN) (2.6 mL, 15 mmol) were added via syringe. The reaction flask was cooled in a dry ice/acetone bath, and methacryloyl chloride (1.5 mL, 15 mmol) was added via syringe. The reaction solution was stirred overnight as the dry ice/acetone bath evaporated allowing the reaction solution to warm to rt. The solution was concentrated, and the crude yellow solid was dried under vacuum (8.72 g). The solid was dissolved in CH_2Cl_2 (100 mL) and washed with deionized water (3×50 mL), 10% citric acid (3×50 mL), 10% K_2CO_3 (3×50 mL), saturated $NaHCO_3$ (3×50 mL), and saturated NaCl (3×50 mL). The organic layer was dried over anhydrous Na_2SO_4. After filtration, the clear, pale yellow solution was concentrated and dried under vacuum to give an off-white/yellow solid (4.63 g, 81 %). The crude product, dissolved in $CHCl_3$, was spotted on a TLC plate and eluted with multiple mixtures of hexanes/EtOAc (v/v): 80/20, 70/30, 50/50. Three spots were observed in the various eluents—80/20: R_f = 0.06, 0.18, 0.53; 70/30: R_f = 0.08, 0.18, 0.44; 50/50:

R_f = 0.31, 0.54, 0.79. The crude product was purified via flash chromatography with a gradient mobile phase; the fractions collected were analyzed on TLC plates with a 50/50 (v/v) hexanes/EtOAc eluent. The total mass recovered was 80% of the mass loaded, the majority of which was found in fractions 15–17 (28%, R_f = 0.72) and fractions 20–22 (68%, R_f = 0.37). The combined fractions were concentrated and dried under vacuum. With ^{1}H NMR, the combined fractions were identified as a di-substituted methacrylate (**MII**), an undesirable side product, and the targeted mono-substituted methacrylate (**5a, MI**), respectively. The presence of small amounts of impurities and/or solvent resulted in a white tacky solid or a gel. In this case, column chromatography procedure was repeated on the material isolated from fractions 20–22 to achieve a white solid, which was dried under vacuum at 45 °C. **MI (5a)**: mp 84.7–85.2 °C; ^{1}H NMR (400 MHz, $CDCl_3$): δ 1.43 (s, 27H), 1.95 (m, 9H), 2.23 (m, 6H), 3.43 (q, 2H) 4.20 (t, 2H), 4.57 (t, 1H), 4.80 (s, 1H), 5.60 (quin, 1H), 6.13 (m, 1H); ^{13}C NMR (100 MHz, $CDCl_3$): δ 18.3, 27.9, 29.8, 30.5, 39.3, 56.5, 64.2, 80.5, 126.0, 136.0, 156.3, 167.4, 173.0; FTIR: 3333, 2950, 1718, 1133; HRMS (m/z): $[M+H]^+$ calcd for $C_{29}H_{51}N_2O_9$, 571.3595; found 571.3611; analysis for $C_{29}H_{50}N_2O_9$: % calcd C, 61.03; H, 8.83; N, 4.91; % found C, 60.97; H, 8.95; N, 4.81.

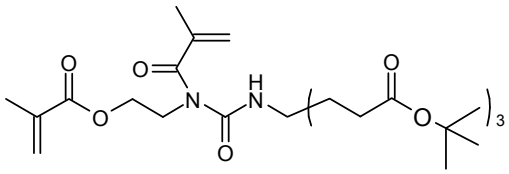

MII

The di-substituted methacrylate (**MII**), an undesirable side product, was analyzed with ^{1}H NMR: ^{1}H NMR (400 MHz, $CDCl_3$): δ 1.39 (s, 27H), 1.89 (m, 3H), 1.95 (m, 9H), 2.17 (m, 6H), 4.02 (t, 2H) 4.26 (t, 2H), 5.14 (br s, 1H), 5.24 (m, 1H), 5.56 (quin, 1H), 6.05 (m, 1H), 8.85 (s,

1H). The di-substituted methacrylate had a tendency to cross-link under ambient conditions. No further analyses were performed.

*3.3.4 Synthesis of Di-tert-butyl 4-(2-tert-Butoxycarbonylethyl)-4-[3-methyl-3-(2-methacryoloxyethyl)ureido]heptanedioate (**5b, MIII**)*

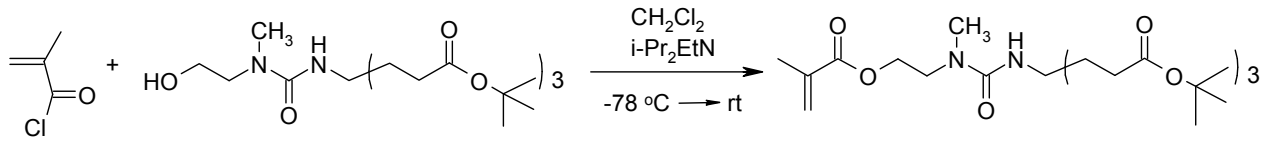

5b, MIII

To prepare the methacrylate macromonomer, **5b** (**MIII**), alcohol **3b** (3.00 g, 5.78 mmol) was placed in a round-bottom flask, which was sealed with a septum and purged with argon. Dichloromethane (9.0 mL) and *i*-Pr_2EtN (1.5 mL, 8.6 mmol) were added via syringe. The reaction flask was cooled in a dry ice/acetone bath, and methacryloyl chloride (1.5 mL, 15 mmol) was added via syringe. The reaction solution was stirred overnight as the dry ice/acetone bath evaporated allowing the reaction solution to warm to rt. The resulting clear, pale pink solution was diluted with CH_2Cl_2 (20 mL) and washed with deionized water (3×50 mL), 10% citric acid (3×50 mL), 10% K_2CO_3 (3×50 mL), saturated $NaHCO_3$ (3×50 mL), and saturated NaCl (3×50 mL). The organic layer was dried over anhydrous Na_2SO_4, filtered, and concentrated. The off- white/pale pink solid was dried under vacuum (2.49 g, 74 %). The crude product was purified via flash chromatography with a gradient mobile phase; the fractions collected were analyzed on TLC plates with a 50/50 (v/v) hexanes/EtOAc eluent. The total mass recovered was 94% of the mass loaded; the majority of which was found in fractions 18–20 (87%, $R_f = 0.41$). The combined fractions were concentrated and dried under vacuum at 45 °C to give a white solid. **MIII** (**5b**): mp 82.6–83.1 °C; ^{1}H NMR (400 MHz, $CDCl_3$) δ: 1.43 (s, 27H), 1.96 (m, 9H), 2.23 (m, 6H), 2.91 (s, 3H), 3.53 (t, 2H), 4.25 (t, 2H), 4.99 (s, 1H), 5.58 (m,

1H), 6.12 (m, 1H); ^{13}C NMR (100 MHz, $CDCl_3$): δ 18.2, 28.0, 29.9, 30.5, 35.4, 47.5, 56.6, 63.1, 80.5, 125.8, 136.1, 156.7, 167.3, 173.2; FTIR: 2955, 1714, 1148; HRMS (m/z): $[M+H]^+$ calcd for $C_{30}H_{53}N_2O_9$, 585.3751; found 585.3727; analysis for $C_{30}H_{52}N_2O_9$: % calcd C, 61.62; H, 8.96; N, 4.79; % found C, 61.40; H, 9.05; N, 4.71.

3.4 Polymerization of Dendritic Methacrylate Macromonomers

3.4.1 Homopolymerization of Dendritic Methacrylate Macromonomers

Polymerization of the dendritic methacrylate macromonomer, **MIII**, was achieved via conventional free radical polymerization in MeCN employing AIBN as an initiator. A series of reactions, varying macromonomer and initiator concentrations, were performed. The concentration of the macromonomer in MeCN was varied from 10 to 60 wt%, and the initiator concentration from 0.01 to 1.0 mol%. Prior to reaction, a stock solution of AIBN in MeCN was prepared and purged with argon. In general, **MIII** was weighed in a round-bottom flask, which was capped with a copper-wired septum and purged with argon. To the reaction flask, MeCN and AIBN solution were added via syringe to achieve the targeted concentrations. The solution was stirred at ~70 °C for 18–24 h. The reaction solution was allowed to cool to rt. The resulting turbid, viscous liquid was diluted with $CHCl_3$ or CH_2Cl_2 and added drop-wise to rapidly-stirring, chilled (in -20 °C freezer) hexanes. The resulting white precipitate was filtered and dried under vacuum at 50 °C. The precipitation procedure was performed 2–3 times for each polymerization reaction. The filtrate, combined from each precipitation cycle, was concentrated and dried under vacuum to give a viscous liquid. Both the precipitate and the viscous liquid were analyzed via ^{1}H NMR. Reactions that resulted in polymerization formed a precipitate. Analysis of the precipitate via NMR confirmed polymerization by 1) the absence of the peaks attributed to the vinyl protons and 2) a significant broadening of the remaining peaks. Reactions with a

macromonomer concentration < 30 wt% and an initiator concentration < 1.0 mol% resulted in no or low (precipitate collected was ~18–20 wt% of mass recovered) monomer conversion; employing a high macromonomer concentration (60 wt%) and low initiator concentration (0.01 mol%) also proved unsuccessful.

When employing the optimized reaction conditions (> 30 wt% macromonomer and 1.0 mol% AIBN), the dendritic methacrylate macromonomer was successfully polymerized.

A stock solution (5.2 mg/mL) of AIBN in MeCN was prepared and purged with argon. In a typical reaction, **MIII** (0.861 g, 1.47 mmol) was weighed in a round-bottom flask, which was capped with a copper-wired septum and purged with argon. To the reaction flask, MeCN (0.54 mL) and AIBN solution (0.46 mL, 0.015 mmol) were added via syringe. The solution was stirred at ~70 °C for 18–24 h. The resulting viscous liquid was allowed to cool to rt and diluted with minimal CH_2Cl_2 to achieve a low viscosity liquid; the solution was added drop-wise to rapidly-stirring, chilled (in -20 °C freezer) hexanes (100-fold excess); a white precipitate formed. The precipitate was collected via vacuum filtration in a fritted funnel, and the dissolution/precipitation cycle was repeated. Finally, the precipitate was collected by filtration and dissolved in CH_2Cl_2. The solution was concentrated to give a white solid, which was dried under vacuum at 50 °C (0.522 g). The solid proved difficult to transfer because it adhered (static electricity?) to the glass funnel, which resulted in decreased mass recovery: ^{1}H NMR (400 MHz, $CDCl_3$): δ 0.51–1.14 (br, —$CH_2C(CO)(CH_3)$—), 1.17–1.57 (br, —$COOC(CH_3)_3$), 1.59–1.70 (br s, $NCC(CH_3)_2$—), 1.71–2.06 (br, —$NHC[CH_2CH_2COO—]_3$ and —$CH_2C(CO)(CH_3)$—), 2.06–2.45 (br, —$NHC[CH_2CH_2COO—]_3$), 2.69–3.15 (br, —$OCH_2CH_2N(CO)(CH_3)$—), 3.23–3.66 (br, —$OCH_2CH_2NCH_3$—), 3.74–4.23 (br, —$OCH_2CH_2N(CH_3)$—), 4.68–5.09 (br, —$CH_2N(CH_3)(CO)NH$—); T_g: 65 °C; $T_{5\%}$ in air: 218 °C.

Molecular weight characterization via SEC was attempted on three different instruments with various detectors (refractive index, viscosity, and MALLS) in multiple solvents ($CHCl_3$, THF, NMP/LiBr); analysis via MALDI-TOF was also attempted.

The filtrate recovered from the filtration of the polymer precipitate was concentrated and dried under vacuum to give a turbid, viscous liquid, which was weighed (0.043 g) and analyzed. The ^1H NMR spectrum revealed signals primarily attributed to unreacted monomer; however, broad signals attributed to polymer were also observed.

3.4.2 Dendronized Copolymers via copolymerization with Methyl Methacrylate

Methacrylate macromonomer **MIII** was copolymerized with methyl methacrylate (MMA); the copolymer composition was varied. Copolymers incorporating 5–50 mol % of the novel methacrylate macromonomer, **MIII**, were targeted. MMA was polymerized to prepare a reference (0 mol% **MIII**) polymer (PMMA).

Polymerization of MMA

A series of MMA polymerizations, varying in initiator concentration (0.01 to 1.0 mol%), was performed. Prior to reaction, a stock solution (3.9 mg/mL) of AIBN in MeCN was prepared and purged with argon. In a typical reaction, a round-bottom flask was capped with a copper-wired septum and purged with argon. To the reaction flask, MMA (0.50 mL, 4.7 mmol), MeCN (6.0 mL), and AIBN solution (2.0 mL, 0.048 mmol) were added via syringe. The solution was stirred at ~70 °C for 18–24 h. The reaction solution was allowed to cool to rt and concentrated to give an off-white solid, which was dried under vacuum. The solid was dissolved in $CHCl_3$ (0.5 mL) and precipitated in hexanes (40 mL). The precipitate was collected with centrifugation; the hexanes was decanted, and the dissolution/precipitation cycle was repeated twice. Lastly, the

hexanes was decanted, and the precipitate was dissolved in $CHCl_3$. The solution was concentrated to give a white solid, which was dried under vacuum at 50 °C (0.325 g): ^{1}H NMR (400 MHz, $CDCl_3$): δ 0.69–0.89 (br s, —$CH_2C(CO)(CH_3)$—, syndiotactic), 0.88–1.06 (br s, —$CH_2C(CO)(CH_3)$—, atactic), 1.06–1.10 (br, —$CH_2C(CO)(CH_3)$—, isotactic) 1.12–1.29 (br, $NC(CH_3)_2CCH_2$—), 1.29–1.47 (br, —$CH_2C(CO)(CH_3)$—), 1.58 (s, $NCC(CH_3)_2$—), 1.65–2.06 (br, —$CH_2C(CO)(CH_3)$—), 3.56 (br s, —$COOCH_3$); SEC (THF; MALLS): M_n = 15,400 g/mol; PDI= 1.7; T_g = 93 °C.

All PMMAs were prepared and characterized in a similar fashion.

Copolymerization

To prepare of a copolymer of the novel macromonomer and MMA, **MIII** (0.254 g, 0.435 mmol) was weighed in a round-bottom flask, capped with a copper-wired septum, and purged with argon. A stock solution (5.2 mg/mL) of AIBN in MeCN was prepared and purged with argon. Acetonitrile (4.0 mL), MMA (0.070 mL, 0.66 mmol), and AIBN solution (0.35 mL, 0.011 mmol) were added via syringe. The solution was stirred at ~70 °C for 24 h. The reaction solution was concentrated to give a flaky, off-white solid (0.093 g), which was dried under vacuum at rt. The solid was dissolved in minimal $CHCl_3$ and precipitated in hexanes (30-fold). The precipitate was collected with centrifugation; the hexanes was decanted and the dissolution/precipitation cycle was repeated twice. Lastly, the hexanes was decanted, and the precipitate was dissolved in $CHCl_3$. The solution was concentrated to give a white solid, which was dried under vacuum at 50 °C: ^{1}H NMR (400 MHz, $CDCl_3$) δ: 0.55–1.08 (br, —$CH_2C(CO)(CH_3)$—), 1.25–1.48 (br, —$COOC(CH_3)_3$), 1.58–2.05 (br, —$NHC[CH_2CH_2COO—]_3$ and —$CH_2C(CO)(CH_3)$—), 2.05–2.28 (br, —$NHC[CH_2CH_2COO$—), 2.75–2.98 (br, —

$CH_2N(CH_3)(CO)$—), 3.38–3.54 (br s, —$OCH_2CH_2N(CH_3)$—), 3.54–3.74 (br s, —$COOCH_3$), 3.82–4.09 (br, —$OCH_2CH_2N(CH_3)$—), 4.78–5.01 (br, —$CH_2N(CH_3)(CO)NH$—).

From ^{1}H NMR, the copolymer composition was estimated by the ratio of signals at 2.75–2.98 δ and 3.54–3.74 δ. SEC (THF, MALLS): M_n = 36,300 g/mol and PDI = 1.5; T_g = 66 °C.

The remaining copolymers in the series were prepared and characterized in a similar fashion.

3.4.3 Employing a Chain Transfer Agent (CTA) for Molecular Weight Control

Model Study

As a means to achieve low molecular weight polymers, a chain transfer agent (CTA), methyl 3-mercaptopropionate (MMP), was employed. A model study was performed by polymerizing MMA in MeCN with AIBN as an initiator, varying the MMP concentration (0, 5, 10 mol %).

In a typical reaction, a round-bottom flask containing a stir bar was capped with a copper-wired septum and purged with argon. A stock solution (10.5 mg/mL) of AIBN in MeCN was prepared and purged with argon. To the reaction flask, MMA (0.25 mL, 2.3 mmol), MeCN (3.0 mL), AIBN solution (0.36 mL, 23 mmol), and MMP (0.025 mL, 0.23 mmol) were added via syringe. The resulting clear, colorless solution was purged with argon and stirred at ~70 °C for 24 h. The reaction solution was allowed to cool to rt and concentrated to give a flaky, off-white solid (0.135 g, material lost in transfer; however, most cases resulted in quantitative mass recovery), which was dried under vacuum. The solid was dissolved in $CHCl_3$ (0.5 mL) and precipitated in hexanes (40 mL). The precipitate was collected with centrifugation; the hexanes was decanted and the dissolution/precipitation cycle was repeated twice. Lastly, the hexanes was

decanted, and the precipitate was dissolved in $CHCl_3$. The solution was concentrated to give a white solid, which was dried under vacuum at 40 °C: ^{1}H NMR (400 MHz, $CDCl_3$): δ 0.69–0.86 (br s, —$CH_2C(CO)(CH_3)$—, syndiotactic), 0.90–1.05 (br s, —$CH_2C(CO)(CH_3)$—, atactic), 1.05–1.10 (br, —$CH_2C(CO)(CH_3)$—, isotactic), 1.13–1.24 (br, —$CH_2C(CO)(CH_3)$—), 1.29–1.48 (br, —$CH_2C(CO)(CH_3)$—), 1.66–2.17 (br, —$CH_2C(CO)(CH_3)$—), 2.39–2.57 (m, —$(CO)CH_2CH_2S$—), 2.61–2.81 (m, —$(CO)CH_2CH_2S$—), 3.46–3.70 (br s, —$COOCH_3$); SEC (THF; MALLS): M_n = 4,300 g/mol; PDI= 1.3; T_g = 85 °C.

In the model study employing 5 mol % MMP, the following was observed: ^{1}H NMR (400 MHz, $CDCl_3$): δ 0.70–0.90 (br s, —$CH_2C(CO)(CH_3)$—, syndiotactic), 0.93–1.08 (br s, —$CH_2C(CO)(CH_3)$—, atactic), 1.08–1.12 (br, —$CH_2C(CO)(CH_3)$—, isotactic), 1.15–1.28 (br, $NC(CH_3)_2CCH_2$—), 1.32–1.51 (br, $NC(CH_3)_2CCH_2$—), 1.84 (s, $NCC(CH_3)_2$—), 1.70–2.20 (br, —$CH_2C(CO)(CH_3)$—), 2.48–2.60 (m, —$(CO)CH_2CH_2S$—), 2.64–2.76 (m, —$(CO)CH_2CH_2S$—), 3.47–3.73 (br s, —$COOCH_3$); SEC (THF; MALLS): M_n = 6,700 g/mol; PDI= 1.2; T_g = 97 °C.

Homopolymerization

Dendronized methacrylate macromonomer, **MIII**, was polymerized in the presence of MMP (0–10 mol %) in an effort to achieve a series of homopolymers of varying molecular weight. The synthetic procedure was similar to that previously described (3.4.1).

A stock solution (5.8 mg/mL) of AIBN in MeCN was prepared. In a typical reaction, **MIII** (0.813 g, 1.40 mmol) was weighed in a round-bottom flask, which was capped with a septum and purged with argon. To the reaction flask, MeCN (0.60 mL), AIBN solution (0.40 mL), and MMP (0.015 mL, 0.14 mmol) were added via syringe. The solution was stirred at ~70 °C for 18 h. The reaction solution was concentrated to give a flaky, off-white solid. The solid

was dissolved in minimal CH_2Cl_2 and precipitated (3×) in chilled hexanes (100-fold). The precipitate was collected in a fritted funnel and dried under vacuum at 45 °C to give a white powder (0.369 g): ^{1}H NMR (400 MHz, $CDCl_3$): δ 0.68–1.16 (br, —$CH_2C(CO)(CH_3)$—), 1.26–1.48 (br, —$COOC(CH_3)_3$), 1.58–2.06 (br, —$C[CH_2CH_2COO—]_3$ and —$CH_2C(CO)(CH_3)$—), 2.06–2.33 (br s, —$C[CH_2CH_2COO—]_3$), 2.47–2.59 (m, —$(CO)CH_2CH_2S$—), 2.60–2.76 (m, —$(CO)CH_2CH_2S$—), 2.79–3.01 (br, —$N(CO)(CH_3)$—), 3.31–3.56 (br, —$OCH_2CH_2N(CH_3)$—), 3.58–3.68 (s, $CH_3O(CO)CH_2CH_2S$—), 3.82–4.21 (br s, —$OCH_2CH_2N(CH_3)$—), 4.74–5.01 (br, —$CH_2N(CH_3)(CO)N(H)$—); T_g: 55 °C; $T_{5\%}$ in air: 212 °C.

Molecular weight characterization via SEC was attempted on three different instruments with various detectors (refractive index, viscosity, and MALLS) in multiple solvents ($CHCl_3$, THF, NMP/LiBr); analysis via MALDI-TOF was also attempted.

For each polymer in the series, the recovered filtrate was concentrated and dried under vacuum to give a yellow, viscous liquid, which was weighed and analyzed. The ^{1}H NMR spectrum revealed signals attributed to monomer, solvent, and thiol; however, broad signals attributed to polymer were also observed. A greater percentage of the total mass (filtrate concentrate plus precipitate) collected was recovered as polymer in the absence of MMP. For polymer reactions without MMP, ~60–90% of the total mass collected was polymer; however, for reactions with 10 mol% MMP, only ~45–70 % of the total mass collected was polymer.

Copolymerization

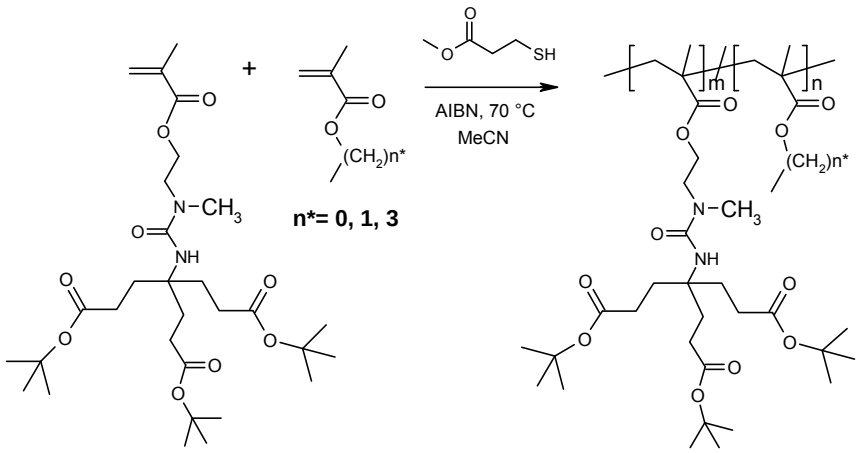

MIII (5b)

Methyl 3-mercaptopropionate (MMP) (10 mol%) was also employed to achieve low molecular weight dendronized copolymers. MMA (n*= 0), ethyl methacrylate (EMA) (n*= 1), and *n*-butyl methacrylate (BMA) (n*= 3) were copolymerized, respectively, with **MIII** (5, 10, 25 mol %).

In a typical copolymerization with MMA, **MIII** (0.830 g, 1.42 mmol) was weighed in a round-bottom flask, which was capped with a copper-wired septum and purged with argon. A stock solution (21 mg/ mL) of AIBN in MeCN was prepared. To the reaction flask, MMA (1.4 mL, 13 mmol), MeCN (20 mL), AIBN solution (1.2 mL, 0.15 mmol), and MMP (0.16 mL, 1.5 mmol) were added via syringe. The solution was stirred at ~70 °C for 18 h. The reaction solution was concentrated to give a flaky, off-white solid, which was dried under vacuum overnight (1.59 g, material lost in transfer). The solid was dissolved in minimal CH_2Cl_2 and precipitated in chilled hexanes (~600 mL). The hexanes was decanted and the dissolution/precipitation cycle was repeated twice. Lastly, the precipitate was collected via vacuum filtration in a fritted funnel. The resulting white solid was dried under vacuum at 45 °C

(0.809 g). The solid proved difficult to transfer because it adhered to the glass funnel (static electricity?), which resulted in decreased mass recovery. ^{1}H NMR (400 MHz, $CDCl_3$) δ: 0.67–0.92 (br s, —$CH_2C(CO)(CH_3)$—, syndiotactic), 0.92–1.08 (br s, —$CH_2C(CO)(CH_3)$—, atactic), 1.08–1.13 (br, —$CH_2C(CO)(CH_3)$—, isotactic), 1.16–1.31 (br, —$CH_2C(CO)(CH_3)$—), 1.31–1.54 (br s, —$COOC(CH_3)_3$), 1.71–2.08 (br, —$NHC[CH_2CH_2COO—]_3$ and —$CH_2C(CO)(CH_3)$—), 2.09–2.29 (br, —$NHC[CH_2CH_2COO—]_3$), 2.47–2.61 (m, —$(CO)CH_2CH_2S$—), 2.64–2.77 (m, —$(CO)CH_2CH_2S$—), 2.83–2.99 (br s, —$OCH_2CH_2N(CO)(CH_3)$—), 3.32–3.51 (br s, —$OCH_2CH_2N(CH_3)$—), 3.51–3.74 (br, —$CH_2C(CH_3)(COOCH_3)$— and $CH_3O(CO)CH_2CH_2S$—), 3.93–4.16 (br, —$OCH_2CH_2N(CH_3)$—), 4.85–5.02 (br, —$CH_2N(CH_3)(CO)NH$—).

From ^{1}H NMR, the copolymer composition was estimated by the ratio of signals at 2.83–2.99 δ and 3.51–3.74 δ.

Similar procedures were employed for the copolymerization of EMA and BMA with **MIII**.

For the **MIII**/EMA copolymer series, ^{1}H NMR (400 MHz, $CDCl_3$) δ: 0.76–0.93 (br s, —$CH_2C(CO)(CH_3)$—, syndiotactic), 0.93–1.08 (br s, —$CH_2C(CO)(CH_3)$—, atactic), 1.08–1.12 (br, —$CH_2C(CO)(CH_3)$—, isotactic), 1.16–1.30 (br s, —$COOCH_2CH_3$), 1.33–1.48 (br s, —$COOC(CH_3)_3$), 1.64–2.07 (br, —$NHC[CH_2CH_2COO—]_3$ and —$CH_2C(CO)(CH_3)$—), 2.08–2.25 (br m, —$NHC[CH_2CH_2COO—]_3$), 2.48–2.59 (m, —$(CO)CH_2CH_2S$—), 2.63–2.76 (m, —$(CO)CH_2CH_2S$—), 2.84–2.97 (br s, —$OCH_2CH_2N(CH_3)(CO)$—), 3.36–3.53 (br s, —$OCH_2CH_2N(CH_3)$—), 3.65 (s, $CH_3O(CO)CH_2CH_2S$—), 3.91–4.16 (br s, —$COOCH_2CH_3$)— and —$OCH_2CH_2N(CH_3)$—), 4.83–4.99 (br, —$CH_2N(CH_3)(CO)NH$—).

From ^{1}H NMR, the copolymer composition was estimated by the ratio of signals at 2.84–2.97 δ and 1.16–1.30 δ.

In the case of the **MIII**/nBMA series, copolymers with 5, 10, 25, and 70 mol% **MIII** were targeted. Due to increased hydrophobicity, purification via precipitation of CH_2Cl_2 in cold hexanes was not feasible. At low **MIII** content, the crude copolymer was soluble in hexanes. For copolymers prepared with 5 or 10 mol% **MIII,** the reaction solution was concentrated and dried under vacuum. The resulting hazy, colorless viscous liquid was dissolved in minimal THF, and the solution was added drop-wise to rapidly stirring, chilled MeOH/H_2O (60:40) (100-fold). The resulting tacky, white precipitate was removed from solution with a spatula and chilled in a -20 °C freezer overnight. The precipitate was dissolved in Et_2O or THF; the solution was concentrated to give a clear, colorless gel, which was dried under vacuum. The precipitation process was repeated twice; the resulting tacky solid was dried under vacuum at room temperature. The result was clear, colorless coating on the round bottom flask that when scraped with a spatula produced a white, tacky solid which was freeze-dried overnight. The result was a clear, colorless coating that when scraped with a spatula produced a white solid; the solid was significantly less tacky.

For the **MIII**/nBMA copolymer with 25 mol% **MIII**, the reaction solution was concentrated and dried under vacuum to give a hazy, colorless viscous liquid. Purification was achieved via hexane extraction alone; the crude polymer was stirred in hexanes (300-400 mL) at room temperature overnight. After the first extraction, a tacky white solid resulted; multiple extractions, typically three, were required to completely remove residual monomer (as determined by ^{1}H NMR). After the final extraction, the hexanes was decanted and the solid was dried under vacuum to give a white, flaky solid.

Purification via precipitation of CH_2Cl_2 in cold hexanes proved a successful means of purifying the **MIII**/nBMA copolymer with 70 mol % **MIII**, a white flaky solid resulted. ^{1}H

NMR (400 MHz, $CDCl_3$) δ: 0.68–1.10 (br, —$CH_2C(CO)(CH_3)$— and —$COOCH_2CH_2CH_2CH_3$), 1.24–1.44 (br, —$COOC(CH_3)_3$ and —$COOCH_2CH_2CH_2CH_3$) , 1.47–1.60 (br s, —$COOCH_2CH_2CH_2CH_3$) 1.65–1.99 (br, —$NHC[CH_2CH_2COO—]_3$ and —$CH_2C(CO)(CH_3)$—), 2.06–2.21 (br m, —$NHC[CH_2CH_2COO—]_3$), 2.42–2.52 (m, —$(CO)CH_2CH_2S$—), 2.57–2.70 (m, —$(CO)CH_2CH_2S$—), 2.77–2.93 (br s, —$OCH_2CH_2N(CO)(CH_3)$—), 3.29–3.52 (br s, —$OCH_2CH_2N(CH_3)$—), 3.60 (s, $CH_3O(CO)CH_2CH_2S$—), 3.76–4.10 (br, —$COOCH_2CH_2CH_2CH_3$ and —$OCH_2CH_2N(CH_3)$—), 4.76–4.95 (br, —$CH_2N(CH_3)(CO)NH$—).

From ^{1}H NMR, the copolymer composition was estimated by the ratio of signals at 2.77–2.93 δ and 1.47–1.60 δ.

A series of copolymers was prepared with **MI** (5, 10, 25 mol% **MI**) and MMA; the procedure used was similar to that employed for the **MIII**/MMA copolymer series. For the **MI**/MMA copolymer, ^{1}H NMR (400 MHz, $CDCl_3$) δ: 0.70–0.93 (br s, —$CH_2C(CO)(CH_3)$—, syndiotactic), 0.93–1.11 (br s, —$CH_2C(CO)(CH_3)$—, atactic), 1.11–1.19 (br, —$CH_2C(CO)(CH_3)$—, isotactic), 1.19–1.32 (br, —$CH_2C(CO)(CH_3)$—), 1.35–1.54 (br s, —$COOC(CH_3)_3$), 1.67–2.11 (br, —$NHC[CH_2CH_2COO—]_3$ and —$CH_2C(CO)(CH_3)$—), 2.11–2.29 (br, —$NHC[CH_2CH_2COO—]_3$), 2.43–2.66 (m, —$(CO)CH_2CH_2S$—), 2.66–2.88 (m, —$(CO)CH_2CH_2S$—), 3.25–3.52 (br , —$OCH_2CH_2N(H)$—), 3.52–3.76 (br, —$CH_2C(CH_3)(COOCH_3)$— and $CH_3O(CO)CH_2CH_2S$—), 3.87–4.17 (br, —$OCH_2CH_2N(H)$—), 4.74–5.04 (br, —$CH_2N(H)(CO)NH$—), 5.07–5.38 (br, —$CH_2N(H)(CO)NH$—) .

The copolymer composition was determined from ^{1}H NMR from the ratio of the signals at 3.25–3.52 δ and 3.52–3.76 δ.

A series of polymers was prepared with *tert*-butyl methacrylate (*t*BMA, 10, 25, 50, 100 mol% *t*BMA) and MMA; the synthesis and purification used was similar to that employed for

the **MIII**/MMA copolymer series. For the *t*BMA/MMA copolymer with 10 mol% *t*BMA, ^{1}H NMR (400 MHz, $CDCl_3$) δ: 0.72–1.19 (br s, —$CH_2C(CO)(CH_3)$—), 1.19–1.33 (br, —$CH_2C(CO)(CH_3)$—), 1.35–1.50 (br s, —$COOC(CH_3)_3$), 1.66 (br s, $NCC(CH_3)_2$—), 1.75–2.21 (br, —$CH_2C(CO)(CH_3)$—), 2.50–2.61 (m, —$(CO)CH_2CH_2S$—), 2.68–2.79 (m, —$(CO)CH_2CH_2S$—), 3.52–3.75 (br,—$COOCH_3$ and $CH_3O(CO)CH_2CH_2S$—). SEC (THF, MALLS): Mn = 2,300 g/mol; PDI= 1.2

The copolymer composition was determined from ^{1}H NMR from the ratio of the signals at 1.35–1.50δ and 3.52–3.75 δ.

3.4.4 Acidolysis

In a typical reaction, **MIII** (0.119 g, 0.203 mmol) was dissolved in neat TFA (Alfa Aesar, 99.5+%) (1 mL; 14 mmol) to achieve a clear, pale yellow solution and stirred at rt for 1 h. The solution was diluted with CH_2Cl_2 and concentrated (~40 °C) to give a yellow, viscous liquid; the dilution/concentration procedure was repeated (typically 3 or 4 times) until an off-white/yellow solid was obtained and the odor of TFA was no longer detectable. The solid was stirred in Et_2O for 2 h; the solvent was decanted leaving an off-white/white solid. Et_2O was added to the white solid; the suspension was placed on a rotary evaporator to remove the Et_2O (3×). Finally, CH_2Cl_2 was added to the white solid and removed by rotary evaporation to give a white solid, which was dried under vacuum at 50 °C (0.0786 g). The deprotected macromonomer will be denoted as **MIII**(OH), ^{1}H NMR (400 MHz, CD_3OD/ $CDCl_3$) δ: 1.88 (m, 3H), 1.98 (m, 6H), 2.24 (m, 6H), 2.86 (s, 3H), 3.48 (t, 2H), 4.18 (t, 2H), 4.54–4.81 (br s, —$CH_2N(CH_3)(CO)NH$—, —$COOH$, and CD_3OH), 5.56 (m, 1H), 6.07 (m, 1H). Note: Sample was dissolved in CD_3OD to give a cloudy solution; $CDCl_3$ was added drop-wise until clear.

In ^{1}H NMR, the disappearance of the large singlet at 1.43 δ , attributed to the *tert*-butyl ester groups, served as evidence of successful deprotection.

Acidolysis was performed on the dendronized homo- and copolymers in a similar fashion. Upon increasing the reaction scale to > 0.2 grams, CH_2Cl_2 was employed as a diluent to achieve homogeneous solutions.

For the dendronized **MIII**(OH) homopolymer (prepared with 10 mol% CTA), ^{1}H NMR (400 MHz, $CD_3OD/CDCl_3$): δ 0.69–1.40 (br, —$CH_2C(CO)(CH_3)$—), 1.44 (br s, $NC(CH_3)_2CCH_2$), 1.76–2.21 (br, —$C[CH_2CH_2COO—]_3$ and —$CH_2C(CO)(CH_3)$—), 2.21–2.49 (br, —$C[CH_2CH_2COO—]_3$), 2.52–2.65 (m, —$(CO)CH_2CH_2S$—), 2.68–2.79 (m, —$(CO)CH_2CH_2S$—), 2.91–3.07 (br s, —$N(CO)(CH_3)$—), 3.38–3.73 (br, —$OCH_2CH_2N(CH_3)$— and $CH_3O(CO)CH_2CH_2S$—), 3.92–4.20 (br, —$OCH_2CH_2N(CH_3)$—), 4.72–5.10 (br, —$CH_2N(CH_3)(CO)N(H)$—, —COOH , and CD_3OH).

Acidolysis of the dendronized copolymers (prepared with 10 mol% CTA) resulted in the following spectra:

For the **MIII**(OH)/MMA series, ^{1}H NMR (400 MHz, $CD_3OD/CDCl_3$) δ: 0.60–0.93 (br s, —$CH_2C(CO)(CH_3)$—, syndiotactic), 0.93–1.15 (br s, —$CH_2C(CO)(CH_3)$—, atactic), 1.15–1.29 (br s, —$CH_2C(CO)(CH_3)$—, isotactic), 1.39–1.59 (br, —$CH_2C(CO)(CH_3)$—), 1.71–2.19 (br, —$NHC[CH_2CH_2COO—]_3$ and —$CH_2C(CO)(CH_3)$—), 2.21–2.43 (br, —$NHC[CH_2CH_2COO—]_3$), 2.52–2.64 (m, —$(CO)CH_2CH_2S$—), 2.65–2.77 (m, —$(CO)CH_2CH_2S$—), 2.90–3.07 (br s, —$OCH_2CH_2N(CO)(CH_3)$—), 3.37–3.75 (br s, —$OCH_2CH_2N(CH_3)$—, —$CH_2C(CH_3)(COOCH_3)$— , and $CH_3O(CO)CH_2CH_2S$—), 3.91–4.13 (br, —$OCH_2CH_2N(CH_3)$—), 4.68–5.01 (br, —$CH_2N(CH_3)(CO)NH$—, —COOH, and CD_3OH).

From ^{1}H NMR, the copolymer composition was estimated by the ratio of signals at 2.90–3.07 δ and 3.37–3.75 δ. Due to an overlap of the signals (3.37–3.75 δ), 2.00 was subtracted from the integration of the range to obtain the integral value for the methoxy protons of the MMA comonomer.

For the **MIII**(OH)/EMA dendronized copolymers (prepared with 10 mol% CTA), ^{1}H NMR (400 MHz, $CD_3OD/CDCl_3$) δ: 0.76–0.93 (br s, —$CH_2C(CO)(CH_3)$—, syndiotactic), 0.93–1.16 (br s, —$CH_2C(CO)(CH_3)$—, atactic), 1.20–1.37 (br, —$COOCH_2CH_3$), 1.77–2.21 (br, —$NHC[CH_2CH_2COO—]_3$ and —$CH_2C(CO)(CH_3)$—), 2.24–2.44 (br, —$NHC[CH_2CH_2COO—]_3$), 2.54–2.66 (m, —$(CO)CH_2CH_2S$—), 2.67–2.80 (m, —$(CO)CH_2CH_2S$—), 2.93–3.06 (br s, —$OCH_2CH_2N(CH_3)(CO)$—), 3.45–3.66 (br, —$OCH_2CH_2N(CH_3)$—), 3.69 (s, $CH_3O(CO)CH_2CH_2S$—), 3.94–4.19 (br, —$COOCH_2CH_3$— and —$OCH_2CH_2N(CH_3)$—), 4.67–4.97 (br, —$CH_2N(CH_3)(CO)NH$—, —COOH, and CD_3OH).

From ^{1}H NMR, the copolymer composition was estimated by the ratio of signals at 2.93–3.06 δ and 1.20–1.37 δ.

For the **MIII**(OH)/nBMA dendronized copolymers (prepared with 10 mol% CTA), ^{1}H NMR (400 MHz, $CD_3OD/CDCl_3$) δ: 0.68–1.13 (br, —$CH_2C(CO)(CH_3)$— and —$COOCH_2CH_2CH_2CH_3$), 1.17–1.30 (br, —$CH_2C(CO)(CH_3)$—), 1.30–1.49 (br, —$COOCH_2CH_2CH_2CH_3$) , 1.52–1.69 (br, —$COOCH_2CH_2CH_2CH_3$) 1.72–2.14 (br, —$NHC[CH_2CH_2COO—]_3$ and —$CH_2C(CO)(CH_3)$—), 2.18–2.37 (br, —$NHC[CH_2CH_2COO—]_3$), 2.50–2.61 (m, —$(CO)CH_2CH_2S$—), 2.64–2.75 (m, —$(CO)CH_2CH_2S$—), 2.86–3.02 (br s, —$OCH_2CH_2N(CO)(CH_3)$—), 3.38–3.60 (br, —$OCH_2CH_2N(CH_3)$—), 3.64 (s, $CH_3O(CO)CH_2CH_2S$—), 3.83–4.15 (br, —$COOCH_2CH_2CH_2CH_3$ and —$OCH_2CH_2N(CH_3)$—), 4.63–4.96 (br, —$CH_2N(CH_3)(CO)NH$—, —COOH , and CD_3OH).

From ^{1}H NMR, the copolymer composition was estimated by the ratio of signals at 2.86–3.02 δ and 1.52–1.69 δ.

For the **MI**(OH)/MMA series (prepared with 10 mol% CTA), ^{1}H NMR (400 MHz, $CDCl_3$) δ: 0.55–0.77 (br s, —$CH_2C(CO)(CH_3)$—, syndiotactic), 0.77–0.99 (br s, —$CH_2C(CO)(CH_3)$—, atactic), 1.00–1.13 (br, —$CH_2C(CO)(CH_3)$—, isotactic), 1.18–1.40 (br, —$CH_2C(CO)(CH_3)$—), 1.53–1.98 (br, —NHC[CH_2CH_2COO—]$_3$ and —$CH_2C(CO)(CH_3)$—), 2.03–2.44 (br, —NHC[CH_2CH_2COO—]$_3$), 2.34–2.47 (m, —(CO)CH_2CH_2S—), 2.47–2.66 (m, —(CO)CH_2CH_2S—), 3.34–3.65 (br, —OCH_2CH_2N(H)— ,—$CH_2C(CH_3)(COOCH_3)$—, and CH_3O(CO)CH_2CH_2S—), 3.71–3.90 (br, —OCH_2CH_2N(H)—), 3.90–4.34 (br, —CH_2N(*H*)(CO)N*H*—,—COO*H* , and CD_3OH) .

The ***t*BMA**/MMA copolymer series was deprotected to give methacrylic acid/MMA (**MA**/MMA) copolymers. ^{1}H NMR (400 MHz, $CD_3OD/CDCl_3$) δ: 0.68–1.33 (br s, —$CH_2C(CO)(CH_3)$—), 1.39–1.59 (br, —$CH_2C(CO)(CH_3)$—), 1.75–2.20 (br, —$CH_2C(CO)(CH_3)$—), 2.51–2.65 (m, —(CO)CH_2CH_2S—), 2.65–2.84 (m, —(CO)CH_2CH_2S—), 3.50–3.73 (br,—$COOCH_3$ and CH_3O(CO)CH_2CH_2S—).

3.4.5 Solubility

The solubilities of the macromonomers and the dendronized homo- and copolymers were investigated.

The solubilities of the **MIII** macromonomer and a **MIII**/MMA (10 mol% **MIII**) copolymer were investigated in hexanes, MeOH, DI H_2O, and Et_2O. In a 20-mL vial, solvent (2 mL) was added to the sample (20 mg), and the solubility was determined visually. The **MIII** macromonomer was insoluble in hexanes—a clear solution with insoluble particulates was observed. The **MIII**/MMA (10 mol% **MIII**) copolymer demonstrated partial solubility in

hexanes—a cloudy solution and insoluble particulates were observed. In MeOH, a clear, homogeneous solution was observed for the **MIII**/MMA (10 mol% **MIII**) copolymer. **MIII** dissolved in MeOH; however, the solution was slightly cloudy. In DI H_2O, the copolymer yielded a slightly turbid solution with insoluble particulates floating on the liquid surface; **MIII** was also insoluble, yielding a clear solution with insoluble particulates adhered to the walls of the vial. Both **MIII** and **MIII**/MMA (10 mol% **MIII**) were soluble in Et_2O; clear, homogeneous solutions were observed.

MIII (0.024 g) was dissolved in EtOH (1 mL, ~ 3 wt% **MIII**); a clear, homogeneous solution was obtained.

MI was dissolved in THF (10 wt %), and a clear, homogeneous solution was observed.

MI and **MIII** were observed to be slightly water soluble based on the initial work-up procedure for the acidolysis reaction, which included a DI H_2O wash.

The *n*BMA copolymer series demonstrated increased solubility in hexanes at low **MIII** composition (5 and 10 mol %). Solubilities of **MIII**/nBMA copolymers with 5 and 10 mol% **MIII** were investigated in various solvents in an effort to identify a non-solvent for purification. The crude product (~1.5 g) was stirred in solvent (~100–150 mL) at rt; solubility was observed to give the following results: cyclohexane (soluble), hexanes (soluble), heptane (partially soluble), toluene (mostly soluble, some particulates), petroleum ether (soluble), *i*-PrOH (soluble), EtOH (soluble), MeOH (soluble), and DI H_2O (insoluble). As a result of this study, a mixed solvent system (MeOH/H_2O) was investigated for use in purification via precipitation.

The **MIII**/*n*BMA copolymers were moderately soluble in several polar organic solvents: CH_2Cl_2, $CHCl_3$, EtAc, MeCN, and THF. Precedence suggested the use of THF as the solvent for purification. **MIII**/*n*BMA (10 mol% **MIII**) was dissolved in minimal THF and added drop-wise

to a rapidly stirring mixture of MeOH and DI H_2O (80/20). A milky, white emulsion resulted; the emulsion was chilled (-20 °C) overnight. After chilling, the emulsion remained and a precipitate was not observed. DI H_2O (25–40 mL aliquots) was added to the emulsion until the solution became transparent and a tacky, a white precipitate was observed at 60/40 MeOH/H_2O. (The stir bar was rendered immobile.)

In the case of the **MIII**/*n*BMA copolymer with 25 mol % **MIII**, the crude material (~ 1.5 g), a pale yellow, viscous liquid, was stirred in an excess of hexanes (~250 mL) to achieve a white solid. **MIII**/*n*BMA copolymers with > 25 mol % **MIII**, for example 50 and 70 mol% **MIII**, were not soluble in hexanes; in this case, the precipitation of CH_2Cl_2 solutions in chilled hexanes was successful.

In preparation for biological testing, solubility in a biologically compatible media was investigated. Aqueous solubility of **MIII**(OH) and several P**MIII**(OH) copolymers were investigated. The **MIII**(OH) macromonomer was soluble at 6.0 mg/mL in DI H_2O, clear and homogeneous solutions were observed. Aqueous solubility at 7.0 mg/mL was investigated for dendronized homopolymers P**MIII**$(OH)_0$ and P**MIII**$(OH)_{10}$, prepared with 0 and 10 mol% MMP, respectively; both polymers were insoluble.

Solubility in 5 w/v % aqueous triethanolamine (aq TEA) was investigated for the deprotected macromonomers and dendronized polymers. For each acid, a sample (25.0 mg) was weighed in a vial, and aq TEA (2 mL) was added to a final concentration of 12.5 mg/mL. The samples were vortexed and sonicated; solubility was observed to give the following results (in cases of insolubility, sonication was repeated in 30 min increments for up to 2 h): **MI**(OH), the acid-functional **MI** macromonomer, and the **MI**(OH)/MMA copolymer series, (5, 10, and 25 mol % **MI**) were all soluble in aq TEA. **MIII**(OH), the acid-functional **MIII** macromonomer,

yielded a slightly turbid solution; however, clear, homogeneous solutions were observed for the **MIII**(OH)/MMA copolymer series (5, 10, and 25 mol % **MIII**). For the **MIII**(OH)/EMA series, the copolymer with 5 mol % **MIII** produced a turbid solution; however, the EMA copolymers with 10 and 25 mol % **MIII** produced clear, homogeneous solutions. **MIII**(OH)/nBMA copolymers (25 and 70 mol% **MIII**) produced turbid solutions in aq TEA at 12.5 mg/mL; diluting the solutions with aq TEA to 2.1 mg/mL did not seem to lessen the turbidity.

Due to the limited solubility demonstrated in DI H_2O and aq TEA, an alternate solvent was investigated for biological testing. The solubility of a **MIII**(OH) homopolymer (prepared in the absence of CTA) was investigated in dimethylsulfoxide/H_2O , v/v, 1/10 (aq DMSO). The polymer sample (11.1 mg) was weighed in a vial, and aq DMSO (1 mL) was added; a film formed on the liquid surface. Additional aq DMSO (1 mL) was added; the polymer remained insoluble. To this solution, pure DMSO was added in 0.1 mL increments. With the first addition (0.1 mL), the polymer aggregated into a sphere and sank to the bottom of the vial. Multiple DMSO additions were made (up to 1.9 mL total); the polymer remained an insoluble, aggregated sphere.

A second **MIII**(OH) homopolymer sample (prepared in the absence of CTA) (12.0 mg) was weighed in a vial; DMSO (1.0 mL) was added to the sample and highly viscous solution resulted. With additional DMSO (0.5 mL), the viscosity decreased.

After two months under ambient conditions, the solutions were re-evaluated. In the case of the aq DMSO solution, the insoluble, aggregated sphere was no longer observed; however, a clear, colorless solution was observed; in addition, the walls of the vial above the solution were coated with a clear, insoluble material. The same observation was made for the solution prepared with pure DMSO.

The solubilities of **MI**(OH), **MIII**(OH), P**MIII**(OH) (**MIII** homopolymer prepared with 10 mol% MMP), the **MIII**(OH)/MMA copolymer series (5, 10, 25 mol% **MIII**), and a **MIII**(OH)/*n*BMA copolymer (25 mol % **MIII**) in aq DMSO were investigated in aq DMSO. The sample was weighed in a vial, aq DMSO (1 mL) was added via syringe, and the solution was agitated by hand. The macromonomers, **MI**(OH) (10.5 mg) and **MIII**(OH) (11.5 mg), exhibited partial solubility; clear solutions with a few free-flowing, insoluble particulates were observed. Clear, homogeneous solutions were achieved with the addition of aq DMSO (1 mL) and stirring. A slightly turbid solution with 'wet' solid particulates adhered to the vial walls was observed for the homopolymer sample, P**MIII**(OH) (12.7 mg). The **MIII**(OH)/MMA copolymer series (~ 12.5 mg samples) was insoluble; turbid solutions with insoluble particulates were observed. The solution prepared from the **MIII**(OH)/MMA copolymer with 5 mol % **MIII** appeared more turbid than the solutions prepared from copolymers with higher **MIII** content. The **MIII**(OH)/*n*BMA copolymer (25 mol % **MIII**) was also insoluble; a clear solution and insoluble aggregated clumps were observed.

To compare solubility in aq TEA, model copolymers, containing one acid group per repeat unit, were prepared. A copolymer series was prepared from *tert*-butyl methacrylate (***t*BMA**) and MMA (10, 25, and 50 mol% ***t*BMA**), and subsequently deprotected to achieve poly(methacrylic acid-co-methyl methacrylate) (**MAA**/MMA). A sample (25 mg) was weighed in a vial; aq TEA (2 mL) was added. The solutions were vortexed and sonicated (~20 min). The solution prepared from the **MAA**/MMA copolymer with 10 mol% **MAA** was completely insoluble—a clear solution with insoluble particulates was observed. The solution prepared from the copolymer with 25 mol% **MAA** appeared very hazy and insoluble particulates were observed. The solution

prepared from the copolymer with 50 mol% **MAA** was turbid but to a lesser extent compared to the 25/75 **MAA**/MMA solution; however, insoluble particulates were observed.

Solubility was also investigated in 0.05M PBS buffer solution prepared by Myra Williams in the laboratory of Dr. Joseph O. Falkinham, III of Biological Sciences at Virginia Tech. The solubilities of macromonomer **MIII**(OH), two P**MIII**(OH) homopolymer samples, two M**III**(OH)/MMA copolymer samples, and a poly(methacrylic acid) homopolymer P(**MAA**) were investigated. In each case, the sample was weighed in a vial, 0.05M PBS buffer solution was added via syringe, and the solution was agitated by hand. The macromonomer, **MIII**(OH) (7.9 mg in 0.5 mL 0.05M PBS), was soluble; a clear, homogeneous solution was observed. In 1 mL 0.05M PBS, slightly turbid solutions were observed for P**MIII**(OH) prepared with 0 mol% MMP (12.4 mg) and P**MIII**(OH) prepared with 1.0 mol% MMP (12.3 mg). The poly(methacrylic acid) homopolymer prepared in the presence of 10 mol% MMP, P(**MAA**), (7.0 mg in 0.5 mL 0.05M PBS) was soluble; a clear, homogeneous solution was observed. Two samples from the **MIII**(OH)/MMA copolymer series were investigated. The **MIII**(OH)/MMA (5 mol% **MIII**) copolymer (7.8 mg in 0.5 mL 0.05M PBS buffer solution) was partially soluble; a turbid solution with insoluble particulates was observed. The **MIII**(OH)/MMA (25 mol% **MIII**) copolymer (8.0 mg in 0.5 mL 0.05M PBS) was insoluble; a clear solution and insoluble particulates were observed.

3.5 Preliminary Biological Studies

3.5.1 Microbial strains, culture conditions, and preparation of inocula for susceptibility testing

Strains of *S. aureus* (ATCC 6538) and *Mycobacterium smegmatis* (ATCC 607) were obtained from the American Type Culture Collection. A methicillin-resistant isolate of *Staphylococcus aureus* (MRSA) was obtained from the Microbiology Laboratory, Danville Community Hospital (Virginia). Colonies of *S. aureus* and MRSA were grown on 1/10-strength Brain Heart Infusion Broth (BBL Microbiology Systems, Cockeysville, MD USA) containing 0.2% (w/v) sucrose (BHIB+S) and 1.5 % (w/v) agar. *Mycobacterium smegmatis* was grown on Middlebrook 7H10 agar (BBL Microbiology Systems). Streaked plates were incubated at 37 °C for 3 days. A single colony for each microbe was used to inoculate 5 mL of 1/10-strength BHIB+S (*S. aureus* and MRSA) and Middlebrook 7H9 broth (*M. smegmatis*) and incubated at 37 °C. After growth, the resulting broth cultures were diluted with buffered saline gelatin [BSG; gelatin (0.1 g/L), NaCl (8.5 g/L), KH_2PO_4 (0.3 g/L), Na_2HPO_4 (0.6 g/L)] to equal the turbidity of a no. 1 McFarland standard. To check for viability and contamination, broth cultures were streaked on plate count agar (BBL Microbiology Systems); the plates were incubated at 37 °C for 3–4 days.

3.5.2 Quality assurance

For the work reported here, all cultures and suspension used as inocula were uncontaminated and the colonies had the expected morphologies. All viable, uncontaminated inocula were stored up to 14 days at 4 °C until used, without any differences in susceptibility to antimicrobial compounds.

3.5.3 Measurement of Minimal Inhibition Concentration (MIC)

The minimal inhibition concentrations (MICs) of compounds dissolved in aqueous triethanolamine (aq TEA) were measured by broth microdilution in 96-well microtitre plates. Microtiter plates (96 wells: rows A–H, columns 1–12) were filled by the following protocol to give twofold serial dilutions of the drug of interest. Aliquots (50 μL) of 1/10-strength BHIB+S (pH 7.4) were placed in all wells except for those in column 1. An aliquot (100 μL) of a stock solution of the drug in triethanolamine (570 μg/mL) was placed in column 1. An aliquot (50 μL) was removed from well 1 and mixed with the 1/10-strength BHIB+S in the well 2. Then, an aliquot (50 μL) of this mixture was removed and mixed with BHIB+S in well 3. This process was repeated through well 11, at which point an aliquot (50 μL) was removed and discarded. For each row, well 12 was the positive growth control, BHIB+S only. An aliquot (50 μL) of the microbial inoculums (10^4 CFU/0.1 mL) was added to all wells of a given row. The concentration of the amphiphile ranged from 570 μg/mL (well 1) to 0.5 μg/mL (well 11). The plates were incubated at 37 °C for 4 d; MIC was determined by comparing the turbidity (due to growth of microbes) of each test well to the positive control wells (well 12). The MIC of each compound was measured in triplicate and defined as the lowest concentration of drug resulting in the absence of visible turbidity compared with the drug-free control. Aqueous triethanolamine was also tested for antimicrobial activity using the same protocol; no antimicrobial activity was found.

3.5.4 Hemolysis Assay

Sheep blood (Remel) was washed with phosphate buffer solution (0.05M + 0.85% salt) (PBS) three times to remove previously lysed cells; the blood was diluted with PBS (1:10) and

tempered at 37 °C for 30 min. Eight microfuge tubes were arranged in a series and 500 µL PBS was added to each tube. Five hundred microliters of the amphiphile of interest, dissolved in 5 w/v % aqueous triethanolamine (aq TEA) (570 µg/mL), were added to the first tube. A two-fold dilution was performed from tube 1 to tube 7; 500 µL were removed from tube 7 and discarded. Upon completion, each tube had a total volume of 500 µL. Tube 8 contained 500 µL PBS and served as a negative control. Triton X-100 (1 % in PBS), (*t*-Octylphenoxypolyethoxyethanol; Sigma), a nonionic surfactant, served as positive control; 5 w/v % aqueous triethanolamine (aq TEA) was also employed as a negative control. Five hundred microliters of washed sheep blood (10^{-1}) were added to each of the eight microfuge tubes; the tubes were incubated at 37 °C for 15 min. After 10 min of centrifugation at 5000 × g at room temperature, 100 µL were removed from each microfuge tube and transferred to a 96-well microtitre plate. Hemoglobin absorbance was measured at 540 nm in a Multiskan Ascent spectrophotometer, specific hemolysis was expressed as % total hemolysis at each concentration:

$$\frac{Absorbance\ sample\ supernatant - Absorbance\ PBS\ supernatant}{Absorbance\ detergent\ supernatant} \times 100$$

Chapter 4: Results and Discussion

4.1 Introduction

Polyanionic molecules are well-known potent *in vitro* inhibitors of HIV replication and show promise as effective microbicides.[29] However, the need for sufficient anionic character per molecule proves an important factor in the design of antiviral agents. To date, polyanionic antiviral agents have evolved from polysaccharides and their derivatives to conventional polymers to dendrimers.

The objective of this research was to synthesize a compound for formulation of a topical microbicide that could be used to curtail the rampant spread of HIV and other STDS and mucosal pathogens. Antimicrobial activity of a homologous series of dendritic amphiphiles, as triethanolammonium salts, with hydrophobic tail lengths of 12–22 carbons and tri-functional hydrophilic headgroups were investigated by Gandour et al.[30, 31] Here we propose, dendronized amphiphilic polymer analogues, which are expected to show enhanced anti-HIV activity compared to the small molecule dendritic amphiphiles given the significant increase in functionality imparted by the dendritic side chains.

Toward this goal, novel dendritic methacrylate macromonomers were synthesized: **MI** (**5a**) and **MIII** (**5b**) (**Section 4.2**), and subsequently polymerized via conventional free radical polymerization in acetonitrile employing AIBN as an initiator. To achieve a series of copolymers, the dendritic methacrylate macromonomer, **MIII**, was copolymerized with methyl methacrylate; a **MIII**/MMA copolymer series varied in **MIII** (0–100 mol%) was prepared. (**Section 4.3**)

To achieve low molecular weight copolymer analogues, **MIII** was copolymerized, in the presence of methyl 3-mercaptopropionate (MMP), with various alkyl methacrylates (methyl, ethyl, *n*-butyl); the copolymer composition was varied in **MIII** from 5 to 25 mol%. (**Section 4.4**)

Molecular weight characterization of these materials proved challenging. SEC analysis was performed in various solvent systems ($CHCl_3$, THF, and LiBR/NMP) employing various detectors (MALLS, RI, Viscometer, and Triple Detector). End-group analysis via ^1H NMR was employed in the case of the dendronized copolymers. (**Section 4.5**)

Deprotection of dendronized polymers via acidolysis with trifluoroacetic yielded polyelectrolytes. In the case of the copolymer series (5–25 mol% acid groups), ionomers were achieved. (**Section 4.6**)

Solubility of the deprotected dendronized polymers was investigated in biologically compatible media as means to assess their proposed use as biological agents. Aqueous solubility was assessed in aqueous triethanolamine (aq TEA) (5 w/v %) for the macromonomers, homopolymers, and a majority of the copolymers prepared. (**Section 4.7**)

The antimicrobial activities of the macromonomers and copolymers soluble in aq TEA were investigated against *M. smegmatis*, *S. aureus*, and MRSA. Lytic activity served as a measure of toxicity; hemolysis assays were performed with the acid-functional dendritic macromonomers and dendronized polymers. (**Section 4.8**)

Figure 18 depicts the general synthetic scheme toward amphiphilic dendronized copolymers.

4.2 Synthesis and Characterization of Novel Methacrylate Macromonomers

Dendronized polymers may be prepared by one of two synthetic methods: the 'coupling-to' approach or the macromonomer approach. In this study, the macromonomer approach was employed. Synthesis via the macromonomer approach involves the attachment of a polymerizable group to the focal point of a preformed dendron and polymerization of the resulting macromonomer. The advantages here lie in the guarantee of well-defined side chains and complete coverage—one dendron per repeat unit.

The synthesis of the novel dendritic methacrylate macromonomers involved several steps.

*4.2.1 Synthesis of Di-tert-butyl 4-(2-(tert-Butoxycarbonylethyl)-4-[3-(hydroxyethyl)ureido]heptanedioate (**3a**)*

Weisocyanate™ was prepared in a three-step synthesis according to literature procedure[30] and allowed to react with 2-aminoethanol in dry ether at room temperature to afford an alcohol derivative (**3a**) with an ureido linker. The rationale behind this step was two-fold: 1) the incorporation of a two–carbon spacer between the focal point and the dendron and 2) to achieve a reactive end-group for nucleophilic substitution.

Steric congestion of the polymerization site has been identified as the major disadvantage of the macromonomer approach in the synthesis of dendronized polymers; steric congestion decreases the rate of polymerization and results in low degrees of polymerization and in some cases no reaction.[137-139] The incorporation of a two-carbon spacer was a proactive measure in the synthetic design to avoid steric congestion of the polymerization site. Additionally, the hydroxyl

functionality allows for further reaction with methacryloyl chloride to achieve a dendritic methacrylate macromonomer.

Chemical composition and purity were confirmed via ^{1}H NMR, melting point, elemental analysis, FTIR, and X-ray crystallography. **Figure 19** depicts the ^{1}H NMR spectrum of **3a** in $CDCl_3$; the spectrum reveals sharp, well-resolved peaks. The characteristic differences in the splitting pattern of the protons of the linker afford facile identification. X-ray crystallography revealed two molecules per unit cell with different conformations about the hydroxyethyl linker (**Figure 20**). The appearance of two molecules per unit cell demonstrates the strong hydrogen bonding ability imparted by the ureido linker.

*4.2.2 Synthesis of Di-tert-butyl 4-(2-tert-Butoxycarbonyl-ethyl)-4-[3-(2-methacryoloxyethyl)ureido]heptandioate (**5a, MI**)*

In preparation of the dendritic macromonomer, **3a** was allowed to react with methacryloyl chloride in dichloromethane (-78 °C to rt); diisopropylethylamine was employed as an acid scavenger. Two major products were obtained as a result of this reaction: a mono-substituted product (**5a, MI**) and a di-substituted product (**MII**). Column chromatography on silica gel employing a gradient solvent system of hexanes and ethyl acetate proved successful in separating the two products. The desired product, **MI**, was recovered as 60% of the sample loaded onto the column; chemical composition and purity were confirmed via ^{1}H and ^{13}C NMR, melting point, FTIR, HRMS, and elemental analysis. The ^{1}H NMR spectra of **MI** and **MII** were distinctly different (**Figure 21**). However, in both spectra, the peak attributed to the hydroxyl proton of **3a** was not observed; its disappearance served as evidence of a successful reaction. In the spectrum of **MI**, the remaining peaks of the former alcohol precursor (**3a**) and new peaks attributed to the methacrylate vinyl (5.60 and 6.13 ppm) and α-methyl (1.95 ppm) protons were

observed. In the ^{1}H NMR spectrum of **MII**, the dimethacrylate, peaks attributed to a second set of α-methyl protons (1.89 ppm) and a second set of vinyl protons (5.14 and 5.24 ppm) were observed. As a result of the increased electronegativity imparted by the additional carbonyl group of **MII**, the methylene protons in the spacer (closest to the linker) and the lone remaining ureido proton shifted downfield from 3.43 to 4.00 ppm and 4.80 to 8.85 ppm, respectively. A change in the splitting of the peak attributed to methylene protons was also observed. In the ^{1}H NMR spectrum of **MI**, the methylene protons at 3.43 ppm were split by both the ureido proton and the adjacent methylene protons and, therefore, appeared as a quartet. In the ^{1}H NMR spectrum of **MII**, the peak attributed to the same methylene protons (4.00 ppm) was split by the adjacent methylene protons alone and, as a result, appeared as a triplet. The **MII** macromonomer was successfully isolated and characterized via ^{1}H NMR; however, it had a tendency to cross-link under ambient conditions and was not further characterized. The formation of two products from the reaction of **3a** and methacryloyl chloride resulted in the need for tedious purification and decreased yield of the desired product (**MI**).

In an effort to increase the yield of the macromonomer reaction, methyl 2-aminoethanol was employed in the synthesis of the alcohol precursor. By blocking the secondary position, the di-substituted product obtained in the reaction of **3a** with methacryloyl chloride could be avoided.

*4.2.3 Synthesis of Di-tert-butyl 4-(2-tert-Butoxycarbonylethyl)-4-[3-(2-hydroxyethyl)-3-methylureido]heptanedioate (**3b**)*

Methyl 2-aminoethanol and Weisocyanate™ were stirred in dry ether at room temperature to produce the *N*-methyl alcohol derivative, **3b**. Chemical composition and purity were confirmed via ^{1}H NMR, melting point, elemental analysis, FTIR, and X-ray

crystallography. The ^{1}H NMR spectrum for **3b** is depicted in **Figure 22**. The major differences between the ^{1}H NMR spectra of **3a** and **3b** were the absence of the peak attributed to one of the ureido protons (4.98 ppm), a slight shift in the peak attributed to the remaining ureido proton, and a new peak attributed to the *N*-methyl substituent (2.98 ppm). The crystal structure of **3b** (**Figure 23**) revealed a single molecule, indicating a loss of the strong hydrogen bonding observed for **3a**, with a single conformation about the hydroxyethyl linker.

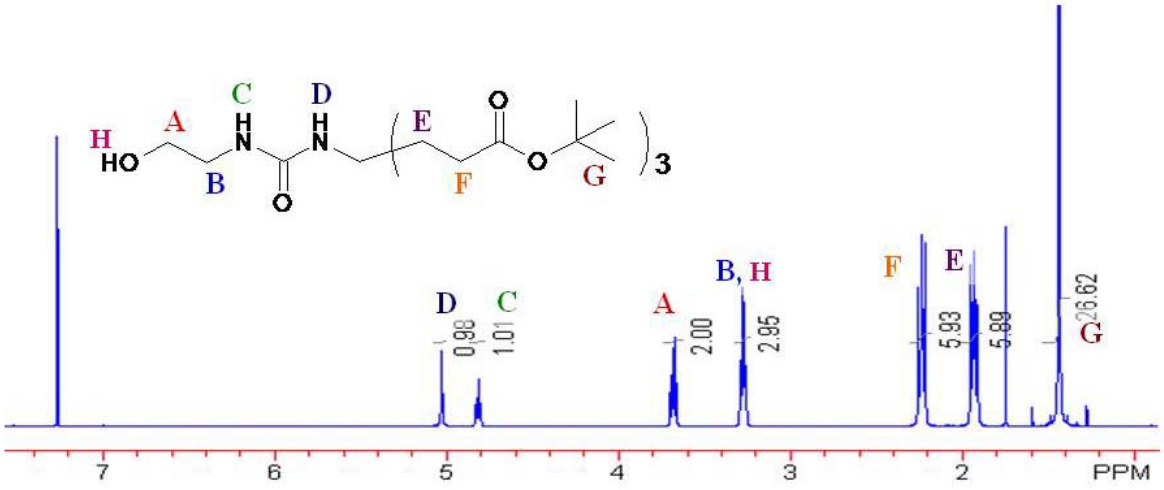

Figure 19. ^{1}H NMR ($CDCl_3$) of alcohol derivative 3a.

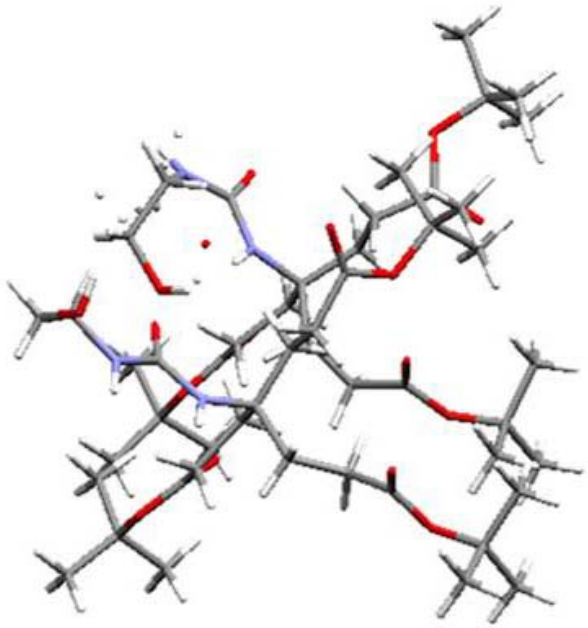

Figure 20. X-ray crystal structure of 3a.

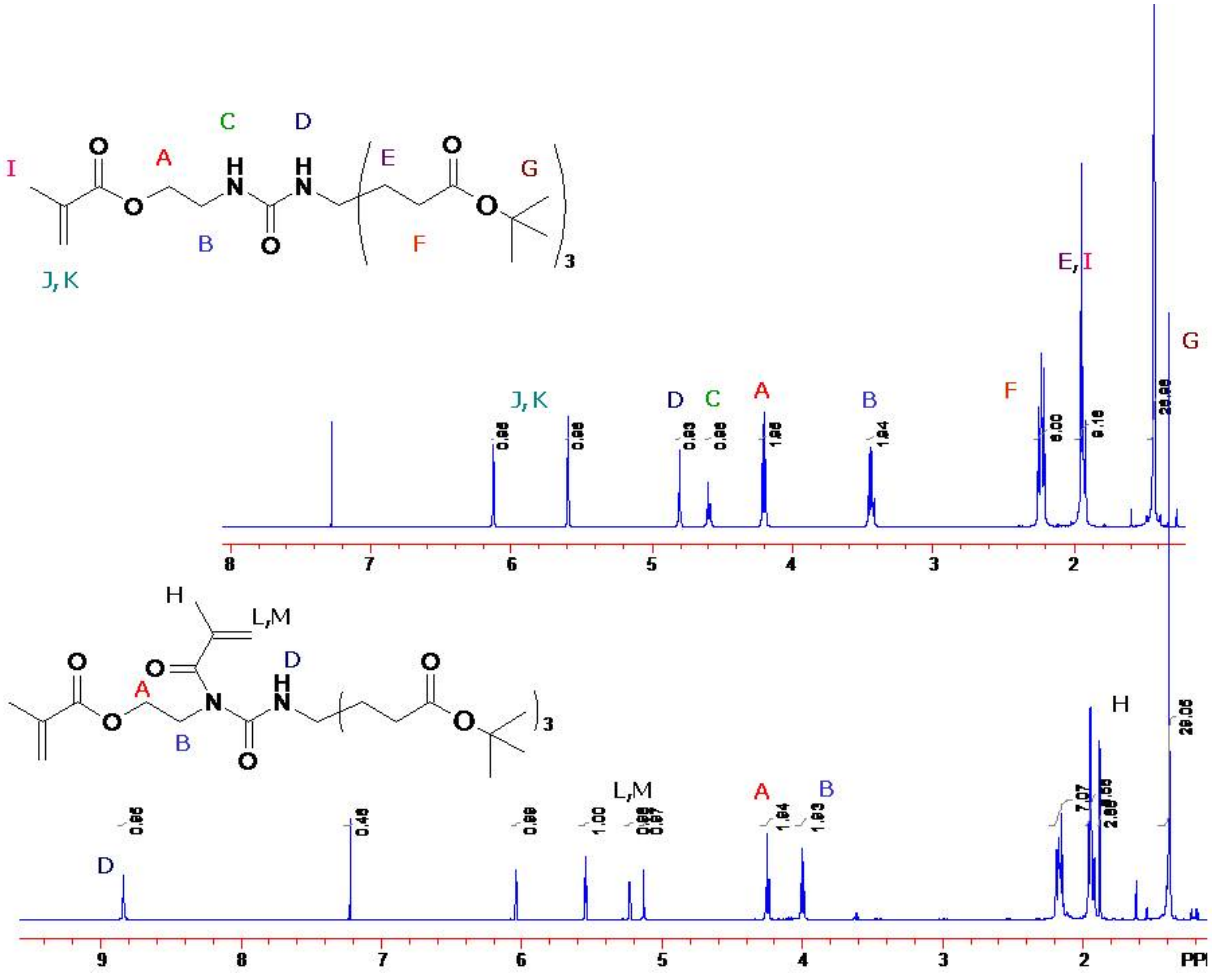

Figure 21. ^{1}H NMR ($CDCl_3$) of dendritic methacrylate macromonomers MI and MII.

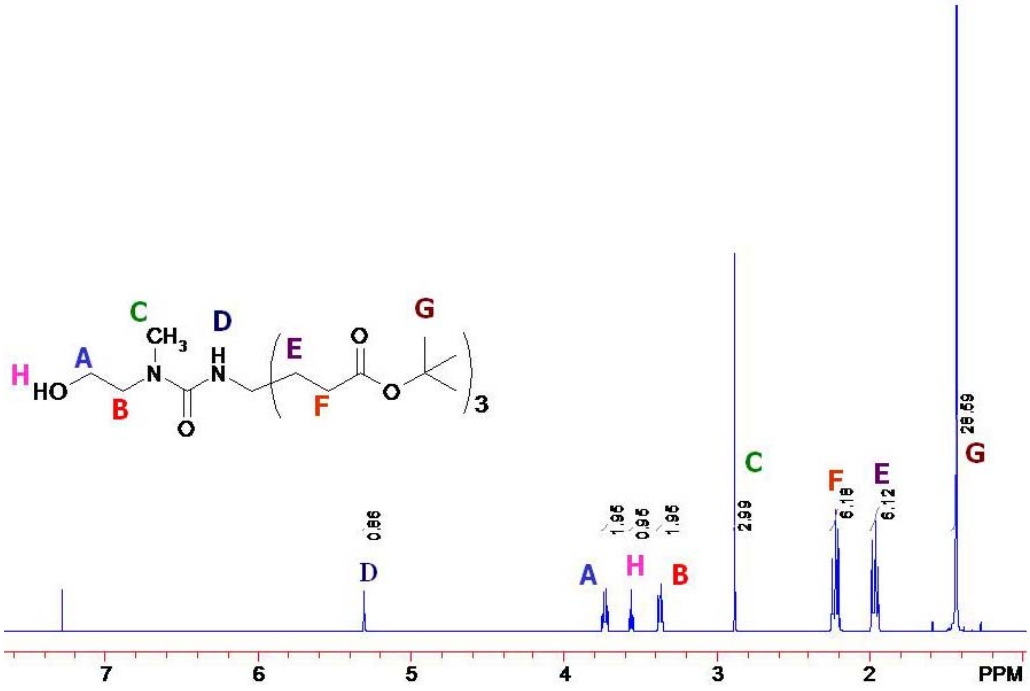

Figure 22. ^{1}H NMR ($CDCl_3$) of alcohol derivative 3b.

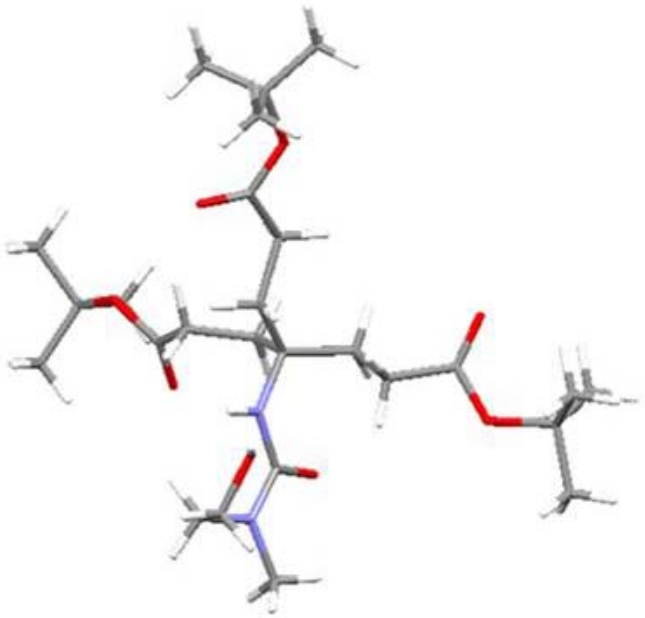

Figure 23. X-ray crystal structure of 3b.

*4.2.4 Synthesis of Di-tert-butyl 4-(2-tert-Butoxycarbonylethyl)-4-[3-methyl-3-(2-methacryoloxyethyl)ureido]heptanedioate (**5b, MIII**)*

Methacryloyl chloride and **3b** were allowed to react in dichloromethane (-78 °C to rt) employing diisopropylethylamine as an acid scavenger to yield the corresponding dendritic methacrylate macromonomer, **MIII**. Purification of **MIII** was achieved via column chromatography on silica gel employing a gradient solvent system of hexanes and ethyl acetate, and resulted in 80–90 % recovery, a significant increase compared to **MI**. The chemical composition and purity were confirmed via ^{1}H and ^{13}C NMR, melting point, FTIR, HRMS, and elemental analysis. The ^{1}H NMR spectrum of **MIII** (**Figure 24**) revealed a new peak attributed to the *N*-methyl substituent (2.91 ppm); in addition, the methylene protons adjacent to the ureido linker appeared as triplet and were shifted downfield slightly compared to the corresponding peaks in **MI**.

The synthesis and characterization of **MIII** proved to be more efficient than that of **MI**; therefore, the majority of the further research proceeded with **MIII**.

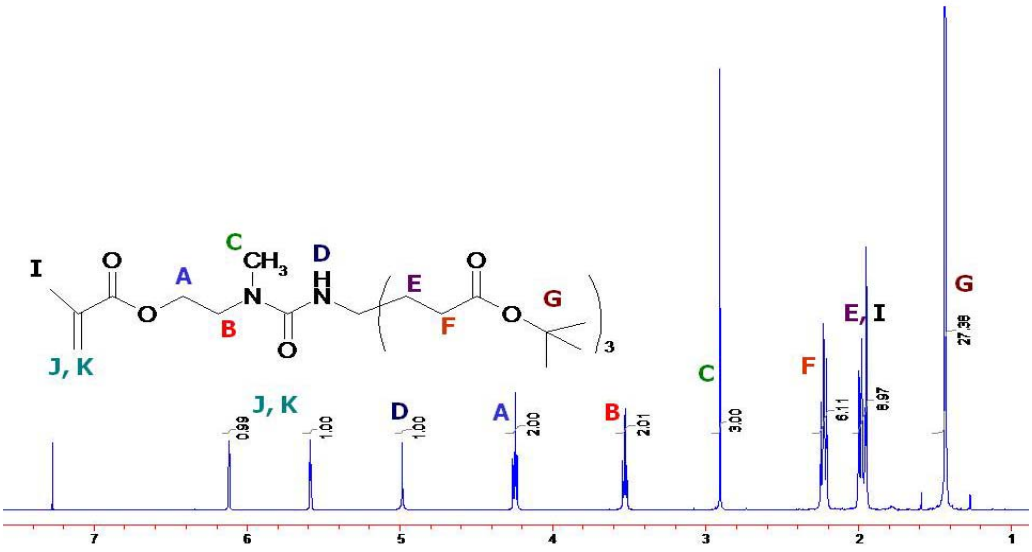

Figure 24. ^{1}H NMR ($CDCl_3$) of dendritic methacrylate macromonomer 5b, MIII.

4.3 Polymerization of Dendritic Methacrylate Macromonomers

4.3.1 Homopolymerization

The novel dendritic methacrylate macromonomer, **MIII**, was polymerized via conventional free radical polymerization in acetonitrile employing AIBN as an initiator; however, polymerization was only achieved above critical monomer and initiator concentrations. Reactions with a macromonomer concentration < 30 wt% and an initiator concentration < 1.0 mol% resulted in no or low (precipitate collected was ~18–20 wt% of mass recovered) monomer conversion; employing a high macromonomer concentration (60 wt%) and low initiator concentration (0.01 mol%) also proved unsuccessful. Successful reactions resulted in a white precipitate. Analysis of the precipitate via NMR confirmed polymerization by 1) the absence of the peaks attributed to the vinyl protons of the macromonomer and 2) a significant broadening of the remaining peaks (**Figure 25**).

The dendronized homopolymers were also characterized with TGA, DSC, and SEC. The thermal stability of the **MIII** homopolymer was analyzed via TGA from 40 to 600 °C at a ramp rate of 10 °C/min. **Figure 26** shows the degradation profile, in air, of three **MIII** homopolymers; in each case, a two-phase degradation profile was observed. In the initial phase, a rapid weight loss was observed with five percent weight loss temperatures, $T_{5\%}$, between 203 and 218 °C and a 55 % weight loss. The second degradation phase exhibited a more gradual weight loss over a broad temperature range and resulted in 0–5 wt% char at the upper temperature limit (500 or 600 °C). In general, the results are similar for each of the three polymers analyzed (**A**, **B**, and **C**); however, homopolymer **A** exhibited a lower $T_{5\%}$ (203 °C) compared to **B** (218 °C) and **C** (215 °C).

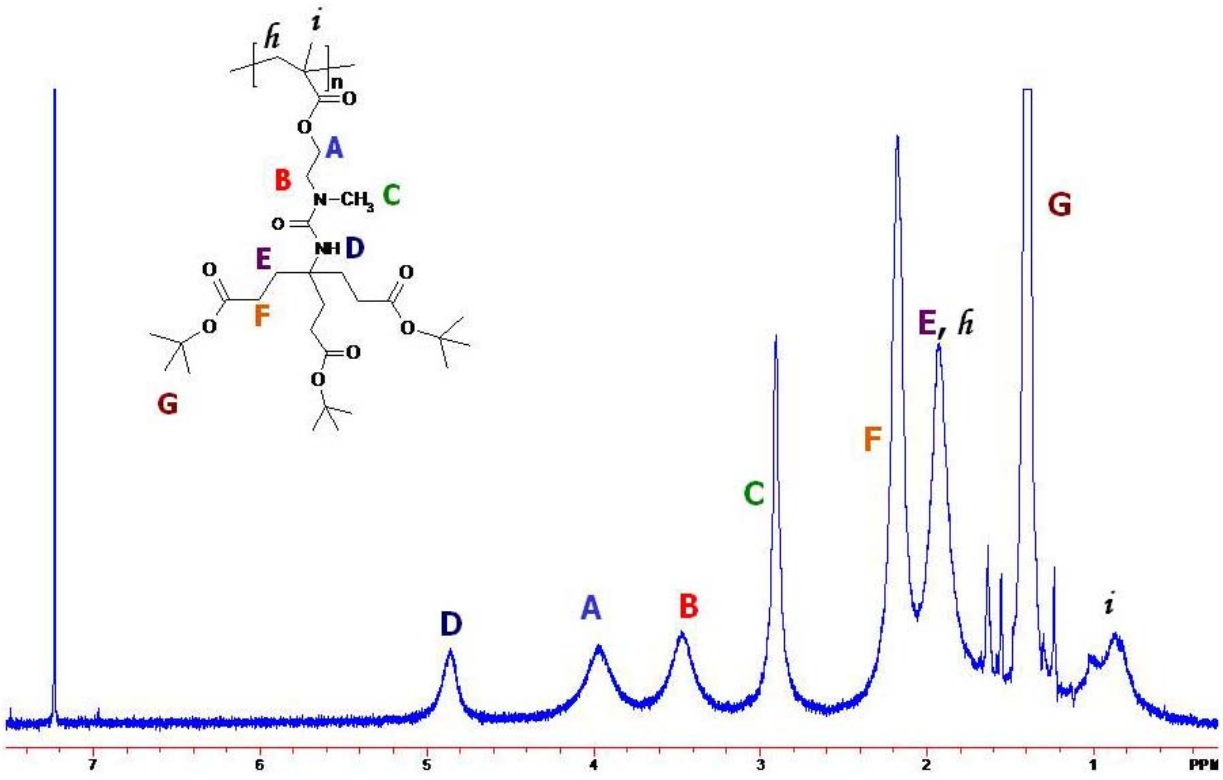

Figure 25. ^{1}H NMR ($CDCl_3$) of MIII homopolymer.

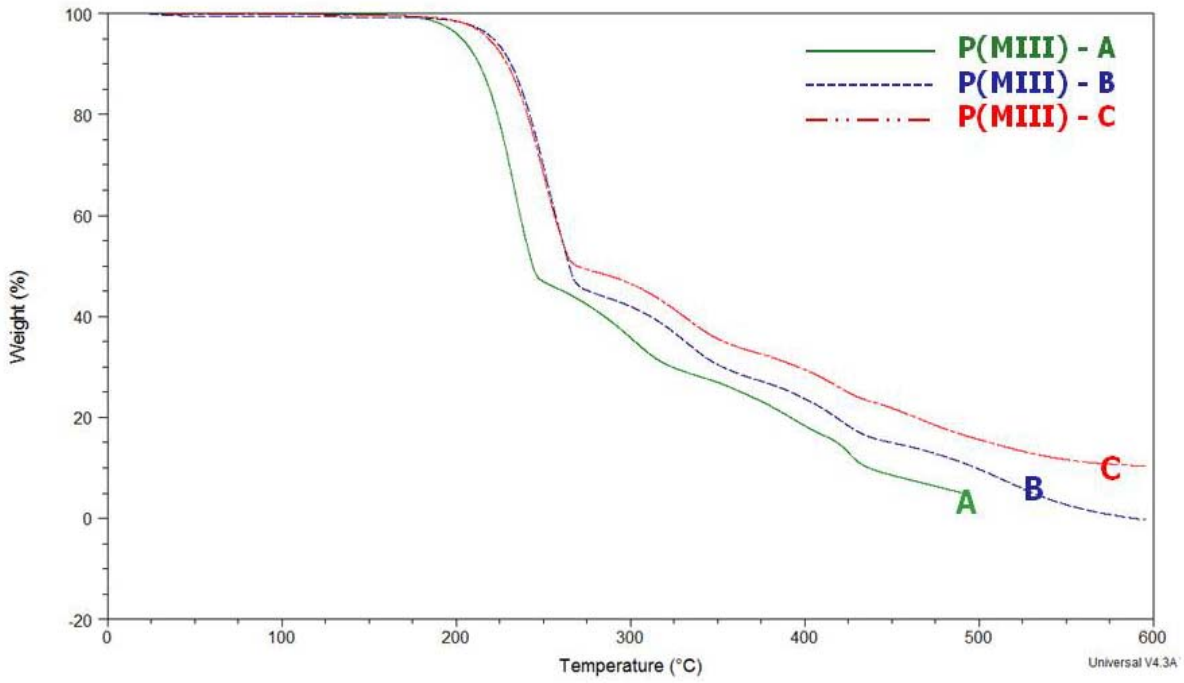

Figure 26. Thermogravimetric analysis of MIII homopolymers in air.

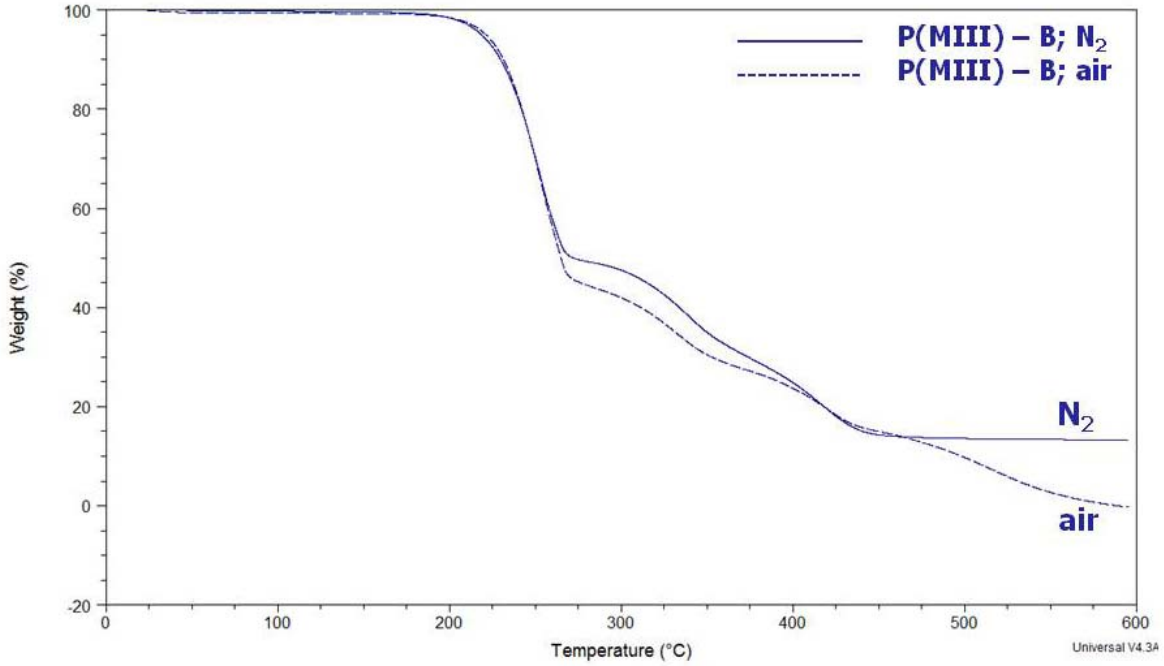

Figure 27. Thermogravimetric analysis of MIII homopolymer in air and Nitrogen.

As illustrated in **Figure 27**, similar degradation profiles were observed in both air and Nitrogen; this data suggests that thermo-oxidative degradation does not play a significant role in the degradation of the **MIII** homopolymer.

In DSC analysis, a range of glass transition temperatures, 52–66 °C, was observed for **MIII** homopolymers; DSC thermograms are illustrated by **Figure 28**. The T_gs observed for the **MIII** homopolymer were lower than that of both PMMA (T_g = 100 °C) and poly(*tert*-butyl methacrylate), P(*t*BMA) (T_g = 118 °C). The branched nature of the repeat unit in P(*t*BMA) sterically hinders rotation about the polymer backbone which results in an increase in T_g compared to PMMA. However, a high level of branching can also function to lower T_g as

observed with high-density polyethylene (HDPE); HDPE (T_g = -115 °C) has a lower T_g than linear low-density polyethylene (LLDPE) (T_g = -93 °C). In the case of the dendronized **MIII** homopolymer, the low glass transition temperatures observed were attributed to the branched nature and bulkiness of the repeat unit. The bulky substituent reduces the packing efficiency of the polymer chains, thereby, increasing the free volume about the polymer chains. The presence of a bulky substituent in the repeat unit and the resulting increase in free volume function to lower T_g. In this case, the bulky substituent is also flexible which also functions to lower T_g. As a result of these structural features, the **MIII** homopolymers exhibited significantly lower T_gs compared to both PMMA and P(*t*BMA).

The variation in glass transition temperature among the homopolymer replicates was attributed to fractionation during purification via precipitation. The purification of homopolymer **A** (T_g = 52 °C) was achieved via precipitation of chloroform solutions in hexanes at room temperature. The resulting solution was chilled in a freezer (-20 °C) overnight; after which, the hexanes was decanted and the polymer was re-dissolved in chloroform, concentrated, and dried under vacuum. Homopolymers **B** (T_g = 65 °C), **C** (T_g = 66 °C), and **D** (T_g = 59 °C) were precipitated from dichloromethane solutions in cold hexanes, chilled at -20 °C prior to use. The change in procedure was made to maintain consistency with the purification of the copolymer systems. The **MIII** homopolymer exhibited a lower T_g compared to homopolymers **B**, **C**, and **D**; a lower T_g is suggestive of decreased molecular weight. It is possible that the homopolymers **B**, **C**, and **D** were fractionation to a lesser extent in the chilled hexanes procedure compared homopolymer **A**, which was precipitated in hexanes at room temperature.

In addition to exhibiting the lowest T_g, homopolymer **A** also exhibited the lowest $T_{5\%}$ (203 °C), which may further support the theory that low molecular weight polymer resulted from

fractionation. These claims could be substantiated with molecular weight data; however, data is not available for these polymers.

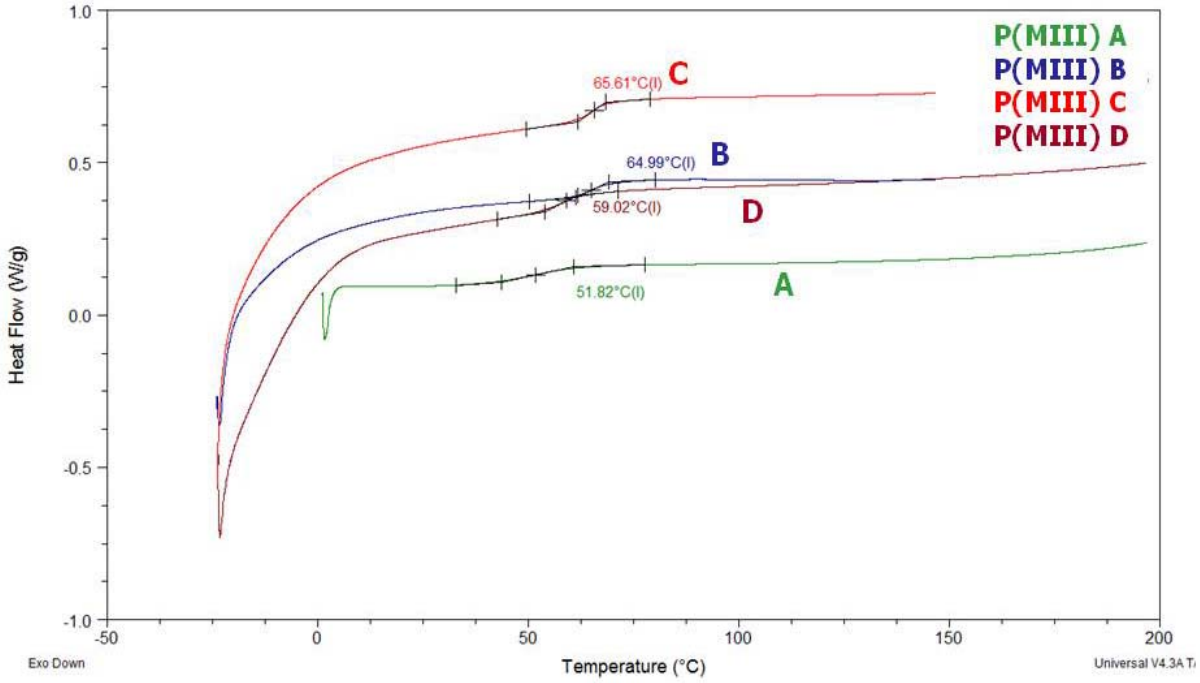

Figure 28. DSC thermograms of MIII homopolymers.

Characterization of the **MIII** homopolymers via SEC was challenging. Samples were analyzed in multiple solvent systems (THF, $CHCl_3$, and LiBr/NMP) employing various detectors (refractometer, viscosity, MALLS, and triple detection); however, reliable quantitative data was not achieved. A more detailed discussion of the attempts at molecular weight characterization is presented in Section 4.4.

4.3.2 Dendronized Copolymers via Copolymerization with Methyl Methacrylate.

Once homopolymerization of the novel dendritic macromonomer proved feasible, copolymers were targeted. **MIII** was copolymerized with methyl methacrylate via conventional

free radical polymerization in acetonitrile; the copolymer composition was varied in **MIII** from 0 to 100%. As a result, the copolymers in the series were predominantly poly(methyl methacrylate) (PMMA); PMMA was synthesized to serve as a reference polymer.

PMMA Model Study

A series of MMA polymerizations, varying in initiator concentration (0.01 to 1.0 mol%), were performed in acetonitrile at a monomer concentration of 10 wt%. The series was characterized via ^{1}H NMR, DSC, and SEC; the properties of the PMMA series are reported in **Table 1**. As expected, increased initiator concentration decreased both molecular weight and T_g. Among the series, the number-average molecular weight ranged from 15,400 to 92,300 g/ mol with polydispersities ranging from 1.6 to 1.7. Glass transition temperatures ranged from 93 °C to 98 °C. As previously discussed, homopolymerization of the **MIII** macromonomer required an initiator concentration of 1.0 mol%; polymerization of MMA at this concentration resulted in a polymer with M_n = 15,400 g/mol and T_g = 93 °C. PMMA is typically synthesized at low initiator concentrations to achieve high molecular weight polymer with T_gs ranging from 105 to 110 °C. The model study revealed the limitations the chosen reaction conditions, specifically initiator concentration, placed on the targeted **MIII**/MMA copolymers which are predominantly poly(alkyl methacrylate)s.

AIBN (mol %)	M_n (10^3) (g/mol)	PDI	DP	T_g (°C)
0.01	92.3	1.7	922	98
0.1	45.2	1.6	451	-
0.5	20.4	1.6	204	-
1	15.4	1.7	154	93

Table 1. Polymerization of MMA with varying AIBN concentration.

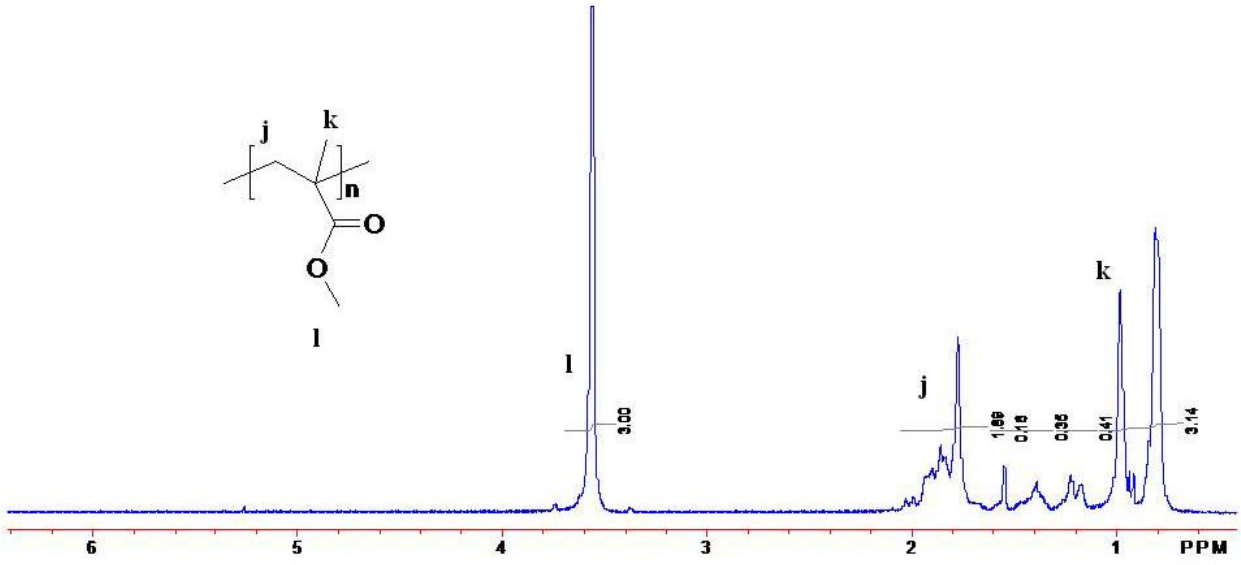

Figure 29. ^{1}H NMR($CDCl_3$) of PMMA.

Copolymer Synthesis

Macromonomer **MIII** was copolymerized with MMA; the copolymer composition was varied in **MIII** from 0 to 100 mol%. Copolymers were achieved via conventional free radical polymerization in acetonitrile employing AIBN as an initiator (1.0 mol %) at a total monomer concentration of 10 wt%. In the case of 100% **MIII**, a higher monomer concentration (34 wt%) was employed due to the issues associated with steric crowding of the polymerization site by the dendritic substituent. Precipitation of $CHCl_3$ solutions in hexanes at room temperature resulted in a white precipitate, which was characterized via ^{1}H NMR, TGA, DSC, and SEC; data are reported in **Table 2**.

As shown in **Figure 30**, the copolymer composition was confirmed via ^{1}H NMR using **Equation 1**; the calculated composition agreed well with the targeted monomer feed. The methylene protons of MMP were distinctly identifiable in the spectrum at 2.54 and 2.70 ppm, and were the major difference between the ^{1}H NMR spectra of this series and the **MIII**/MMA series prepared in the absence of MMP. As a result, end-group analysis could be employed to determine number average molecular weight from ^{1}H NMR (See Section 4.4 for Discussion).

Molecular weight of the copolymer series was characterized via SEC in THF; absolute values from the MALLS detector are reported. At low **MIII** content, the polymers are predominantly PMMA. The number average molecular weight was relatively constant at low **MIII** content (0–10 mol%) ranging from 15,000 to 15,600 g/mol. Upon incorporation of 20 mol% **MIII**, the number average molecular weight doubled and continued to increase with increasing **MIII** content. At low **MIII** content, the degree of polymerization (DP) decreased with increasing **MIII** content; above 20 mol% **MIII**, DP increased with increasing **MIII** content.

The molecular weight trends observed may be attributed to the incorporation of a co-monomer with a bulky substituent. The molecular weight of the repeat unit formed from the dendritic macromonomer is approximately six times that of MMA; each addition of the dendritic macromonomer substantially increased the copolymer molecular weight. It is noteworthy that analysis of the **MIII** homopolymer via this system resulted in a high molecular weight (184,000 g/mol) and a low PDI (1.1). Such low PDIs are typically only observed in "controlled/living" free radical polymerizations; this data may suggest that the copolymer is aggregating in and/or sticking to the column. Upon inspection, the corresponding chromatograph revealed a narrow peak with significant tailing (**Figure 31**). If the tailing is a result of the polymer sticking to the column, then the molecular weight data reported may exclude low molecular weight species and are high. Regardless, the significant tailing makes it impossible to determine an accurate baseline; as a result, the molecular data obtained for the **MIII** homopolymer was deemed inaccurate and unreliable. Although significant tailing was not observed in the chromatographs of the copolymers, the issue observed in the analysis of the **MIII** homopolymer may be a factor in the copolymer system but to a lesser extent and contribute to the increase in molecular weight observed as the copolymer composition increased in **MIII**. Nonetheless, the SEC data, at the very least, presents a qualitative comparison along the series. Characterization of molecular weight via SEC will be discussed further in Section 4.4.

The **MIII** /MMA copolymers were analyzed via DSC; T_g was shown to decrease with increasing **MIII** content. Due to the branched nature of the **MIII** macromonomer, an increase in free volume about the polymer chains was anticipated as the copolymer composition was increased in **MIII**. An increase in free volume results in a decrease in the amount of thermal energy required to promote molecular motion of the polymer chains (i.e. T_g). **MIII**

homopolymer **A** was purified via the same means as the copolymers presented here and exhibited a relatively low T_g (52 °C). As the **MIII** content of the copolymer was increased, the copolymer T_g approached the **MIII** homopolymer T_g. The Fox equation (**Equation 2**) was used to predict the T_g of the copolymers based on PMMA, T_g = 93 °C, and P**MIII**, T_g = 52°C. These data compared well with the experimental values. The predicted and experimental T_gs differed by 7–9 °C for copolymers with 6–32 mol% **MIII**; however, a greater deviation (ΔT_g =16 °C) was observed for the copolymer with 47 mol% **MIII**.

The **MIII**/MMA copolymer series confirmed the ability to successfully synthesize copolymers of the novel dendritic methacrylate macromonomer and an alkyl methacrylate in various targeted compositions.

MIII (mol %)		M_n (10^3) (g/mol)	PDI	DP	T_g (°C)	T_g (°C)	ΔT_g
Monomer Feed	Polymer Composition				Fox Eq		
0	0	15.4	1.7	154	-	93	-
5	6	15.0	1.5	121	89	80	9
10	10	15.6	1.6	109	86	79	7
20	21	28.6	1.3	153	80	73	7
40	32	36.3	1.5	148	74	66	8
50	47	65.0	1.5	198	68	52	16
100	100	-	-	-	-	52	-

Table 2. MIII/MMA copolymer series.

$$\%\ \text{MIII} = \frac{\left(P_A \ / \#\ \text{Protons in } \mathbf{A}\right)}{\left(P_A \ / \#\ \text{Protons in } \mathbf{A}\right) + \left(P_B \ / \#\ \text{Protons in } \mathbf{B}\right)}$$

$P_{\mathbf{A}}$ = integration of peak representative of co-monomer **A**
$P_{\mathbf{B}}$ = integration of peak representative of co-monomer **B**

Equation 1. Copolymer composition determined from ^{1}H NMR.

$$\frac{1}{T_g} = \frac{w_a}{T_{g,a}} + \frac{w_b}{T_{g,b}}$$

Where,
W_a is the weight fraction of monomer 'a'
W_b is the weight fraction of monomer 'b'
$T_{g,\,a}$ is the T_g of a polymer of monomer 'a'
$T_{g,b}$ is the T_g of a polymer of monomer 'b'

Equation 2. Fox Equation.

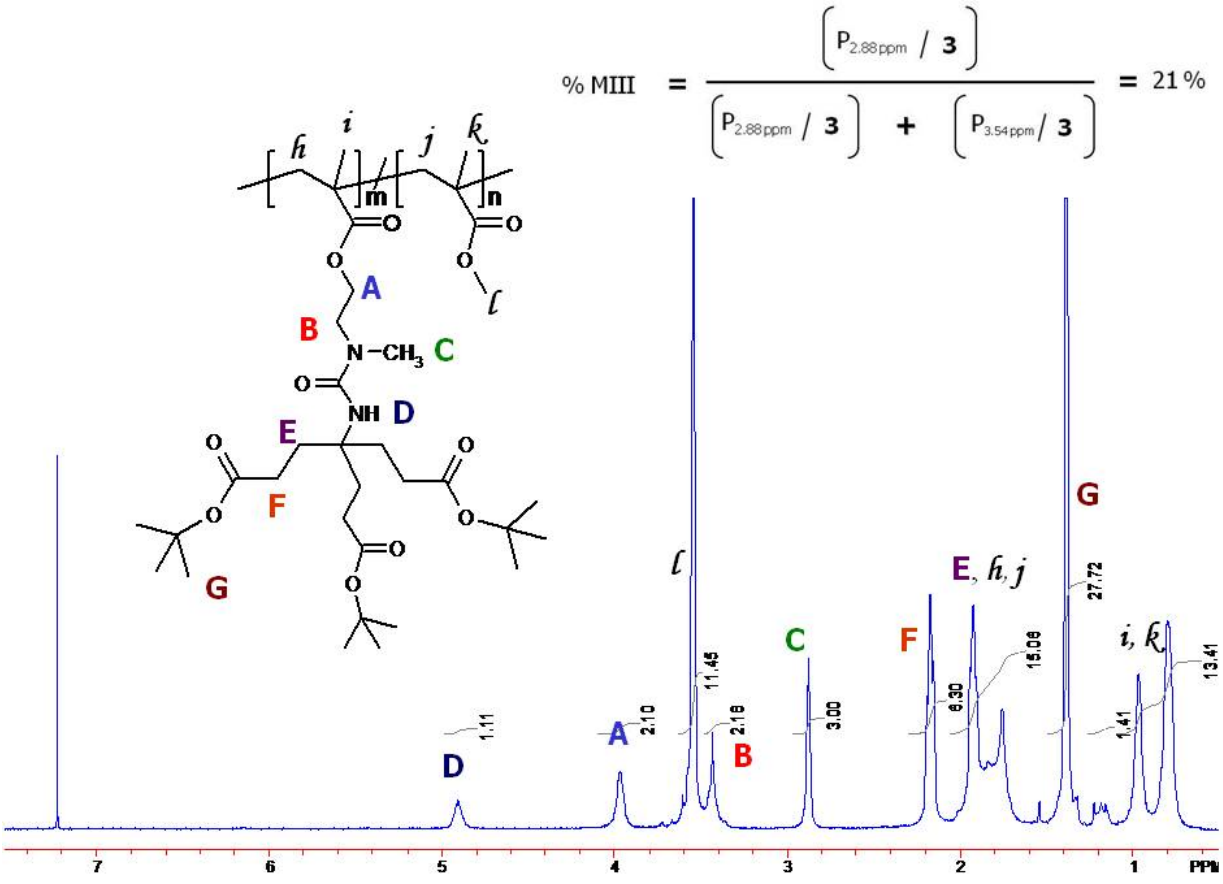

Figure 30. ^{1}H NMR ($CDCl_3$) of MIII/MMA (20:80).

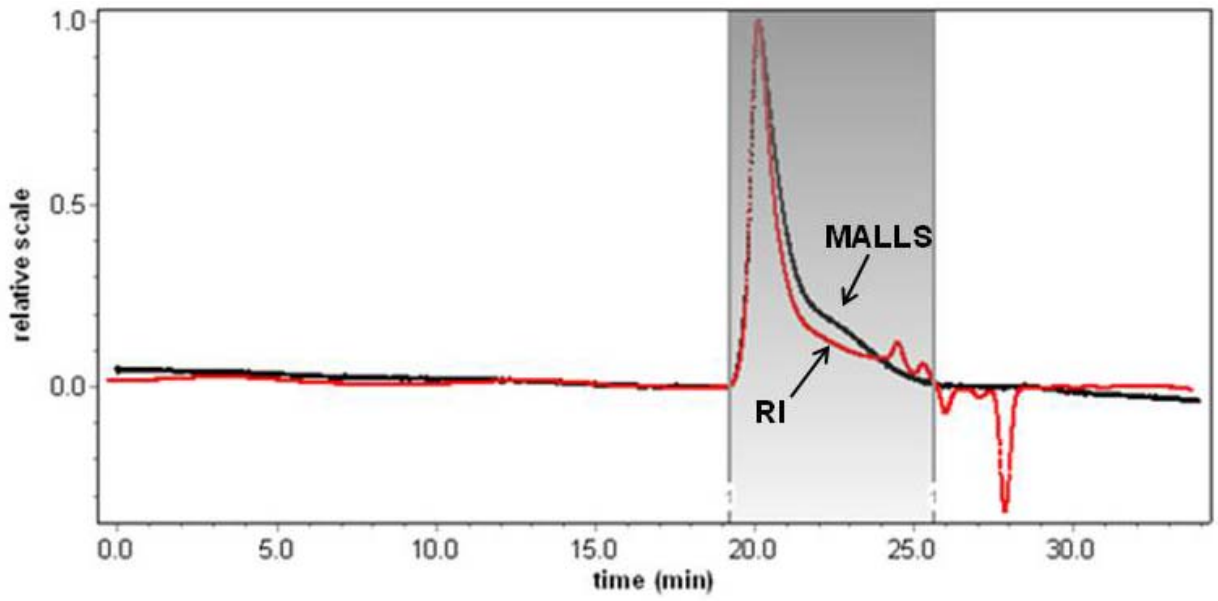

Figure 31. SEC chromatograph of MIII homopolymer from RI (red) and MALLS (black) detectors.

4.4 Employing a Chain Transfer Agent (CTA) for Molecular Weight Control

In much of the literature, low molecular weight polymers have been shown more effective antimicrobials compared to their high molecular weight analogues. This is attributed to increased interaction and mobility between the polymer and the microbe below the polymer's entanglement molecular weight. For this reason, low molecular weight dendronized copolymers were targeted. Molecular weight control was achieved with the use of a chain transfer agent (CTA). A CTA brings about the termination of the growing polymer chain and the initiation of a new one, thereby, reducing the average molecular weight of the polymer.[192] CTAs have at least one weak chemical bond that facilitates the transfer; thiols are effective chain transfer agents. Dodecylmercaptan is most commonly employed in this regard; however, because low molecular weight polymers with a controlled hydrophilic/hydrophobic composition were desired, ultimately, an alternative mercaptan was used: methyl 3-mercaptopropionate (MMP). Methyl 3-mercaptopropionate has a much shorter chain length compared to dodecylmercaptan which should lessen its influence on the hydrophilic/hydrophobic composition of the copolymers post deprotection.

4.4.1 PMMA Model Study

In an effort to determine the concentration of CTA needed to achieve polymers of desired molecular weight (<10K) using the reaction conditions previously determined for the dendronized copolymer series, methyl methacrylate was polymerized incorporating MMP at varying concentrations (0, 5, and 10 mol %). The reaction conditions previously determined suitable for the synthesis of the dendronized amphiphilic copolymers were employed: 10 wt % monomer in acetonitrile, 1.0 mol % AIBN and 70 °C for 24h. The polymers were purified by

precipitation of $CHCl_3$ solutions in hexanes at room temperature. Analysis of the resulting polymers by SEC in THF revealed a decrease in molecular weight as a function of increasing CTA concentration, as expected. The number average molecular weight ranged from 4,300 to 15,400 g/mol. In addition, a decrease in PDI was also observed; the low PDIs (1.2 and 1.3) were attributed to the CTA as well. Analysis via DSC revealed a decrease in T_g as function of CTA concentration; T_gs ranged from 85 to 97 °C. The reaction employing 10 mol% CTA produced PMMA with a number average molecular weight of 4,300 g/mol and PDI of 1.3; these reaction conditions were carried forth in the synthesis of dendronized copolymers in effort to achieve copolymers with number average molecular weights ≤10 K g/mol.

CTA (mol)	M_n (10^3) (g/mol)	PDI	DP	T_g (°C)
1 mol % AIBN				
0	15.4	1.7	154	93
0.05	6.7	1.2	67	97
0.1	4.3	1.3	43	85

Table 3. CTA Model Study: Polymerization of MMA.

4.4.2 Homopolymerization

In an effort to prepare a series of dendronized homopolymers of varying molecular weight a chain transfer agent (CTA), methyl 3-mercaptopropionate (MMP), was employed. The MMP concentration was varied from 0 to 10 mol% in the polymerization of **MIII** while the remaining reaction conditions (≥ 30 wt % monomer in acetonitrile, 1.0 mol% AIBN, 70 °C) were

maintained as previously described. One major difference observed in the preparation of this series was that the polymers proved difficult to precipitate unless the non-solvent was chilled at -20 °C prior to use. Otherwise the polymer would agglomerate resulting in a yellow gel-like material. However, slow precipitation of dilute CH_2Cl_2 solutions in rapidly-stirring, cold hexanes resulted in a white precipitate which was collected by filtration. The precipitate was analyzed via ^{1}H NMR, SEC, TGA, and DSC.

Successful polymerization was evident by the formation of a white precipitate and analysis via ^{1}H NMR. In ^{1}H NMR analysis, the disappearance of the peaks attributed to the vinyl protons and a significant broadening of the remaining peaks served as evidence of a successful polymerization reaction. The ^{1}H NMR spectra of the homopolymers prepared with 0, 0.5, and 1.0 mol% MMP were identical. However, the spectrum of the polymer prepared with 10 mol% MMP differed in that the peaks were not as broad as observed in the other spectra; and, as a result, the peaks attributed to MMP were distinguishable (**Figure 32**).

The thermal stability of the **MIII** homopolymer series prepared in the presence of MMP was analyzed via TGA from 40 to 600 °C at a ramp rate of 10 °C/min. Degradation profiles were examined in both air and Nitrogen; in each case, a two-phase degradation profile was observed. In the initial phase, a rapid weight loss was observed with five percent weight loss temperatures, $T_{5\%}$, between 207 and 221 °C and ~60 % weight loss. The second degradation phase exhibited a more gradual weight loss over a broad temperature range. In air, the degradation profiles were very similar among the series and resulted in 0–5 wt% char at the upper temperature limit (600 °C) (**Figure 33**). However, in Nitrogen, slight deviations among the series were observed (**Figure 34**). In addition, higher char yields (15–20 wt %) were observed for the homopolymers prepared with 0–1.0 mol% MMP in Nitrogen.

Analysis via DSC revealed a decrease in T_g with increasing MMP concentration, which may serve as a first approximation of relative molecular weight among the series (**Figure 35**). A significant decrease in T_g was observed for the homopolymer prepared with 10 mol % MMP (T_g = 55 °C) versus 0 mol % MMP (T_g = 65 °C) (**Table 4**).

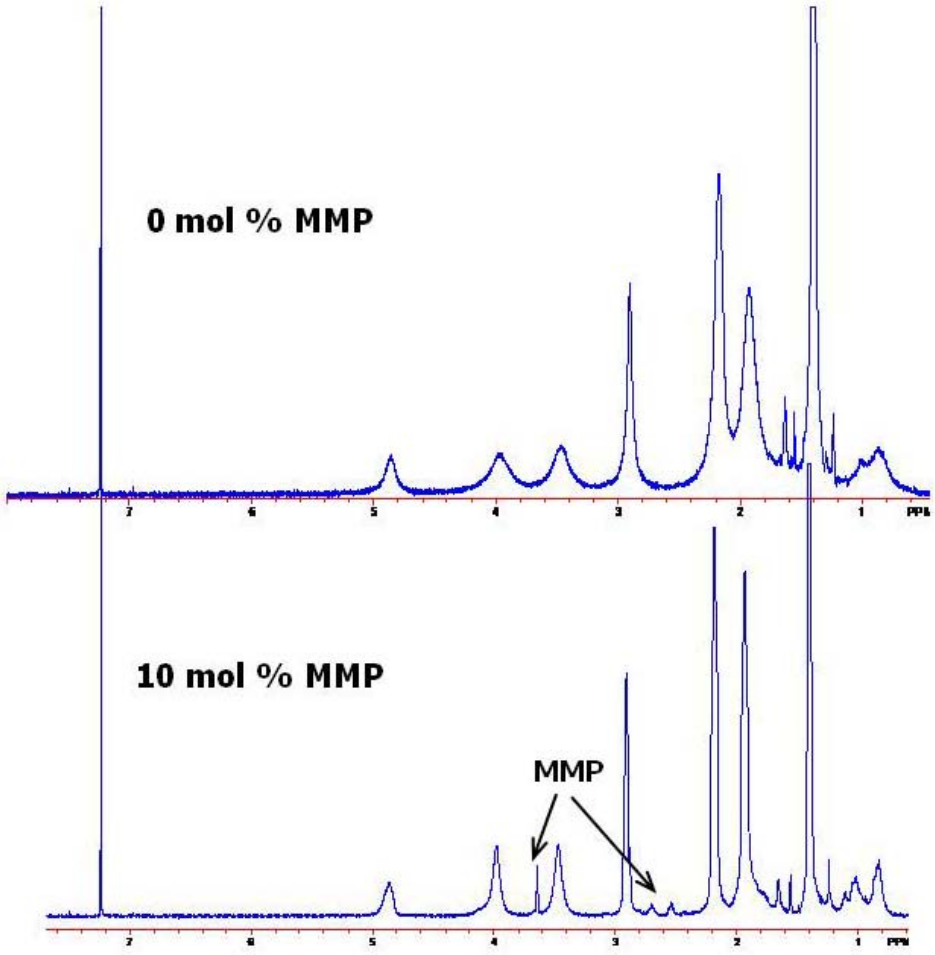

Figure 32. ^{1}H NMR ($CDCl_3$) of MIII homopolymers prepared with 0 and 10 mol% MMP.

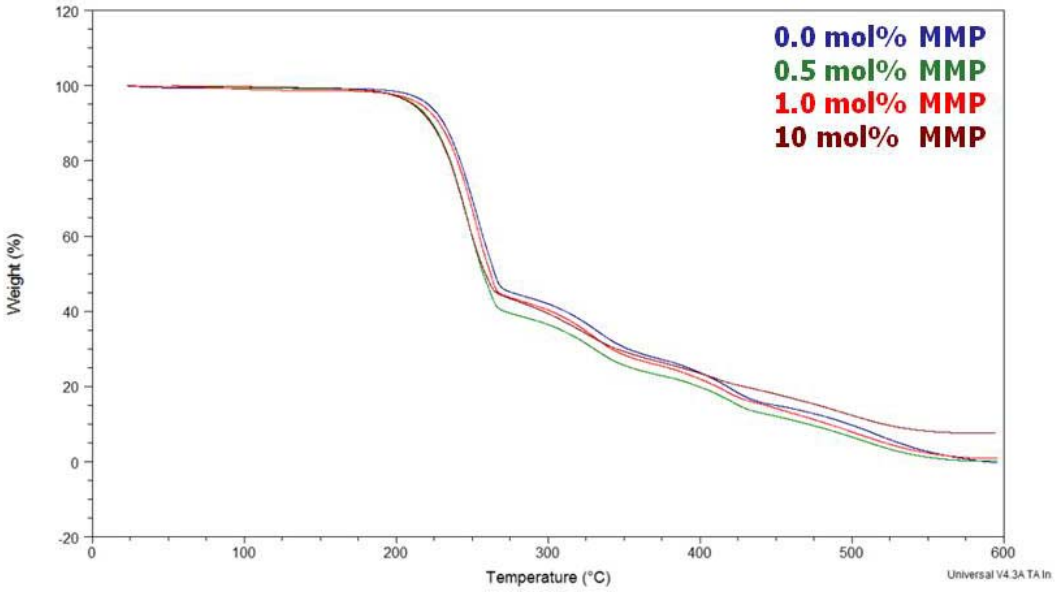

Figure 33. Thermogravimetric analysis of MIII homopolymer series in air.

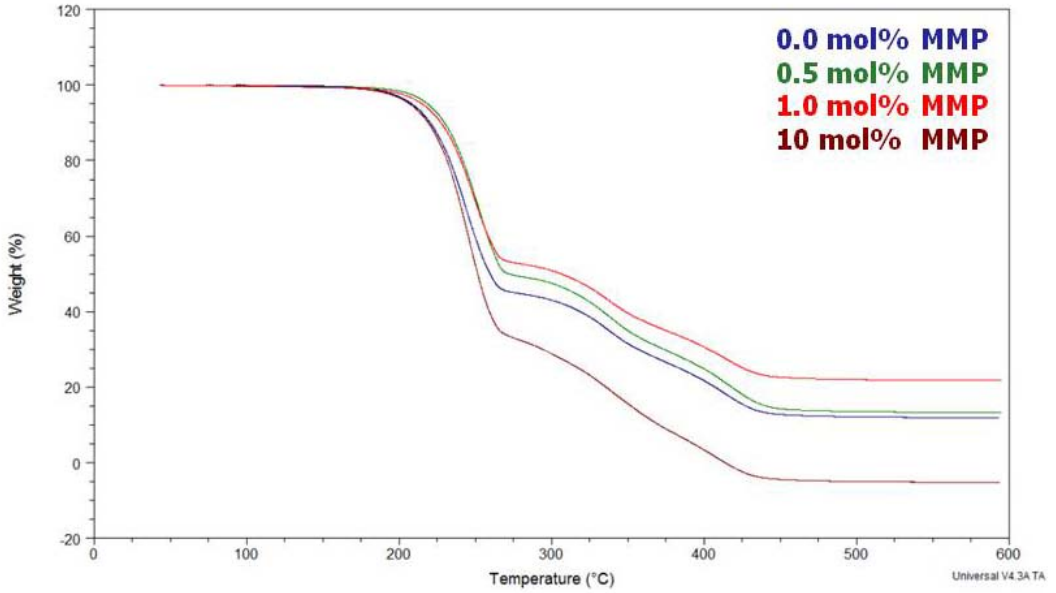

Figure 34. Thermogravimetric analysis of MIII homopolymer series in Nitrogen.

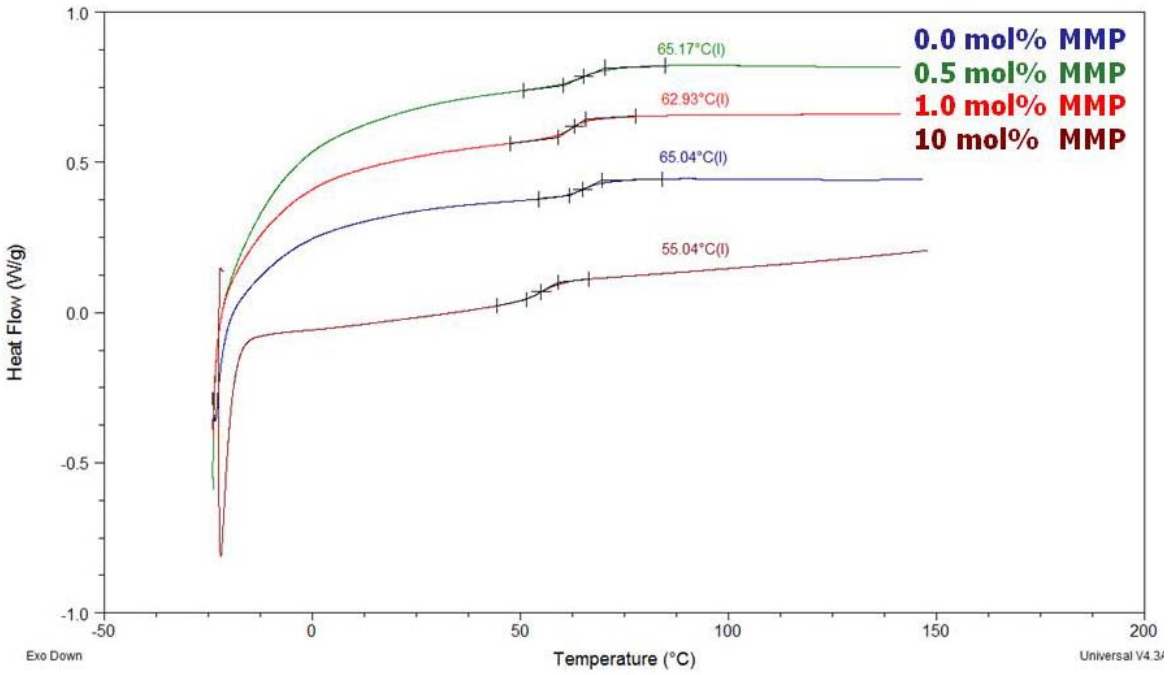

Figure 35. DSC Thermograms of MIII homopolymers prepared in the presence of MMP at various concentrations (0–10 mol%).

Analysis of the homopolymers via SEC proved challenging. Samples were analyzed in multiple solvent systems (THF, $CHCl_3$, and LiBr/NMP) employing various detectors (refractive index, viscosity, MALLS, and triple detection). SEC analysis in THF employing a MALLS detector revealed narrow peaks with significant tailing were observed, which made it difficult to establish a baseline. This result suggested a strong interaction with the column as was also observed in the analysis of the **MIII** homopolymer prepared in the absence of MMP. However, intrinsic viscosity (IV) data was obtained from SEC analysis, in LiBr/NMP, employing triple detection. The IV data revealed a trend which may serve as an approximation of relative molecular weight (**Table 4**) among the series; IV was shown to decrease as a function of increasing MMP concentration.

MMP (mol%)	**IV (dL/g)**	**TGA (°C, $T_{5\%}$)**		**T_g (°C)**
1.0 mol % AIBN	NMP/LiBR	**Air**	**N_2**	
0	0.300	221	219	65
0.5	0.283	212	208	65
1.0	0.076	216	215	63
10	0.039	211	207	55

Table 4. MIII homopolymers: Molecular weight series.

Analysis via matrix-assisted laser desorption/ionization time of flight (MALDI-TOF) mass spectrometry confirmed polymerization of the dendritic macromonomer. However, data was only obtained for the polymer prepared with the highest MMP concentration (10 mol%), which would intuitively be the lowest molecular weight polymer.

A more detailed discussion of the attempts to characterize molecular weight is presented in Section 4.4.

4.4.3 Copolymerization

Copolymerization Employing MIII

Low molecular weight dendronized copolymers prepared from the novel dendritic methacrylate macromonomer, **MIII**, and various alkyl methacrylates were the major goal of this research. Methyl, ethyl, and *n*-butyl methacrylate were employed as alkyl methacrylate co-monomers. For each alkyl methacrylate, a series of copolymers was prepared with varying **MIII** content: 5, 10, and 25 mol%. Conventional free radical polymerization was carried out in acetonitrile (10 wt % total monomer concentration) at 70 °C employing AIBN (1.0 mol %) as a free radical initiator, and methyl 3-mercaptopropionate (MMP) (10 mol %), a chain transfer agent, was used to limit the degree of polymerization (DP). For the methyl and ethyl methacrylate series, purification was achieved by precipitation of CH_2Cl_2 solutions in cold hexanes. In the case of the *n*-butyl methacrylate series, purification was achieved via precipitation of THF solutions in cold MeOH/H_2O (60:40) or extraction with hexanes. Each polymer series was characterized via ^{1}H NMR, SEC, TGA, and DSC; the results are reported in **Table 5**.

The **MIII**/MMA copolymer series described here represents a low molecular weight analogue of that previously described (Section 4.2.2); similar trends were observed. For example, the number average molecular weight was shown to increase with increasing **MIII** content. The number average molecular weight ranged from 4,000 to 9,000 g/mol for the series, and low PDIs (1.1–1.3) were obtained. The molecular weight trends observed may be attributed to the incorporation of a comonomer with a bulky substituent.

	MIII (mol%)		M_n (10^3) (g/mol)	PDI	DP	TGA (°C, $T_{5\%}$)		T_g (°C)
	Monomer Feed	Copolymer Composition				Air	N_2	
MMA	**0**	**0**	**4.3**	**1.3**	**43**	**264**	**-**	**85**
	5	**5**	**4.2**	**1.2**	**34**	**215**	**220**	**71**
	10	**10**	**4.8**	**1.2**	**32**	**211**	**215**	**67**
	25	**23**	**8.8**	**1.1**	**42**	**203**	**204**	**58**
EMA								
	5	**9**	**4.4**	**1.2**	**28**	**211**	**213**	**52**
	10	**14**	**4.7**	**1.2**	**26**	**201**	**200**	**48**
	25	**26**	**6.4**	**1.2**	**27**	**187**	**185**	**51**
nBMA								
	5	**4**	**2.6**	**1.4**	**20**	**210**	**210**	**24**
	10	**6**	**3.1**	**1.3**	**22**	**188**	**202**	**30**
	25	**25**	**5.3**	**1.3**	**23**	**213**	**214**	**29**
	70	**65**	**12.6**	**1.2**	**31**	**192**	**192**	**44**
	100	**100**	**-**	**-**	**-**	**215**	**220**	**55**

Table 5. MIII and alkyl methacrylate copolymer series.

As shown in **Figure 36**, the copolymer composition was confirmed via ^{1}H NMR using **Equation 1**; the copolymer composition agreed well with the targeted monomer feed. The methylene protons of MMP were distinctly identifiable in the spectrum at 2.54 and 2.70 ppm, and were the major difference between the ^{1}H NMR spectra of this series and the **MIII**/MMA

series prepared in the absence of MMP. As a result, end-group analysis could be employed to determine number average molecular weight from ^{1}H NMR (See Section 4.4 for Discussion).

In DSC analysis, the T_gs obtained for this copolymer series were comparably lower than those prepared without MMP. However, in both cases, a similar trend was observed: As the **MIII** content was increased, the copolymer T_g decreased. For the **MIII**/MMA copolymers with 5 to 20 mol% **MIII** prepared in the absence of MMP, T_gs ranged from 80 to 73 °C. Copolymers with 5 to 20 mol% **MIII** prepared with MMP exhibited T_gs between 71 and 58 °C.

The thermal stability of the **MIII**/MMA copolymer series prepared in the presence of MMP was analyzed via TGA from 40 to 500 °C at a ramp rate of 10 °C/min (**Figure 37**). Degradation profiles were examined in both air and Nitrogen. As observed with the **MIII** homopolymers, the copolymers exhibited a two-phase degradation profile. However, degradation in the initial phase was less rapid and the percent weight loss was lower, 18–40 wt% versus ~60 wt %, compared to the homopolymers. The initial degradation phase began to resemble that of the homopolymers more as the copolymer composition was increased in **MIII**; the copolymer with 25 mol% **MIII**, exhibited a rapid 40 wt% loss in the initial degradation phase. In each case, the second degradation phase exhibited a more gradual weight loss over a broad temperature range. TGA analysis in air and Nitrogen revealed similar degradation profiles with $T_{5\%}$ temperatures ranging from 203 to 220 °C for the series; thermal stability ($T_{5\%}$) decreased as **MIII** content was increased. The copolymers proved slightly more stable in Nitrogen than air; however, low char yields (0–5 wt%) were observed at 500 °C in both air and Nitrogen.

As the length of the aliphatic chain of the alkyl methacrylate was increased, an effect on the properties of their respective polymers was expected. Increasing the chain length decreases

the polymer's ability to pack, increasing the free volume about the chains. The effect of increased alkyl chain length was most evident as a decrease in the glass transition temperature. DSC analysis of the **MIII**/ethyl methacrylate (**MIII**/EMA) copolymer series resulted in $T_g s$ ranging from 48 to 52 °C (**Table 5**). Literature values for the glass transition temperature of poly(ethyl methacrylate) ranged from 65 to 71 °C[193, 194], which is substantially lower than that reported for poly(methyl methacrylate) (100–120 °C) [193, 195-197]. Consequently, DSC analysis of the **MIII**/EMA copolymer series resulted in $T_g s$ that were significantly lower than those obtained for the **MIII**/MMA series. However, the values did not deviate much along the series differing by ± 4 °. Homopolymers of **MIII** and MMA, prepared in the presence of 10 mol% MMP and 1.0 mol% AIBN, exhibited glass transition temperatures which differed by ~30 °C. The literature reports $T_g s$ between 65 and 71 °C for high molecular weight EMA homopolymers; however, the T_g of an EMA homopolymer prepared in the presence of 10 mol% MMP and 1.0 mol% AIBN (not prepared) would be lower, as observed in the model studies of the polymerization of MMA varying in AIBN (Section 4.2.2) and MMP (Section 4.3.1) concentrations. From this, one may conclude that the T_gs of **MIII** and EMA homopolymers, prepared with similar reaction conditions, are closer in magnitude than the T_gs of **MIII** and MMA homopolymers prepared under the same conditions. As a result, the effect of the incorporation of **MIII** on T_g observed for the **MIII**/MMA copolymers, decreased T_g with increasing **MIII** content, was not observed for the **MIII**/EMA series.

In TGA, **MIII**/EMA copolymers exhibited trends similar to the **MIII**/MMA copolymer series. A two-phase degradation profile was observed (**Figure 38**). For the copolymers with 5 and 10 mol% **MIII**, degradation in the initial phase was less rapid and the percent weight loss was lower compared to **MIII** homopolymers. As the copolymer composition was increased in

MIII, the initial degradation phase began to resemble that of the **MIII** homopolymer, and the $T_{5\%}$ temperatures decreased. The second degradation phase exhibited a more gradual weight loss over a broad temperature range. TGA analysis in air and Nitrogen revealed similar degradation profiles with $T_{5\%}$ temperatures ranging from 185 to 213 °C for the series. The copolymers proved slightly more stable in Nitrogen than air; however, low char yields (0–5 wt%) were observed at 500 °C in both.

Similar to the MMA copolymer series, the number average molecular weight increased with increasing **MIII** content for the **MIII**/EMA copolymer series and narrow PDIs were obtained. The DPs did not deviate much along the series but were lower than the DPs of the **MIII**/MMA series.

Chemical composition was determined by ^{1}H NMR using **Equation 1**. **Figure 39** depicts the ^{1}H NMR spectrum of the **MIII**/EMA copolymer with a target copolymer composition of 25 mol % **MIII**; the **MIII** content was determined to be 26%. Copolymer composition for the EMA series was slightly higher than the targeted monomer feed for each polymer of the series.

Employing *n*-butyl methacrylate (*n*BMA) as a co-monomer lead to a further reduction in copolymer T_g; **MIII**/*n*BMA copolymers with 5, 10, 25, and 70 mol% **MIII** were targeted. The T_gs for the *n*BMA series ranged from 24 to 44 °C (**Table 5**). Poly(*n*-butyl methacrylate) reportedly has a T_g of 20–26 °C[193, 194]. Due to the increased hydrophobicity, purification via precipitation of CH_2Cl_2 in cold hexanes was not feasible. At low **MIII** content, the crude copolymer was soluble in hexane; however, copolymers with ≥25 mol% **MIII** were insoluble in hexanes. Copolymers with 5 or 10 mol% **MIII** were purified via precipitation of THF solutions in cold MeOH/H_2O (60:40) and vacuum drying at room temperature; a tacky gel was obtained. The **MIII**/*n*BMA copolymer with a target of 25 mol% **MIII** was purified via extraction in

hexanes; in this case, a white flaky solid was obtained. Purification via precipitation of CH_2Cl_2 in cold hexanes also proved a successful means of purifying the **MIII**/*n*BMA copolymer with 70 mol % **MIII**, a white flaky solid resulted.

Analysis of the **MIII**/*n*BMA copolymer series via TGA revealed trends similar to that of the MMA and EMA series. Each copolymer exhibited a two-phase degradation profile (**Figure 40**). At low **MIII** content, the degradation of the initial phase was shallow and only exhibited a 15–20 wt% loss. A more rapid and significant (40 wt %) weight loss was observed in the initial degradation phase of the copolymer with 25 mol% **MIII**. TGA analysis in air and Nitrogen revealed similar degradation profiles with $T_{5\%}$ temperatures ranging from 188 to 214 °C for the series. The copolymers were slightly more stable in Nitrogen than air; however, low char yields (0–5 wt%) were observed at 500 °C in both air and Nitrogen.

Figures 41 and **42** depict the ^{1}H NMR spectra of **MIII**/*n*BMA copolymers with **MIII** targets of 25 and 70 mol%, respectively. Comparison of the spectra revealed the conversion of the copolymer from predominantly P(*n*BMA) to P**MIII**. The change in copolymer composition was evident in the change of the ratio of the peaks between 3.76 and 4.10 ppm, which are labeled '**A**' and '**l**', respectively. The '**A**' peak represents the methylene protons in the linker of the dendritic macromonomer; the '**l**' peak represents the methylene protons in the aliphatic chain of the *n*-butyl methacrylate comonomer Using **Equation 1**, the copolymer composition was confirmed via ^{1}H NMR; the calculated composition agreed well with the targeted monomer feed. The methylene protons of MMP were distinctly identifiable in the spectrum at 2.47 and 2.64 ppm; as a result, end-group analysis could be employed to determine number average molecular weight from ^{1}H NMR (See Section 4.4).

The number average molecular weight, determined by SEC/MALLS analysis in THF, was shown to increase with increasing **MIII** content. In addition, an increase in DP was observed with the increase in **MIII** content from 25 to70 mol% **MIII**. The number average molecular weight ranged from 2,600 to 12,600 g/mol for the series, and low PDIs (1.2–1.4) were obtained.

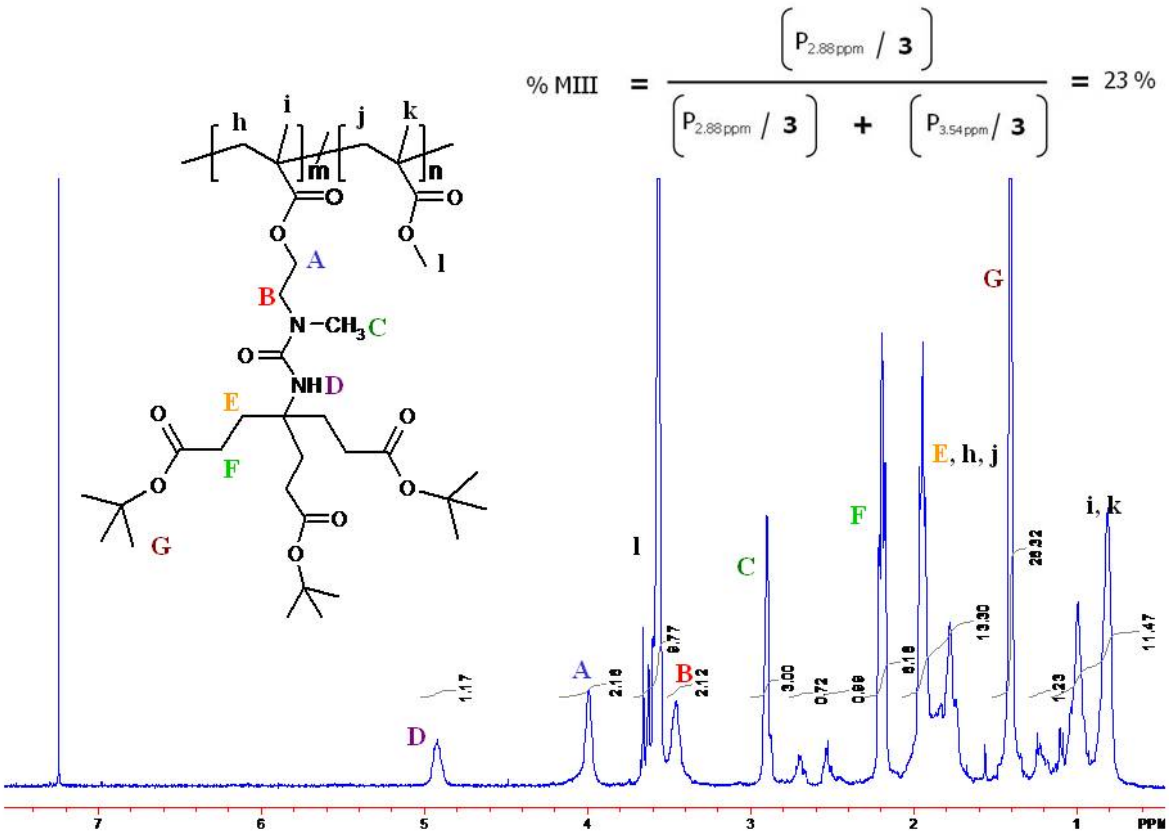

Figure 36. ^{1}H NMR ($CDCl_3$) of MIII/MMA copolymer (25:75).

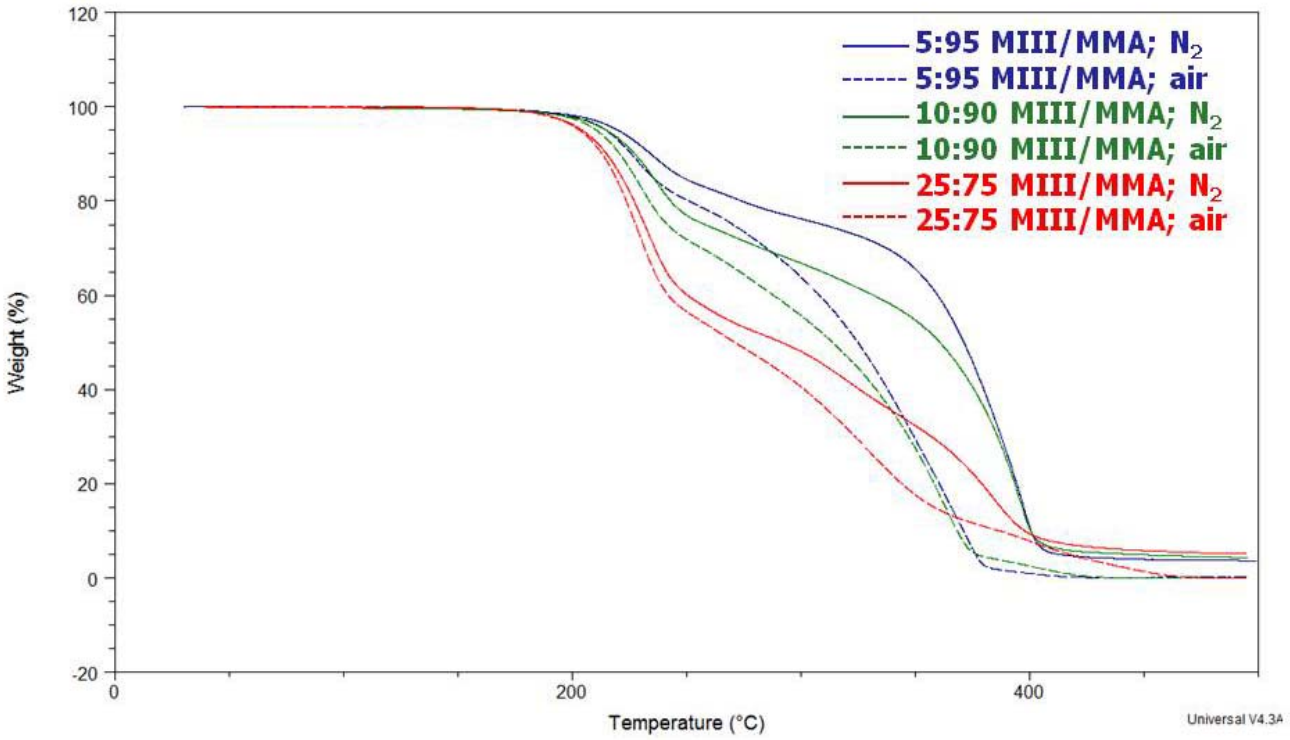

Figure 37. TGA of MIII/MMA copolymer series in air and Nitrogen.

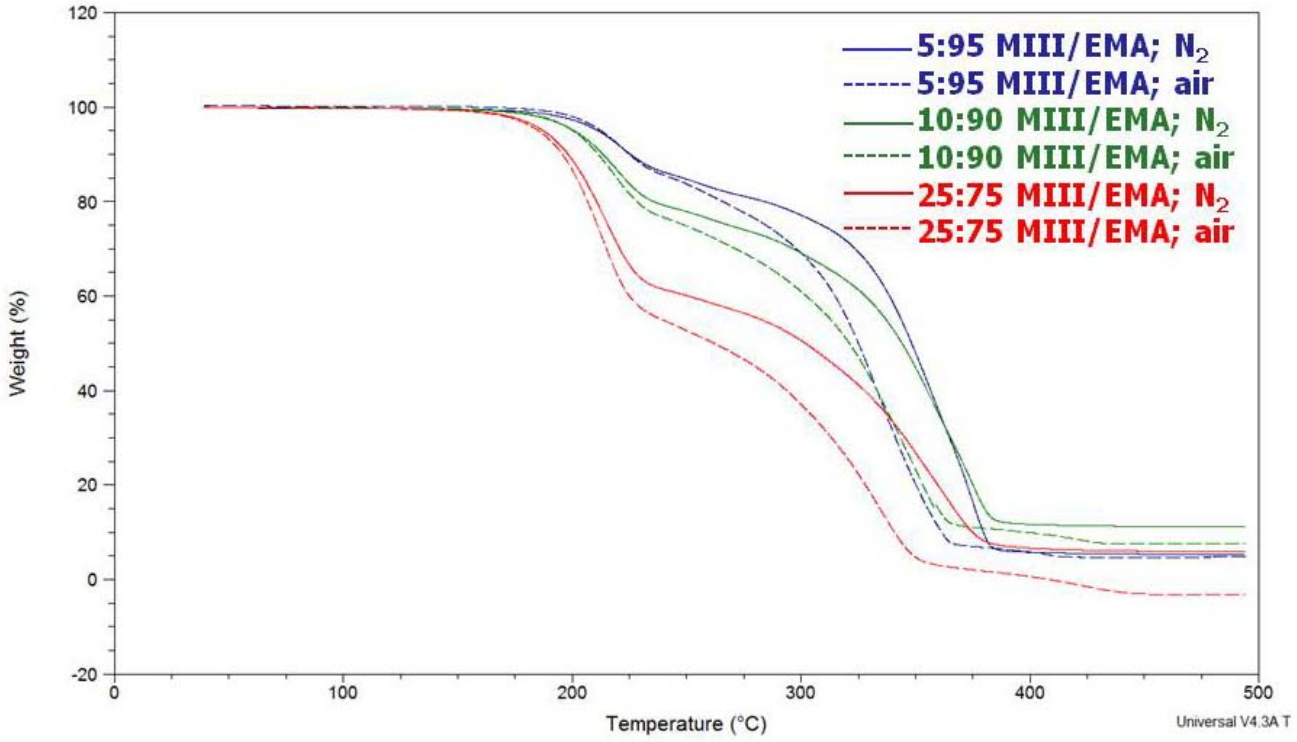

Figure 38. TGA of MIII/EMA copolymer series in air and Nitrogen.

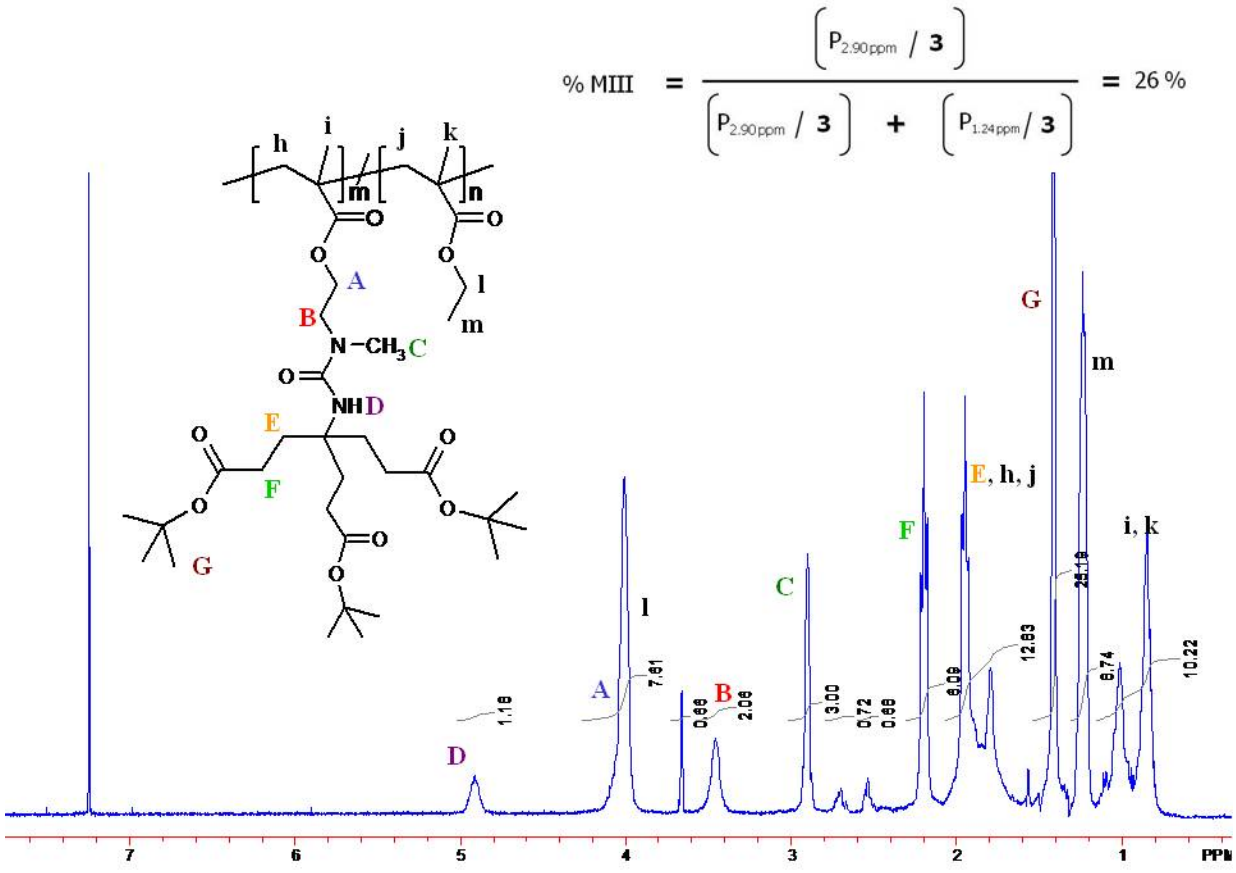

Figure 39. ^{1}H NMR ($CDCl_3$) of MIII/EMA (25:75).

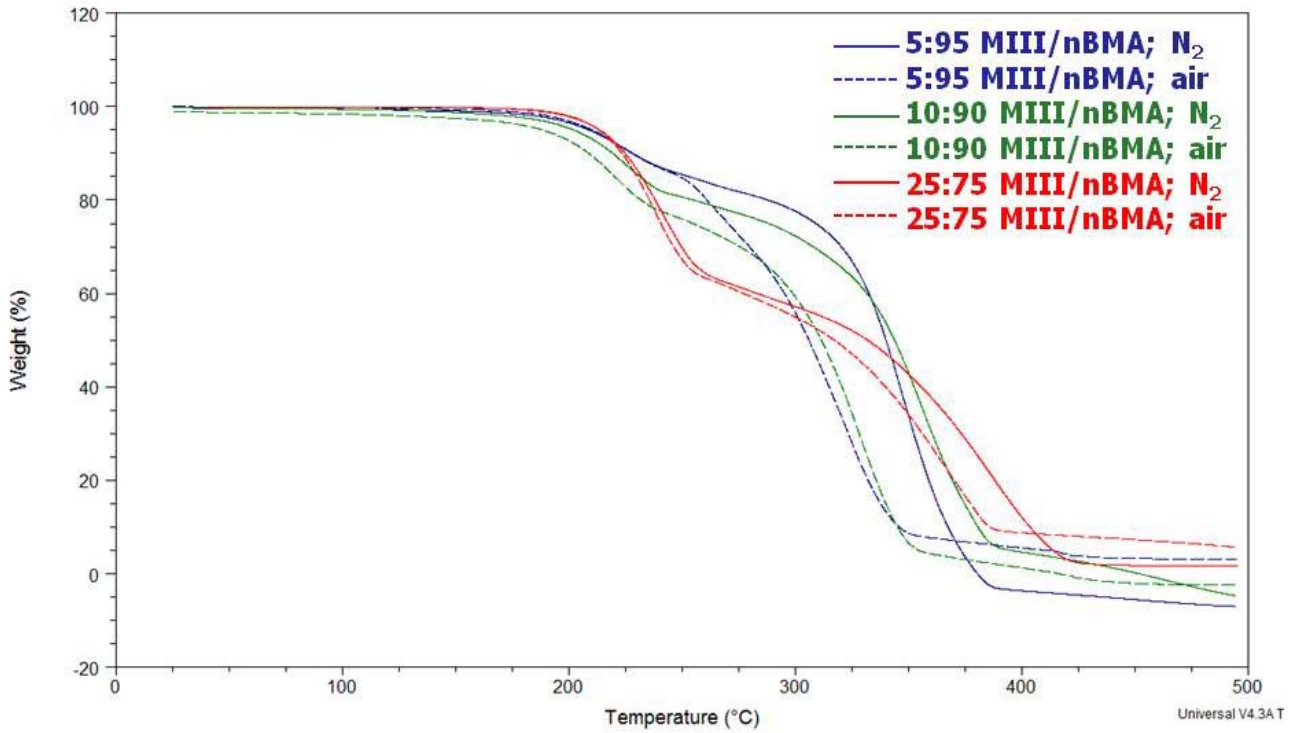

Figure 40. TGA of MIII/nBMA copolymer series in air and Nitrogen.

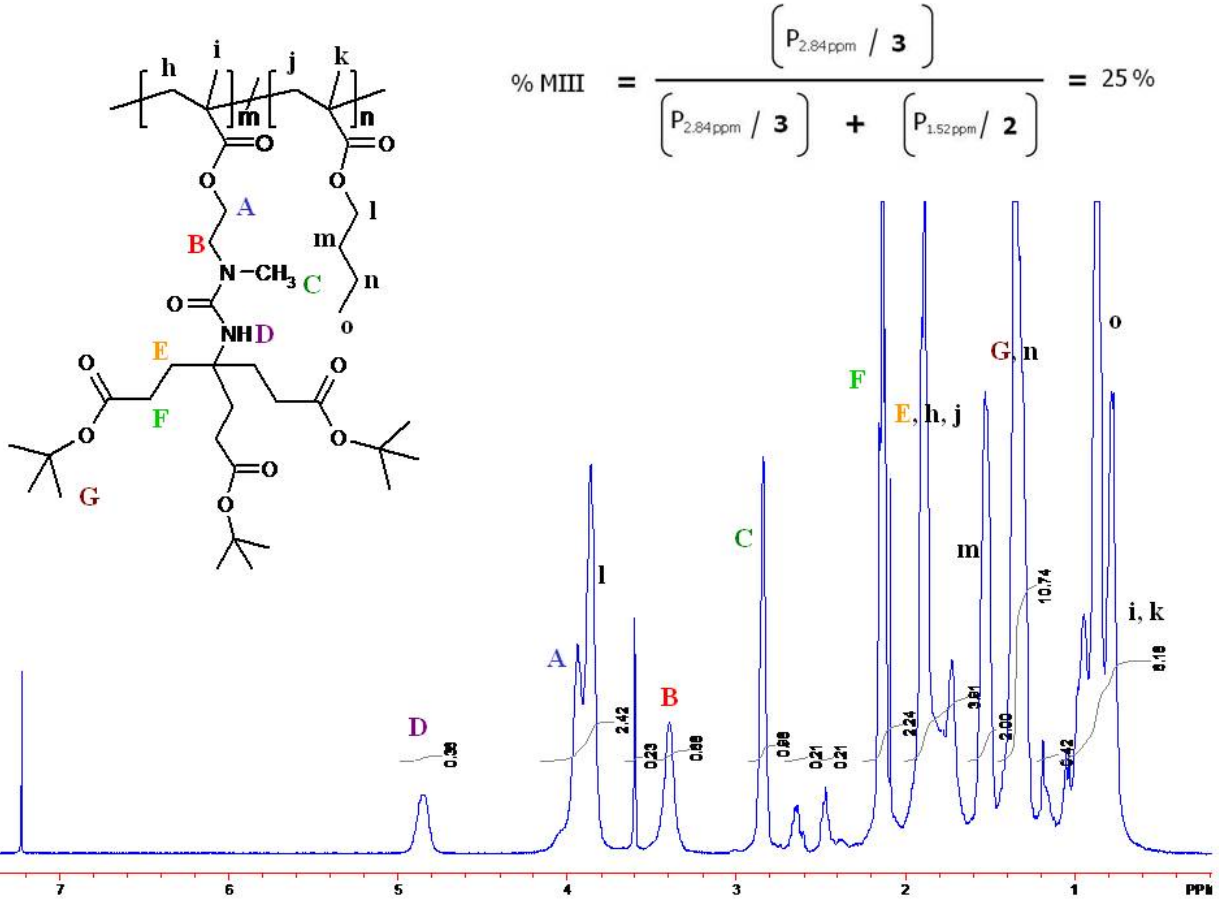

Figure 41. ^{1}H NMR ($CDCl_3$) of MIII/nBMA (25:75).

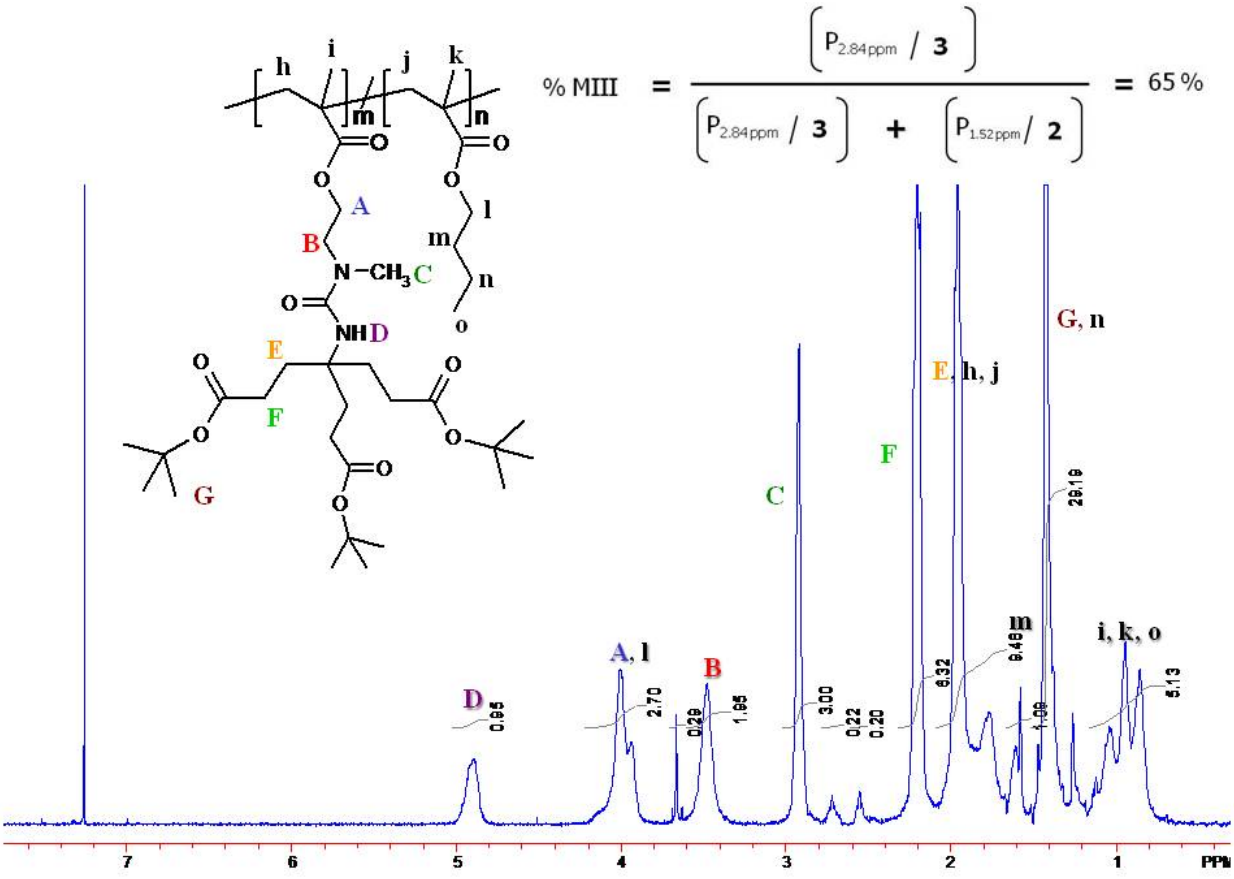

Figure 42. ^{1}H NMR ($CDCl_3$) of MIII/nBMA (70:30).

Copolymerization Employing MI

Dendritic methacrylate macromonomer **MI** was copolymerized with MMA; the copolymer composition was varied in **MI** from 0 to 100 mol%. Copolymers were achieved via conventional free radical polymerization in acetonitrile employing AIBN as an initiator (1.0 mol %) at a total monomer concentration of 10 wt%. Precipitation of $CHCl_3$ solutions in hexanes at room temperature resulted in a white precipitate, which was characterized via ^{1}H NMR, TGA, DSC, and SEC; data are reported in **Table 6**.

Analysis of the precipitate via ^{1}H NMR confirmed polymerization by 1) the absence of the peaks attributed to the vinyl protons of each of the co-monomers and 2) broadening of the remaining peaks. **Figure 43** depicts the ^{1}H NMR spectrum of a **MI**/MMA copolymer with a targeted **MI** composition of 5 mol%. Copolymer composition was determined from ^{1}H NMR using **Equation 1**. The **MI** content determined from ^{1}H NMR was higher than the monomer feed for copolymers with targets of 5 and 10 mol% **MI** but correlated well for the copolymer in which 25 mol% **MI** was targeted. The spectrum shown in **Figure 43** represents a copolymer in which 5 mol% **MI** was targeted, however, 9 mol% **MI** was calculated from NMR. The peaks (2.55 and 2.77 ppm) attributed to the methylene protons of MMP, a chain transfer agent, were well resolved and available for use in end-group analysis.

Molecular weight of the copolymer series was characterized via SEC in THF; absolute values from the MALLS detector are reported in **Table 6**. At low **MI** content, the polymers are predominantly PMMA; however, the incorporation of 5 mol% **MI** resulted in a decrease in the number-average molecular weight. The control polymer, PMMA, exhibited a number-average molecular weight of 4,300 g/mol; the **MI**/MMA copolymer with 5 mol% **MI** exhibited a number-average molecular weight of 3,100 g/mol. From there, the number-average molecular

weight increased as a function of increased **MI** content (5–25 mol%) ranging from 3,100 to 5,200 g/mol. Low PDIs were observed (1.2–1.4) and attributed the use of a chain transfer agent.

The thermal stability of the **MI**/MMA copolymer series was analyzed via TGA, in air, from 40 to 600 °C at a ramp rate of 10 °C/min. The results revealed a slight decrease in $T_{5\%}$ temperatures as a function of increasing **MI** content. At 5 mol% **MI**, $T_{5\%}$ was 211 °C, and decreased to 203 °C for the copolymer with 25 mol% **MI**. A similar trend was observed for the **MIII**/MMA copolymer series; in addition, the $T_{5\%}$ temperatures spanned the same range (215–203 °C).

Analysis of the copolymers via DSC, revealed a decrease in T_g as a function of **MI** content; the T_gs ranged from 66 to 61 °C. The copolymers with 5 and 10 mol% **MI** had the same T_g (66 °C). Similar results were exhibited by the **MIII**/MMA copolymer series; T_gs ranged from 71 to 58 °C for the **MIII**/MMA series, and decreased as a function of increasing **MIII** content.

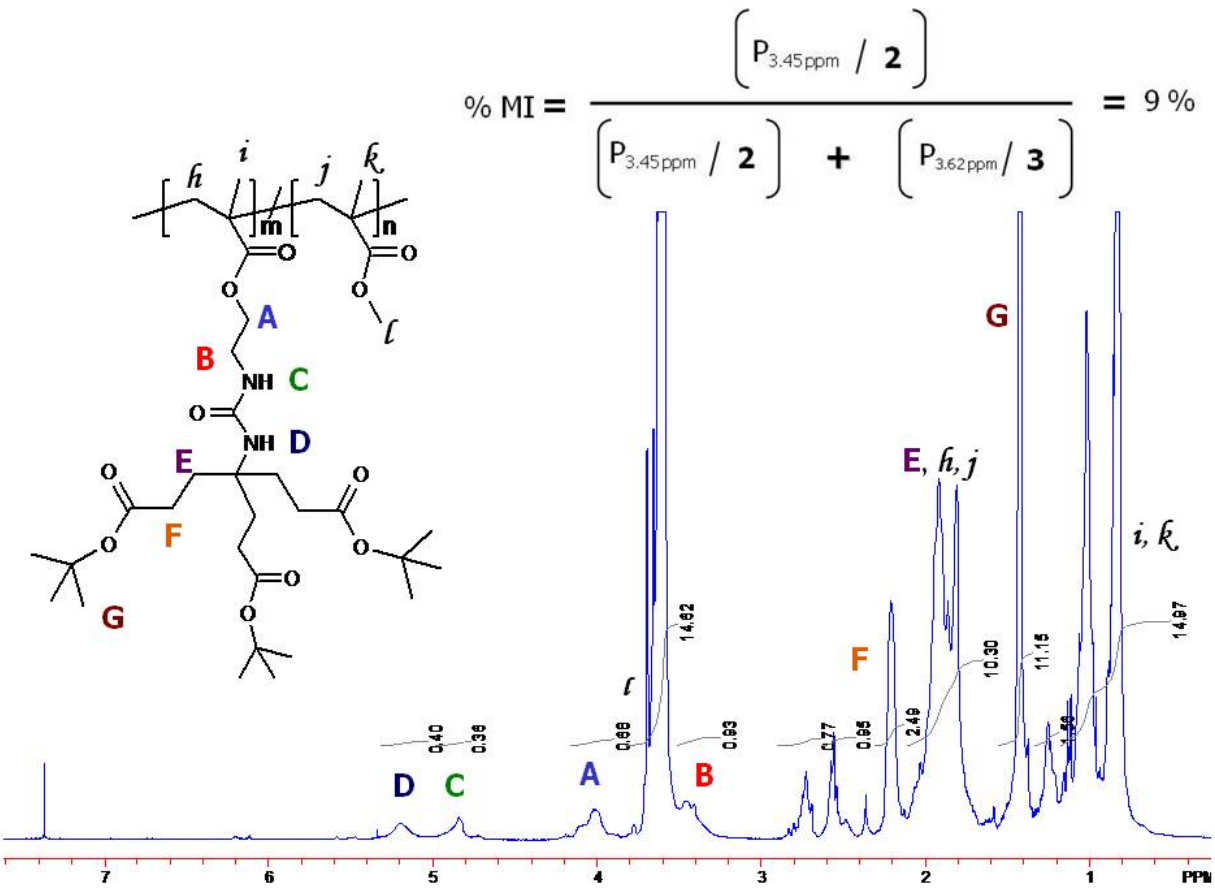

Figure 43. ^{1}H NMR ($CDCl_3$) of MI/MMA copolymer (5:95).

	MI (mol%)		M_n (10^3) (g/mol)	PDI	DP	TGA (°C, $T_{5\%}$)	T_g (°C)
	Monomer Feed	Copolymer Composition				Air	
MMA	0	0	4.3	1.3	43	264	85
	5	9	3.1	1.2	22	211	66
	10	13	4.7	1.2	29	206	66
	25	24	5.2	1.4	24	203	61

Table 6. Copolymer series of MI and MMA.

4.5 Molecular Weight Characterization

The characterization of dendronized polymers via conventional methods can prove challenging.[136] For instance, size exclusion chromatography (SEC) is only useful if the hydrodynamic volume of the polymer under consideration and the polymer used for calibration, typically polystyrene, are in the same range.[198] However, the hydrodynamic volume of dendronized polymers strongly deviates from that of polystyrene. The steric-induced spatial demand of dendron substituents causes a random polymer coil to stretch and subsequently stiffens the polymer chain.[136] This phenomenon results in an increased hydrodynamic volume causing the molar mass reported from SEC to be larger than the actual molar mass. As one can imagine, this effect is propagated as the dendron generation is increased. Additionally, dendronized polymers have a much larger mass per unit length compared to polystyrene. As a

result, an opposing effect is observed in SEC; the molar mass reported from SEC, based on comparison with polystyrene standards, is lower than the true molar mass. For these reasons, SEC methods that rely on relative means to determine molecular weight are not applicable in dendronized systems; methods that report absolute measurements are necessary. Light scattering (LS) is one such method; however, this method may be complicated by the fact that aggregation is common for these polymers.

4.5.1 SEC Analysis of Dendronized Homopolymers

The novel dendritic methacrylate macromonomer, **MIII**, was polymerized via conventional free radical polymerization in acetonitrile (50–60 wt%) employing AIBN as an initiator (1 mol%). Successful reactions resulted in a white precipitate. Analysis of the precipitate via ^{1}H NMR confirmed polymerization by 1) the absence of the peaks attributed to the vinyl protons of the macromonomer and 2) a significant broadening of the remaining peaks. In addition to ^{1}H NMR, the dendronized homopolymers were also characterized with TGA, DSC, and SEC. Four homopolymers were synthesized and characterized: P**MIII A**, **B**, **C** and **D**.

The thermal stability of the P**MIII** homopolymers was analyzed via TGA from 40 to 600 °C at a ramp rate of 10 °C/min. In general, the results were similar for each of the three polymers analyzed (**A**, **B**, and **C**); however, homopolymer **A** exhibited a lower $T_{5\%}$ (203 °C) compared to **B** (218 °C) and **C** (215 °C).

In DSC analysis, a range of glass transition temperatures, 52–66 °C, was observed for P**MIII** homopolymers. Homopolymer **A** exhibited the lowest T_g. Variations in the thermal analysis data, including TGA, among the homopolymer replicates were attributed to fractionation during purification via precipitation. Purification of homopolymer **A** (T_g = 52 °C) was achieved via precipitation of chloroform solutions in hexanes at room temperature.

Homopolymers **B** (T_g = 65 °C), **C** (T_g = 66 °C), and **D** (T_g = 59 °C) were precipitated from dichloromethane solutions in cold hexanes, chilled at -20 °C prior to use. It is possible that the homopolymers **B**, **C**, and **D** were fractionated to a lesser extent in the chilled hexanes procedure compared homopolymer **A**, which was precipitated from chloroform in hexanes at room temperature. These claims may be substantiated via characterization of molecular weight; however, analysis of the P**MIII** homopolymers via SEC proved challenging.

P**MIII** homopolymers were analyzed via SEC in multiple solvent systems (THF, $CHCl_3$, and 0.05M LiBr/NMP) employing various detectors (refractive index, viscosity, MALLS, and triple detection).

Homopolymer P**MIII A** was analyzed in THF on a SEC equipped with MALLS and RI detectors. In THF, narrow peaks with significant tailing were observed (**Figure 44**). The data suggested that the polymer was aggregating in and/or sticking to the column; in which case, the resulting molecular weight data may exclude low molecular weight species and predict high molecular weights. Regardless the reason, the significant tailing made it impossible to determine an accurate baseline; as a result, the molecular weight data obtained for homopolymer P**MIII A** was deemed inaccurate and unreliable, and alternative means were investigated.

Homopolymer P**MIII D** was analyzed in $CHCl_3$ on a SEC equipped with RI and viscosity detectors; universal calibration was employed. Inspection of the chromatograph revealed a relatively monomodal peak. Homopolymer P**MIII D** exhibited a number-average molecular weight of 2,660 g/mol (DP=5) and a PDI of 1.3. Given that this polymer was prepared without MMP, high molecular weight polymer was anticipated. This may be evidence of the ineffectiveness of the RI detector to accurately predict the molecular weight of dendronized polymers, which have a much larger mass per unit length compared to polystyrene standards. As

a result, the true molar mass should be higher than the SEC molar mass obtained. However, an effective measure of molecular weight would be needed to confirm such a conclusion.

In an effort to achieve a series of polymers of varying molecular weight, four dendronized homopolymers were prepared at various MMP concentrations (0, 0.5, 1.0, and 10 mol% MMP): P(**MIII**)$_0$, P(**MIII**)$_{0.5}$, P(**MIII**)$_{1.0}$, and P(**MIII**)$_{10}$. SEC analysis of these homopolymers in THF employing MALLS and RI detectors resulted in chromatographic traces with broad tailing similar to that observed for homopolymer P**MIII A** (**Figure 45**). As a result, the data was deemed unreliable and molecular weight data was not obtained.

The P**MIII** homopolymer series prepared with varying MMP concentrations was also analyzed in 0.05M LiBr in NMP on a SEC equipped with triple detection–RI, right-angle light scattering, and viscosity detectors. Overall, low intensity signals were observed; the largest signal resulted from the RI detector; in most cases, a signal from the light scattering was not detectable. Broad, relatively monomodal peaks with tailing were observed. It is noteworthy that tailing was also observed in the LiBr/NMP system. For the homopolymers prepared with 0 or 0.5 mol% MMP, the LiBr/NMP system predicted number-average molecular weights between 300 and 500K with PDIs ranging from 1.6 to 2.6; based on these results, the DP of the homopolymer series ranged from 500 to 850. Given the fact that steric congestion of the polymerization site is known to be an issue with this system and that they were achieved by conventional free radical polymerization, molecular weights of this magnitude are most likely unobtainable. The homopolymer prepared with 1.0 mol% MMP had a number-average molecular weight of 2,420 g/mol and PDI of 16.3; the homopolymer prepared with 10 mol% MMP exhibited a number-average molecular weight of 1 and PDI of 1. After analysis, it was

determined that the instrument had been calibrated for high molecular weights, and could not accurately predict "low" molecular weight samples.

The LiBr/NMP system with triple detection did not seem to effectively predict number-average molecular weight for the dendronized homopolymers. However, intrinsic viscosity data obtained from this analysis revealed a trend which may serve as an approximation of relative molecular weight (**Table 7**) among the series. In this analysis, intrinsic viscosity was shown to decrease as a function of increasing MMP concentration; this trend confirms that a series of dendronized homopolymers with a gradient of molecular weights was achieved.

Homopolymer samples were analyzed in LiBr/NMP employing universal calibration with polystyrene standards (3–127K) and the RI and viscosity detectors; the right-angle light scattering detector was not included. P**MIII** homopolymer prepared without MMP (P**MIII C/** P(**MIII**)$_0$) exhibited a broad, relatively monomodal peak with tailing, and a number-average molecular weight of 292K and PDI of 3.6. P(**MIII**)$_{10}$, the homopolymer prepared with 10 mol% MMP, was also analyzed; a number-average molecular weight of 12,040 g/mol and PDI of 1.4 were obtained. Inspection of the chromatographic trace revealed a broad peak with non-distinct shoulders; the peak was not monomodal. Based on what is known of the synthesis, the general trend is correct. In the absence of MMP, high molecular polymer weight was expected; in the case of 10 mol% MMP, low molecular weight polymer was expected.

For comparison, a **MIII**/MMA copolymer, 25 mol% **MIII,** prepared with 10 mol% MMP was also analyzed. A number-average molecular weight of 5,500 g/mol and PDI of 1.5 were obtained. The same copolymer was analyzed in THF on a SEC equipped with a MALLS detector; from this analysis, a number-average molecular weight of 4,800 g/mol and PDI of 1.4 were obtained. Given that the data obtained from two different systems correspond relatively

well for the “low” molecular weight copolymer, the issues with characterization of the dendronized homopolymers may be attributed to the polymers themselves and not the instrumentation.

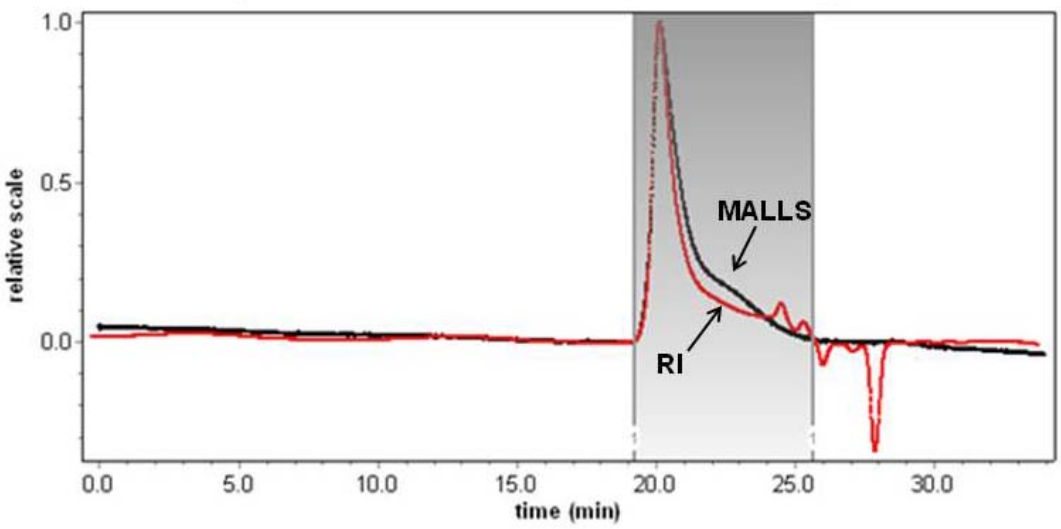

Figure 44. PMIII homopolymer analyzed via SEC in THF.

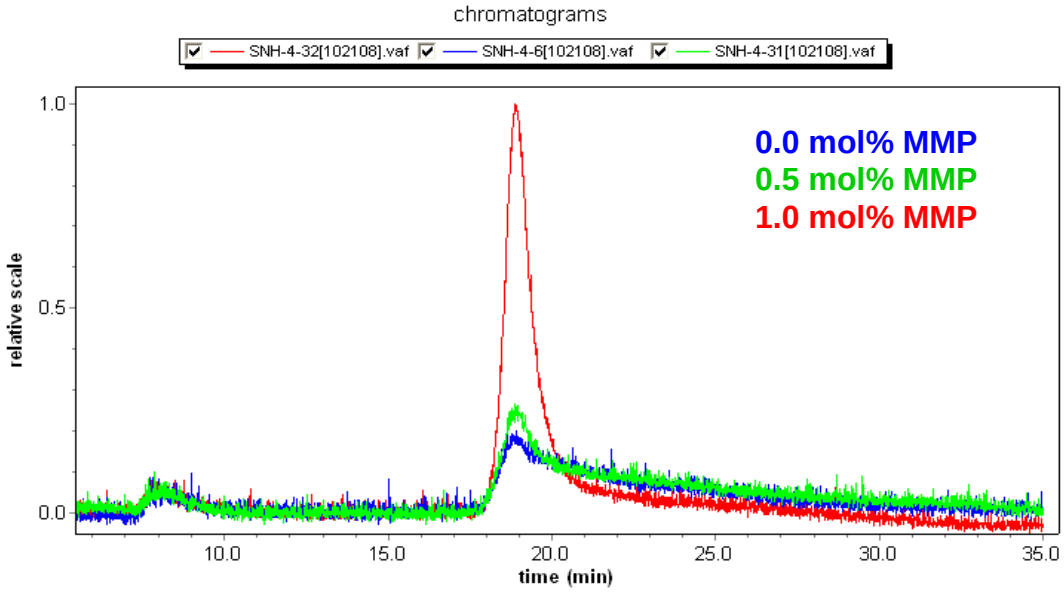

Figure 45. PMIII homopolymer series analyzed via SEC in THF.

MMP (mol%)	IV (dL/g)	T_g (°C)
1.0 mol % AIBN	0.05M LiBr/NMP	
0	0.300	65
0.5	0.283	65
1.0	0.076	63
10	0.039	55

Table 7. Intrinsic viscosity as a function of MMP concentration from SEC in 0.05M LiBr/NMP.

4.5.2 MALDI-TOF MS Analysis of Dendronized Homopolymers

Matrix-assisted laser desorption/ionization time of flight mass spectrometry (MALDI-TOF MS) is a powerful technique for the determination of absolute mass; mass spectrometric analysis of polymers is becoming of increasing importance.[199] The series of dendronized homopolymers prepared with varying MMP concentrations were analyzed via MALDI-TOF MS; however, data was only obtained for P(**MIII**)$_{10,}$ the polymer prepared with the highest MMP concentration (10 mol%), which would intuitively be the lowest molecular weight polymer. Upon inspection of the spectrum (**Figure 46**), each peak represented a different degree of polymerization, as expected. The peak-to-peak distance was 584.7, the molecular mass of the **MIII** macromonomer. The mass exhibited by each peak represented the mass of the repeat unit, MMP end-groups, and sodium. The polymer was assumed to be end-capped by MMP, 120.17 g/mol; the degree of polymerization was determined by subtracting the mass of the end-groups and sodium (23 g/mol) and dividing the resulting mass by the mass of the repeat unit, 584.7 g/mol. The base peak, 2481 m/z, represented a degree of polymerization of 4. For the same

sample, a degree of polymerization of 6 was determined by end-group analysis in ^{1}H NMR, which correlated to a number-average molecular weight of 3,628 g/mol (End-group analysis discussed in Section 4.4.4).

Analysis via MALDI-TOF MS confirmed polymerization of the novel dendritic macromonomer; it also confirmed that low molecular weight polymers were achieved employing MMP (10 mol%) and the presence of MMP end-groups.

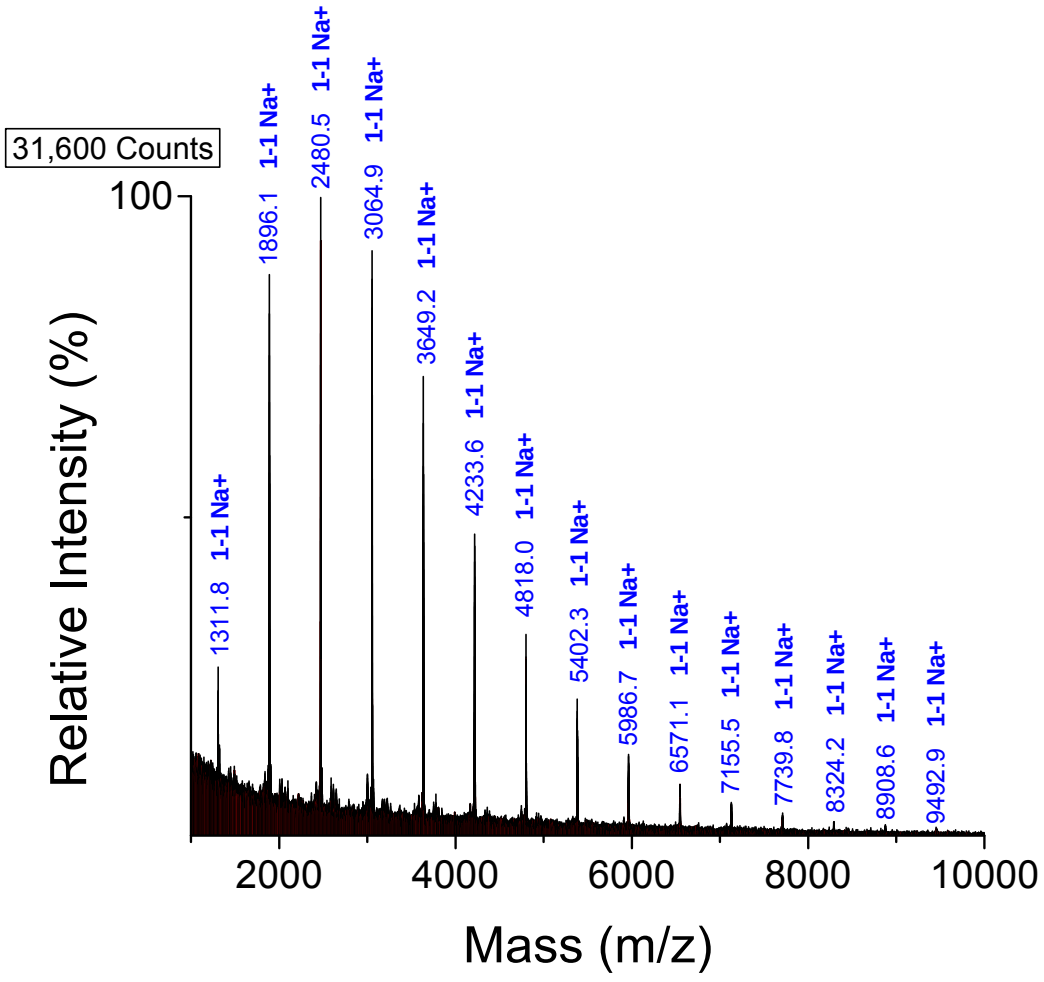

Figure 46. MALDI-TOF spectrum for PMIII homopolymer (10 mol% MMP).

4.5.3 SEC Analysis of Dendronized Copolymers

Macromonomer **MIII** was copolymerized with MMA; the copolymer composition was varied in **MIII** from 5 to 50 mol%. Copolymers were achieved via conventional free radical polymerization in acetonitrile employing AIBN as an initiator (1.0 mol %) at a total monomer concentration of 10 wt%. Precipitation of $CHCl_3$ solutions in hexanes at room temperature resulted in a white precipitate.

SEC analysis in THF was employed to characterize the molecular weight of the copolymer series; absolute values from the MALLS detector were reported. In general, the number-average molecular weight increased as the copolymer composition was increased in **MIII** (**Table 2**). At low **MIII** content, the copolymers are predominantly poly(methyl methacrylate)s. As a result, the tailing observed for the dendronized homopolymers was not observed. However, inspection of the chromatographs revealed that tailing does occur as the copolymer composition was increased in **MIII**. As shown in **Figure 47**, tailing becomes obvious at 30 mol% **MIII** and propagates with the incorporation of 50 mol% **MIII**.

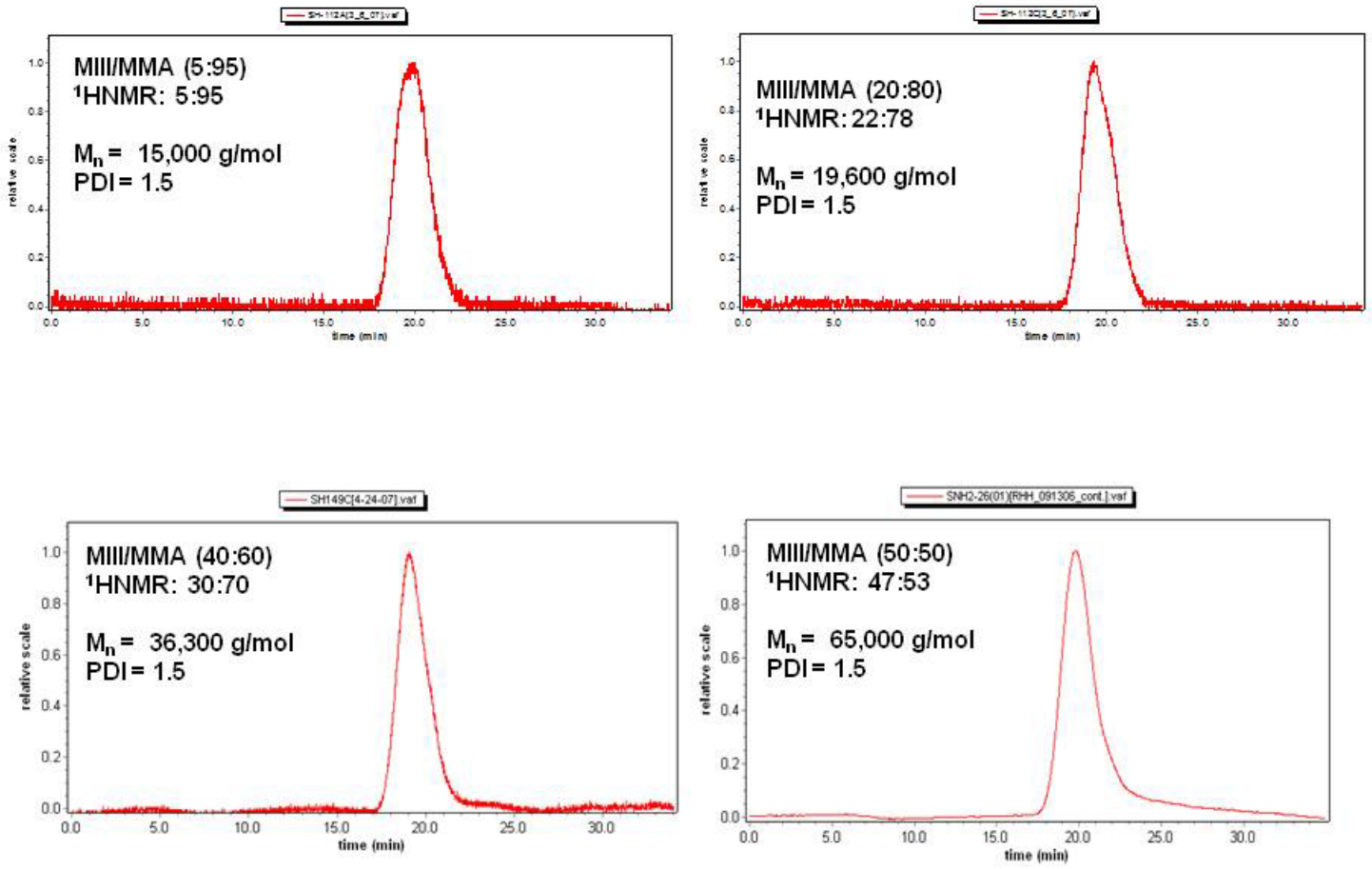

Figure 47. SEC chromatographs of MIII/MMA copolymers analyzed in THF.

Comparison of data obtained from the MALLS and RI detectors revealed a significant discrepancy. In **Figure 48**, the chromatographic traces from both the RI and MALLS detectors are depicted for two **MIII**/MMA copolymers. The number-average molecular weight determined from the RI detector was significantly lower than that determined from the MALLS detector; larger PDIs were obtained employing the RI detector. Chromatographic traces from the RI detector for PMMA and two **MIII**/MMA copolymers analyzed in THF are shown in **Figure 49**. In each case, the elution time was approximately twenty-one minutes; however, significantly lower Mp values were observed for the copolymers compared to PMMA. Employing the MALLS detector, PMMA exhibited a number-average molecular weight of 15,400 g/mol which was more comparable to the **MIII**/MMA copolymers than observed with the RI detector. This result is further evidence of the fact that the RI detector does not accurately predict molecular weight of the dendronized polymers even at low **MIII** content.

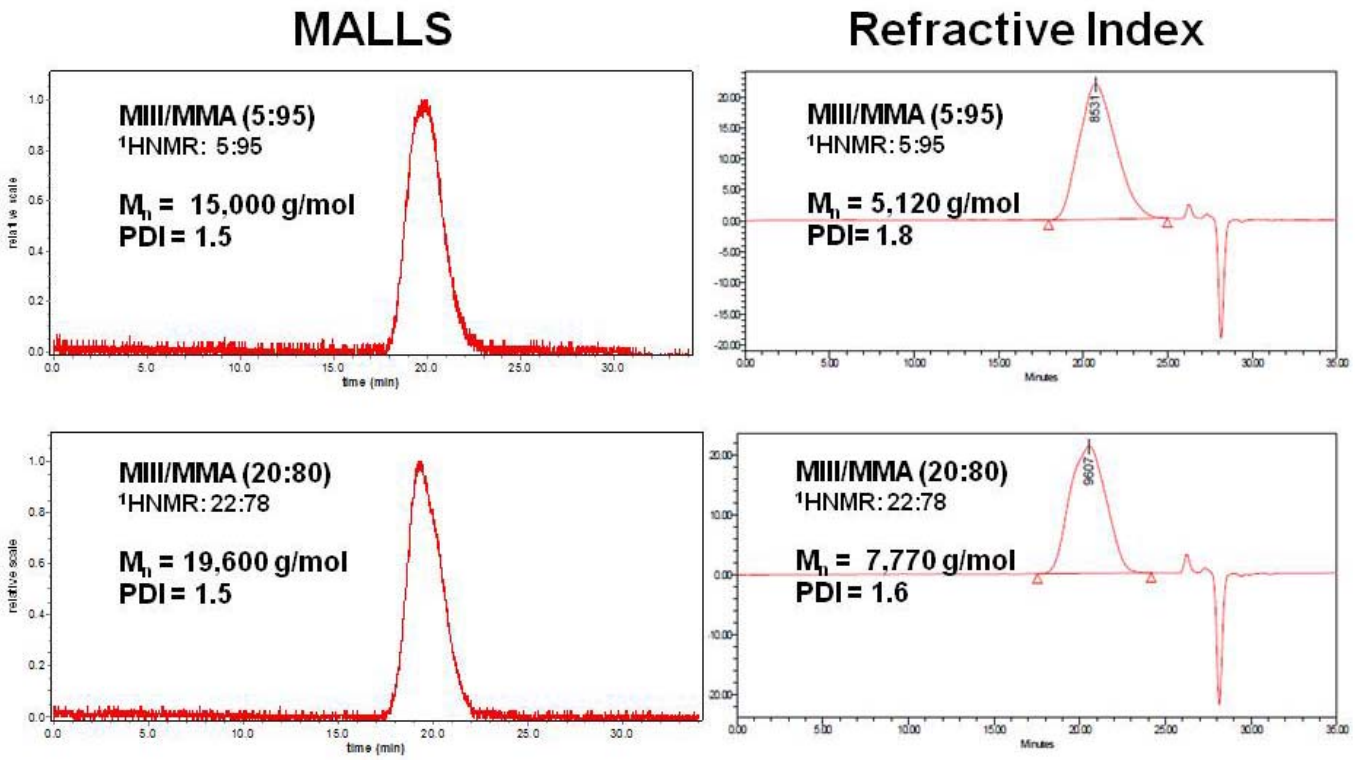

Figure 48. SEC chromatograms from MALLS and RI detectors for MIII/MMA copolymers.

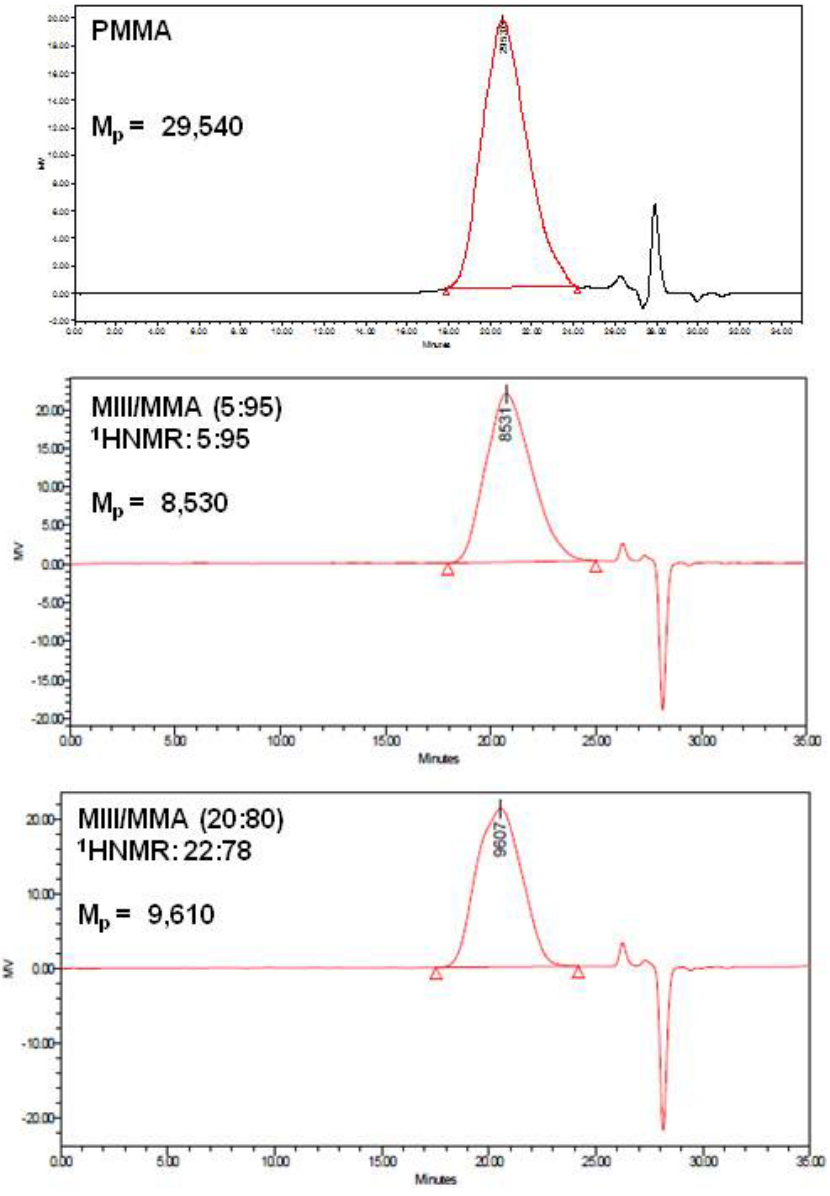

Figure 49. SEC chromatographs from Refractive Index detector.

Low molecular weight dendronized amphiphilic copolymers prepared from the novel dendritic methacrylate macromonomer, **MIII**, and various alkyl methacrylates were the major goal of this research. Methyl, ethyl, and *n*-butyl methacrylate were employed as alkyl methacrylate comonomers. For each alkyl methacrylate, a series of copolymers was prepared with varying **MIII** content: 5, 10, and 25 mol%. Conventional free radical polymerization was carried out in acetonitrile (10 wt % total monomer concentration) at 70 °C employing AIBN (1.0 mol %) as a free radical initiator, and methyl 3-mercaptopropionate (MMP) (10 mol %), a chain transfer agent, was used to limit the degree of polymerization (DP).

Molecular weight characterization was achieved via SEC employing a MALLS detector. Manufacturers of MALLS detectors claim that a monodisperse polystyrene sample of very low molecular weight, as low as 580 g/mol, can be measured accurately by SEC-MALLS; however, this claim received considerable criticism in the polymer community. Xie et al.[200] confirmed the manufacturers' claim through critical examination of the reliability of SEC-MALLS in characterizing absolute molecular weight and molecular weight distribution in the low molecular weight region (2500–10,000) using poly(diisopropyl trimethylene-1,1-dicarboxylate) samples prepared by living anionic ring-opening polymerization. Molecular weights determined by four different analytical techniques were compared: end-group analysis via ^{1}H NMR, vapor pressure osmometry (VPO), SEC-MALLS, and MALDI-TOF MS. The number-average molecular weight data obtained from SEC-MALLS was in agreement with VPO and MALDI-TOF. Saito et al.[201] performed a similar reliability study employing polystyrene certified reference materials (CRMs) whose molecular weights ranged from 500 to 2400 g/mol. Average molecular weights were determined by SEC-MALLS, conventional static light scattering (SLS), MALDI-TOF MS, and ^{1}H NMR and compared with the certified values which were determined by supercritical

fluid chromatography (SFC). For the PS2400 sample, SEC-MALLS data compared well with SFC data; the relative difference between the certified weight-average molecular weight by SEC and that by SEC-MALLS was 5%. However, discrepancies were observed for the PS500 sample. Based on these studies, analysis of the low molecular weight (3,000–10,000 g/mol) polymers by SEC-MALLS should be feasible.

The copolymer series (**MIII**/MMA, **MIII**/EMA, and **MIII**/*n*BMA), prepared with 10 mol% MMP, were analyzed via SEC in THF employing a MALLS detector. For the **MIII**/MMA series, the data obtained revealed the same trends observed for the copolymer series prepared in the absence of MMP–molecular weight increased as the copolymer composition was increased in **MIII**. However, the copolymer series prepared in the presence of MMP exhibited significantly lower molecular weights and PDIs, as anticipated. In the model study of PMMA, MMA was polymerized at various MMP concentrations and the resulting polymers were characterized via SEC in THF employing the MALLS detector (**Table 3**). In the absence of MMP, 'high' molecular weight (15,000 g/mol) polymer with a PDI of 1.7 was obtained. Polymerizations performed in the presence of MMP (5 or 10 mol%) resulted in 'low' molecular weight PMMA (4,300 and 6,700 g/mol) and low PDIs (1.2 and 1.3). From this model study, it may be concluded that the low PDIs observed may be attributed to the high concentration of MMP used, and are not necessary a unique characteristic of the dendronized copolymers themselves.

The **MIII**/MMA and **MIII**/EMA copolymer series prepared in the presence of MMP were analyzed in 0.05M LiBr/NMP on a SEC equipped with triple detection (RI, viscosity, and right-angle light scattering) and in THF on a SEC equipped with MALLS and RI detectors. SEC data from both systems are reported in **Table 8**; data from the MALLS and RI detectors are reported

for the THF system. In general, number-average molecular weight increased as the copolymer composition was increased in **MIII** and low PDIs were obtained; this trend was observed for each system. In THF, the RI detector consistently predicted lower molecular weights than the MALLS detector; this trend was observed, to a much larger extent, for the 'high' molecular weight **MIII**/MMA copolymer series (prepared without MMP). The difference between the values determined from the MALLS and RI detectors seems to increase as a function of increasing **MIII** content. The molecular weight data from the MALLS detector in THF corresponds relatively well with the data obtained from the LiBr/NMP system; the greatest deviation occurs for the copolymer with 25 mol% **MIII**. These data confirm that low molecular weight copolymers (~4,000–9,000 g/mol) were achieved as targeted.

For consistency, molecular weight characterization was performed in THF with the SEC system equipped with the MALLS detector for all copolymers synthesized in this research.

	MIII (mol%)		THF MALLS		THF RI		LiBr/NMP		
	Monomer Feed	Copolymer Composition	M_n (10^3) (g/mol)	PDI	M_n (10^3) (g/mol)	PDI	M_n (10^3) (g/mol)	PDI	T_g (°C)
MMA									
	5	5	4.2	1.2	3.7	1.2	3.9	1.3	71
	10	10	4.8	1.2	4.5	1.3	5.2	1.3	67
	25	23	8.8	1.1	5.6	1.2	6.8	1.2	58
	5	7	2.8	1.4	2.7	1.4	3.7	1.4	66
	10	11	5.1	1.2	3.1	1.4	4.9	1.3	65
	25	23	4.8	1.4	3.7	1.4	6.2	1.3	59
EMA									
	5	9	4.4	1.2	4.2	1.2	5.7	1.2	52
	10	14	4.7	1.2	3.9	1.3	5.5	1.3	48
	25	26	6.3	1.2	4.6	1.2	6.9	1.2	51

Table 8. SEC characterization of MIII/XMA copolymers in THF and LiBr/NMP.

4.5.4 End-Group Analysis

In search of a secondary means by which to determine molecular weight, end-group analysis via ^{1}H NMR was investigated. Spectroscopic analysis of dendronized polymers has been shown to be difficult due to the considerable molecular weight of the repeat units; the proportion of polymer backbone to dendron substituent may become so unfavorable that NMR spectroscopy reaches its limits.[136] However, provided that well resolved peaks can be identified for the end-groups, end-group analysis may be successfully employed. For polymers prepared with 10 mol% MMP; integration of the methylene peaks of MMP were used to determine the degree of polymerization, and to subsequently calculate number-average molecular weight. In some cases, the protons of methoxy methyl of MMP were used.

Equation 3 describes the calculations used to determine number-average molecular weight via end-group analysis. For the random copolymers, the copolymer composition and molecular weight of each comonomer were taken into consideration. The number-average molecular weights determined from both end-group analysis and SEC-MALLS are reported in **Table 9**. End-group analysis of the dendronized copolymers was based on the assumption that all polymer chains possessed a MMP terminus. Although polymerization was initiated with AIBN, given the high concentration of MMP employed, this is a sound assumption. Analysis of the P(**MIII**)$_{10}$ homopolymer via MALDI-TOF MS confirmed the absolute mass as the proposed repeat unit with MMP end-groups.

Number-average molecular weights determined via end-group analysis in ^{1}H NMR were similar among each series; a trend was not discernable. Conversely, a distinct trend was observed in SEC analysis; the molecular weight increased as a function of increasing **MIII** content. The number-average molecular weights obtained from SEC were 2–4 times greater than

those from end-group analysis; the difference between the two values increased with increasing **MIII** content.

End-group analysis revealed a decrease in the degree of polymerization (DP) as a function of increasing **MIII** content. This result may be attributed to the bulky nature of the dendronized macromonomer which has been shown difficult to polymerize due to steric hindrance of the polymerization site (Section 4.2.1). SEC data revealed a decrease in DP for copolymers with □20 mol% **MIII** but an increase in DP at ≥ 20 mol% **MIII**, which may highlight the ineffectiveness of the system to characterize dendronized polymers. In SEC-MALLS, the increase in DP observed at ≥ 20 mol% **MIII** may be attributed to increased mass per unit length attributed to the incorporation of the very dense dendritic macromonomer. However, the increase in DP may also be attributed to aggregation. DP was shown to increase further with the incorporation of 70 mol% **MIII** in the analysis of the **MIII**/*n*BMA series.

These results are evidence of the fact that the branched nature of the dendronized copolymers plays a role in analysis via SEC. However, each method confirms the polymerization of low molecular weight copolymers.

Alternative methods of molecular weight determination may be employed. Other methods employed in this regard include scanning force microscopy (SFM) and analytical ultracentrifugation [189], small angle neutron scattering (SANS)[202] and vapor pressure osmometry (VPO).

$$X_n = M_n / M_0 = \#\ \text{repeat units}$$

$$M_0 = x\,(\mathbf{XMA}\ \text{r.p. unit}) + y(\mathbf{MIII}\ \text{r.p. unit})$$

XMA = alkyl methacrylate

y = % MIII (determined from Eq. 1)
x = 1 - % MIII

From NMR:

$$\#\ \text{repeat units} = \left[x\,(P_a / \#\ \text{protons}) + y\,(P_b / \#\ \text{protons})\right] / (P_c / \#\ \text{protons})$$

P_a = integration of peak representative of monomer 'a'
P_b = integration of peak representative of monomer 'b'
P_c = integration of peak representative of MMP end group

$$M_n = (M_0\ X\ \#\ \text{repeat units}) + MW\ MMP\ \text{end groups}$$

Equation 3. Number-average molecular weight determined by end-group analysis.

	% MIII	M_0 (g/mol)	M_n (g/mol)	X_n	M_n (g/mol)	X_n
			^{1}H NMR	^{1}H NMR	SEC	SEC
MIII/MMA						
	0	100	2623	25	4300	43
	5	124	2109	16	4200	34
	10	149	2349	15	4800	32
	23	212	2025	9	8800	42
	100	585	3628	6	-	-
MIII/EMA						
	9	157	2311	14	4400	28
	14	180	2640	14	4700	26
	26	237	2722	11	6400	27
MIII/nBMA						
	3	156	3541	22	2600	17
	6	169	3665	21	3100	18
	25	253	2138	8	5400	21
	65	430	3559	8	12600	29

Table 9. Molecular weight determined via End-group analysis vs SEC.

4.6 Acidolysis of Dendronized Homo- and Copolymers

Ionomers, ion-containing polymers in which the bulk properties are governed by ionic interactions in discrete regions of the material[203], are of much interest as ion-selective membranes, reversible crosslinkers in thermoplastic elastomers, self-healing polymers, and in biological applications requiring electrostatic attractions. Deprotection of the *tert*-butyl ester functional dendronized homo- and copolymers yielded carboxylic acid functional polymers that may be ionized–polyelectrolytes. In addition to being polyelectrolytes, deprotection of the homo- and copolymers yielded amphiphilic dendronized homo- and copolymers. Amphiphilicity or hydrophilic/hydrophobic ratio of the copolymers may be varied by manipulation of the copolymer composition in two ways: 1) hydrophilic/hydrophobic ratio may be modified by varying the ratio of the alkyl methacrylate and **MIII** comonomers, and 2) hydrophobicity may be modified by varying the length of the aliphatic chain of the alkyl methacrylate comonomer.

Amphiphilic dendronized polymers were achieved via acidolysis of the dendronized homo- and copolymers in trifluoroacetic acid (TFA) at room temperature. After the reaction, the TFA solutions were diluted with CH_2Cl_2 and a series of solvents (CH_2Cl_2, MeOH, and Et_2O in this order) were employed as chase solvents via roto-evaporation to remove the acid and residual chase solvent. Subsequently, the polymers were dried under vacuum at 50 °C (excluding the *n*BMA copolymer series).

^{1}H NMR analysis served as confirmation of successful deprotection (**Figure 50**). The *tert*-butyl ester protons of the ester functional polymer correspond to a large singlet at ~1.4 ppm. After treatment with TFA, the peak at ~1.4 ppm was significantly reduced. The small peak that

remained was attributed to the alkyl methacrylate repeat unit, which was also observed in the spectrum of the PMMA homopolymer (**Figure 51**).

The resulting carboxylic acid functionality significantly increased intermolecular hydrogen bonding, which was evident by the increase in T_g observed for the acid functional copolymers compared to the corresponding esters (**Table 10**). In general, the T_gs of the acids increased with increasing **MIII** content —more acid groups, increased hydrogen bonding. This was also evident in the magnitude of increase (ΔT_g) along the series. For the **MIII**/MMA copolymer series, the glass transition temperature increased by 12–17 °C for the acids. Analysis of the deprotected **MIII**/EMA copolymer series revealed increases in T_g from 8 to 32 °C. The T_gs of the deprotected **MIII**/*n*BMA copolymers also increased as a function of **MIII** content. The magnitude of increase ranged from 8 to 31 °C for copolymers with 5–25 mol% **MIII**; however, a decrease in ΔT_g was observed for the copolymer with 70 mol% **MIII**.

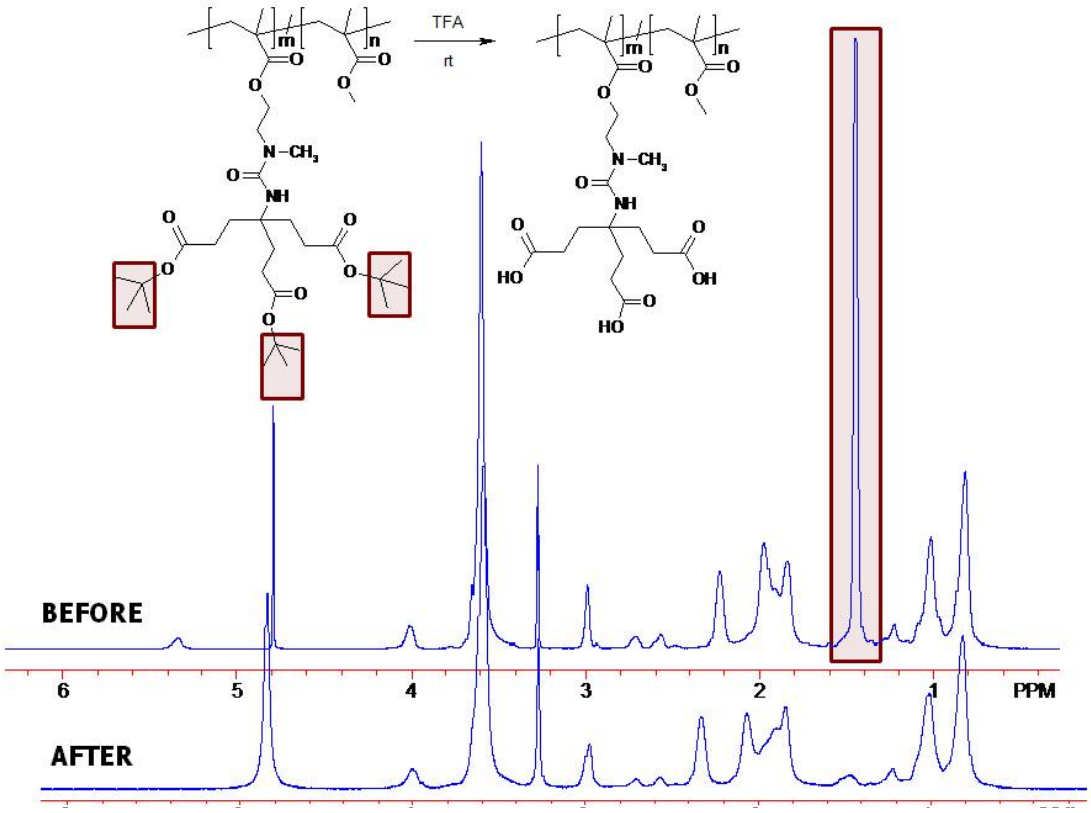

Figure 50. ^{1}H NMR ($CD_3OD/CDCl_3$): Acidolysis of MIII/MMA copolymer in neat TFA.

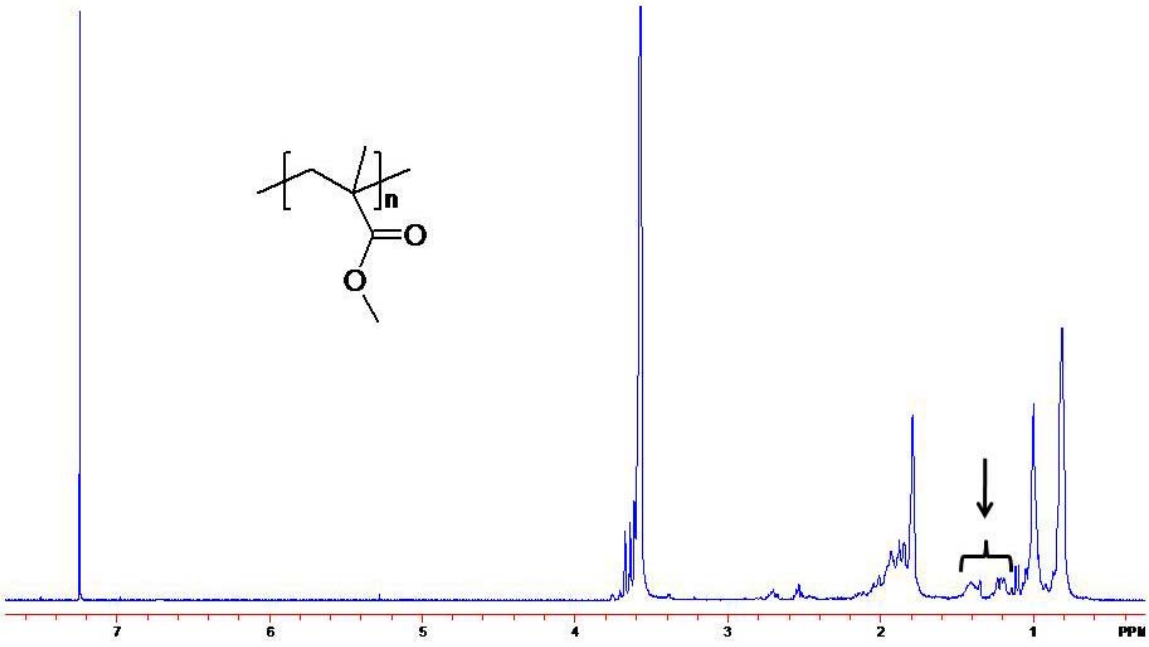

Figure 51. ^{1}H NMR ($CDCl_3$): PMMA homopolymer.

MIII	ESTER	ACID	
	T_g (°C)	T_g (°C)	ΔT_g
MMA			
5	73	85	12
10	67	80	13
25	58	75	17
EMA			
5	52	60	8
10	48	68	20
25	51	83	32
nBMA			
5	24	32	8
10	30	58	28
25	31	62	31
70	44	68	24

Table 10. Glass transition temperatures of carboxylic acid functional copolymers.

A series of **MIII** homopolymers prepared from varying concentrations of the chain transfer agent, methyl 3-mercaptopropionate (MMP), were prepared; deprotection of the homopolymer series was also achieved via treatment with TFA. The glass transition temperatures of the esters and their corresponding acids are reported in **Table 11**. As was observed with the ester functional copolymers, the T_gs of the acid functional copolymers decreased as a function of increasing MMP concentration. The magnitude of change (ΔT_g) also decreased as function of increasing MMP concentration. These trends were attributed to the molecular weight trend resulting from varying MMP concentration. At high MMP concentration, low molecular weight polymers were expected; and as a result, lower T_gs were expected. The homopolymers prepared with little or no MMP were expected to have higher number-average molecular weights and as a result more acid groups. In general, the trend observed for the **MIII** homopolymers is the same trend observed for the **MIII** copolymer series–more acid groups resulted in increased T_gs as a result of a greater number of acid groups and increased intermolecular hydrogen bonding.

	ESTER	ACID	
	T_g (°C)	T_g (°C)	ΔT_g
% MMP			
0	65	86	21
0.5	65	87	22
1	63	77	14
10	51	61	10

Table 11. Glass transition temperatures of carboxylic acid functional homopolymers.

4.7 Solubility in Biologically Compatible Media

4.7.1 Solubility in aqueous triethanolamine solutions

Biological assays of the dendritic amphiphiles reported by Gandour et al.[30, 31], on which the present work is based, were performed in aqueous solutions of triethanolamine (TEA). TEA is a weak base commonly used in cosmetic formulations. In this case, it affords aqueous solubility of the dendritic amphiphile and a loose ion pair. Solubility in biologically compatible media is a key issue in this research endeavor.

The dendronized amphiphilic copolymer series were dissolved in 5 w/v % aqueous triethanolamine (aq TEA) (12.5 mg/mL). In the synthetic design, the hydrophilic head group was expected to impart aqueous solubility despite the presence of the hydrophobic polymer backbone and hydrophobic copolymer repeat unit. **MIII** proved sufficient to solubilize the MMA series at 5, 10, and 25 mol% **MIII**. However, solubility becomes an issue as the aliphatic chain length of the alkyl methacrylate comonomer increased with the incorporation of ethyl methacrylate (EMA). For the EMA copolymer series, solubility was not achieved below 10 mol% **MIII**. Solubility continued to decrease with the incorporation of *n*-butyl methacrylate (*n*BMA). Even at the highest concentration (25 mol%), **MIII** was not sufficient to solubilize the *n*BMA copolymers; turbid solutions resulted. Dilution of these solutions (2.1 mg/mL) yielded no improvement. The *n*BMA copolymer series was expanded to further investigate the solubility issues. Interestingly, a highly loaded copolymer, 70 mol% **MIII**, also produced turbid solutions, which suggested that the issue may not be a lack of solubility but aggregation. **Table 12** summarizes the results of the solubility study in aq TEA.

	TEA (aq)	
	12.5 mg/mL	2.1 mg/mL
MI(OH)	Soluble	NA
MI(OH)/MMA		
5:95	Soluble	NA
10:90	Soluble	NA
25:75	Soluble	NA
MIII(OH)	Soluble	NA
PMIII(OH)	Soluble	NA
MIII(OH)/MMA		
5:95	Soluble	NA
10:90	Soluble	NA
25:75	Soluble	NA
MIII(OH)/EMA		
5:95	Insoluble	-
10:90	Soluble	NA
25:75	Soluble	NA
MIII(OH)/nBMA		
25:75	Insoluble - turbid	Insoluble - turbid
70:30	Insoluble - turbid	Insoluble - turbid

Table 12. Copolymer solubility in 5 w/v% aqueous triethanolamine.

4.7.2 Solubility in 0.05M Phosphate Buffer Solution

The solubilities of macromonomer **MIII**(OH), two P**MIII**(OH) homopolymers, two M**III**(OH)/MMA copolymers, and a poly(methacrylic acid) homopolymer P(**MAA**) were investigated in 0.05M PBS buffer solution. In each case, the sample was weighed in a vial, 0.05M PBS buffer solution was added via syringe, and the solution was agitated by hand. The macromonomer, **MIII**(OH) (7.9 mg in 0.5 mL 0.05M PBS), was soluble; a clear, homogeneous solution was observed. In 1 mL 0.05M PBS, slightly turbid solutions were observed for P**MIII**(OH) (12.4 mg) prepared with 0 mol% MMP and P**MIII**(OH) (12.3 mg) prepared with 1.0 mol% MMP. The poly(methacrylic acid) homopolymer prepared in the presence of 10 mol% MMP, P(**MAA**), (7.0 mg in 0.5 mL 0.05M PBS) was soluble; a clear, homogeneous solution was observed. Two samples from the **MIII**(OH)/MMA copolymer series were also investigated. The **MIII**(OH)/MMA (5 mol% **MIII**) copolymer (7.8 mg in 0.5 mL 0.05M PBS buffer solution) was partially soluble; a turbid solution with insoluble particulates was observed. The **MIII**(OH)/MMA (25 mol% **MIII**) copolymer (8.0 mg in 0.5 mL 0.05M PBS) was insoluble; a clear solution and insoluble particulates were observed.

Based on these results, 0.05M PBS buffer solution would be a suitable solvent in biological testing for the macromonomer and homopolymers but not for the **MIII**(OH)/MMA copolymer series.

4.7.3 Solubility of MAA/MMA copolymers in aqueous triethanolamine

The complexity of and multi-step synthesis required to prepare the dendronized amphiphilic copolymer series begs the question, are three acid groups more effective than one?

In an attempt to address this question, a copolymer series was synthesized from *tert*-butyl methacrylate (***t*BMA**) and methyl methacrylate, and subsequently deprotected to achieve poly(methacrylic acid-co-methyl methacrylate) (**MAA**/MMA) copolymers. The copolymer composition was varied in ***t*BMA** from 10 to 50 mol%. The resulting polymers represent an amphiphilic copolymer analogue of the dendronized system consisting of one acid group per hydrophilic repeat unit. Solubility being a key issue thus far served as a first approximation for comparison.

As illustrated in **Scheme 1**, the **MAA**/MMA copolymers were synthesized and deprotected in the same fashion as the dendronized amphiphilic copolymer series; characterization data for the series are reported in **Table 13**. **Figure 52** depicts the ^{1}H NMR spectrum of the ***t*BMA**/MMA copolymer (10 mol% *t*BMA) and the determination of its composition using **Equation 1**. The degree of polymerization, X_n, was determined via end-group analysis from ^{1}H NMR; using these data and the copolymer composition the number of acid groups was estimated to afford a means of direct comparison.

Solubility of the **MAA**/MMA series was investigated in 5 w/v % aqueous triethanolamine (aq TEA). The copolymers (25 mg) were dissolved in aq TEA (2.0 mL) and their solubility determined visually. In general, solubility increased as the copolymer composition was increased in methacrylic acid (**Scheme 1**). However, at 10 mol% **MAA**, the copolymer was completely insoluble; a clear, colorless solution with white solid particulates was observed. A solution of the **MAA**/MMA copolymer with 25 mol% **MAA** appeared turbid and solid particulates were observed; in this case, turbidity suggested dissolution to an extent. Increasing the **MAA** content to 50 mol% seemed to increase the solubility. Although the solution remained slightly turbid, it was less turbid than the solution of the 25:75 **MAA**/MMA copolymer and

insoluble particulates were not observed. Even in the case where the number of acid groups were comparable, the **MIII**(OH)/MMA copolymers were soluble while the **MAA**/MMA copolymers were only partially soluble. Based on these results, the ability of the methacrylic acid group to impart aqueous solubility proved inferior to that of the novel **MIII** macromonomer. The **MIII**(OH)/MMA copolymers were soluble in aq TEA even at low **MIII**(OH) content (5 mol%). Consequently, if 50 mol% **MAA** was insufficient to solubilize the MMA copolymer further issues are anticipated as the aliphatic chain length of alkyl methacrylate comonomer is increased. Based on these results, three acid groups per repeat unit are indeed more effective than one.

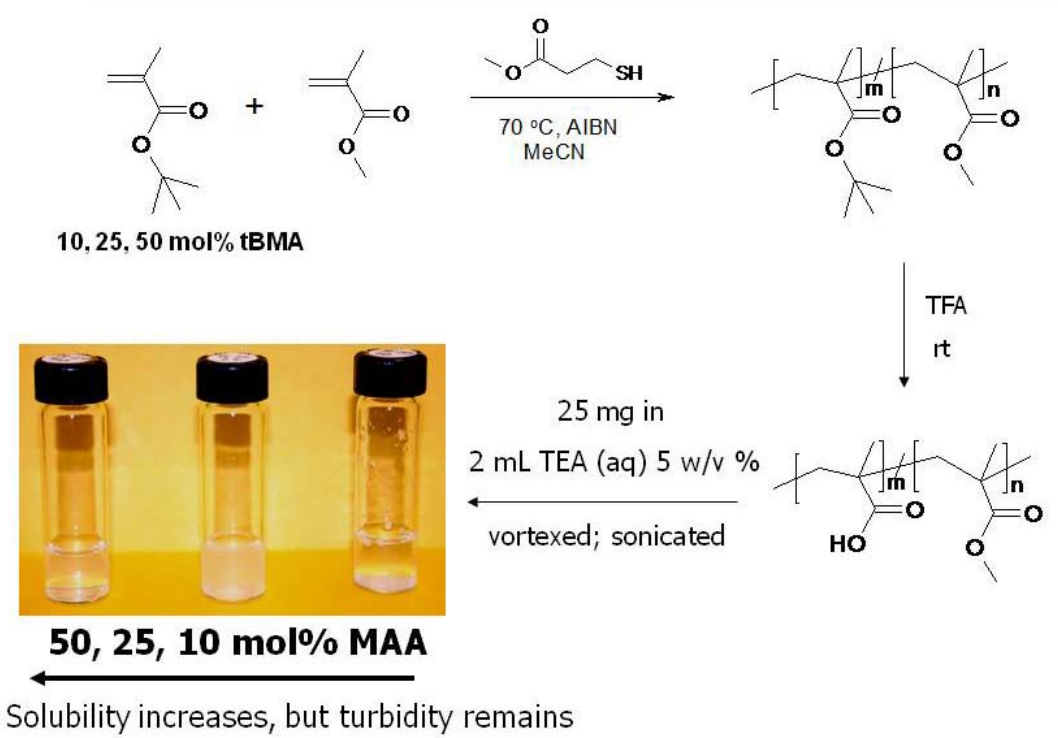

Scheme 1. Synthesis and solubility of MAA/MMA copolymers.

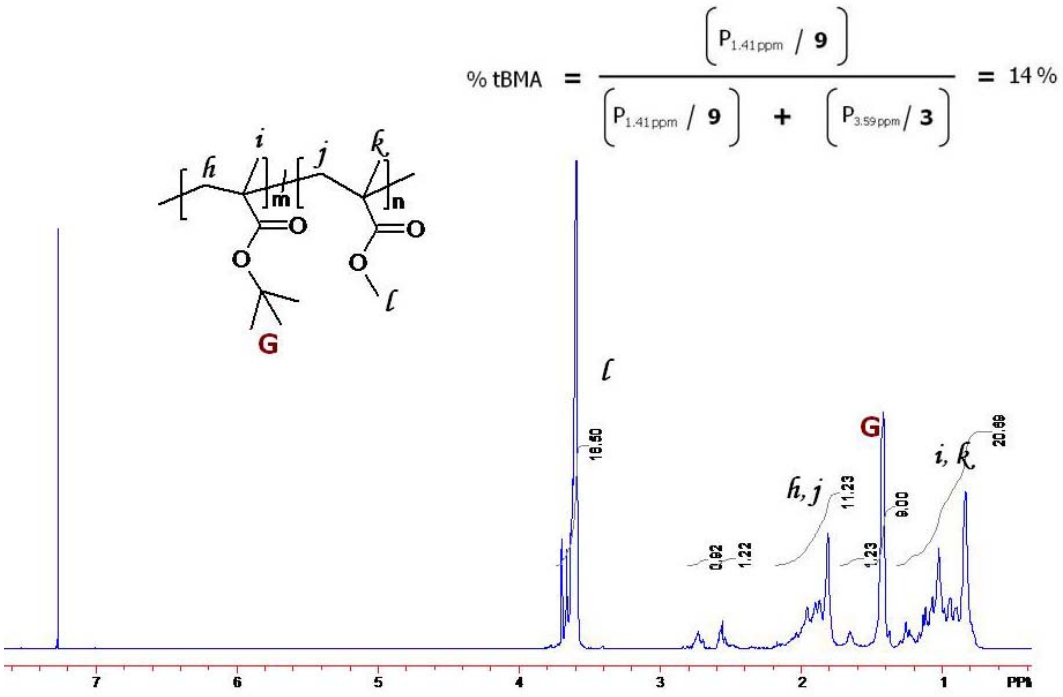

Figure 52. ^{1}H NMR spectrum: *t*BMA/MMA copolymer (10:90).

		X_n [a]	#COOH[b]	aq TEA[c]
MIII/MMA	% MIII			
Monomer Feed	Copolymer			
5	5	16	3	S
10	10	15	6	S
25	23	9	6	S
100	100	6	18	S
tBMA/MMA	% tBMA			
Monomer Feed	Copolymer			
10	14	12	2	I
25	25	11	3	PS
50	47	6	3	PS
100	100	18	18	PS

[a]Calculated from ^{1}H NMR. [b]Estimated from X_n. [c]Solubility in aq TEA.

Table 13. Characterization of *t*BMA/MMA and MAA/MMA copolymer series.

4.8 Preliminary Biological Studies

4.8.1 Antimicrobial Activity

The antimicrobial activity of dendritic macromonomer **MI**(OH), the **MI**(OH)/MMA copolymer series (5, 10, and 25 mol% **MI**), the **MIII**(OH)/MMA copolymer series (5, 10, and 25 mol% **MIII**), and the **MIII**(OH)/EMA copolymer series (10 and 25 mol% **MIII**) were investigated for *Mycobacterium smegmatis* (*M. smegmatis*), *Staphylococcus aureus* (*S. aureus*), and a methicillin-resistant isolate of *Staphylococcus aureus* (MRSA). Complete inhibition of growth was observed for the microbes studied (**Table 14**).

In the case of *M. smegmatis*, a non-pathogenic model for tuberculosis, macromonomer **MI**(OH) and the most of the **MI**(OH)/MMA copolymers showed modest activity; complete inhibition was observed in well 3 (140 μg/mL). Well 4 (71 μg/mL) activity was observed for **MI**(OH)/MMA copolymer with 5 mol% **MI**. The **MIII**(OH)/MMA and **MIII**(OH)/EMA copolymers studied also exhibited well 3 activity (140 μg/mL).

The changes in activity observed for *S. aureus* and MRSA, Gram positive bacteria, revealed that the observed activity was species specific. Against *S. aureus*, macromonomer **MI**(OH) and the **MI**(OH)/MMA copolymer series (10 and 25 mol% **MIII**) exhibited complete inhibition in well 3 (140 μg/mL); the **MI**(OH)/MMA copolymer exhibited complete inhibition at well 4, (71 μg/mL). The **MIII** copolymer series (MMA and EMA) showed complete inhibition at the highest concentration of drug, well 1 (570 μg/mL). Against MRSA, **MI**(OH) and a **MI**(OH)/MMA copolymer with 5 mol% **MI** showed well 2 (280 μg/mL) activity while the **MIII** copolymer series (MMA and EMA) only showed complete inhibition at the highest concentration of drug, well 1 (570 μg/mL).

The **MI**(OH) macromonomer and **MI**(OH)/MMA copolymers exhibited similar MICs. The greatest activity, lowest MIC, was observed for *M. smegmatis*; the **MI**(OH) series showed better activity than the **MIII**(OH) series. In general, the dendritic macromonomer and dendronized amphiphilic copolymers effectively inhibited the growth of each microbe tested. Complete inhibition was achieved in each case; however, high concentrations were needed.

	MIC (μg/mL)		
	M. Smegmatis	***S. aureus***	**MRSA**
MI(OH)	**140**	**140**	**280**
MI(OH)/MMA			
5:95	**71**	**71**	**280**
10:90	**140**	**140**	**570**
25:75	**140**	**140**	**570**
MIII(OH)/MMA			
5:95	**140**	**570**	**570**
10:90	**140**	**570**	**570**
25:75	**140**	**570**	**570**
MIII(OH)/EMA			
5:95	-	-	-
10:90	**140**	**570**	**570**
25:75	**140**	**570**	**570**

Table 14. MICs of macromonomers and copolymers against Mycobacteria and Gram-Positive bacteria.

4.8.2 Hemolysis Assay

It is not only important that the dendronized amphiphilic polymers are potent antimicrobials and antivirals but that they also lack toxicity to human cells. Lytic activity against mammalian red blood cells (hemolytic activity) was evaluated as a measure of toxicity. Hemolysis assays were performed with the dendritic macromonomers, **MI**(OH) and **MIII**(OH), dendronized homopolymers, P**MIII**$(OH)_0$ and P**MIII**$(OH)_{10}$, and the **MIII**(OH)/MMA dendronized copolymer series (5, 10, and 25 mol% **MIII**). One hundred percent hemolysis was determined from an assay using Triton X-100, a nonionic surfactant. The assay results for the amphiphiles were corrected based on hemolytic activity observed for PBS, the diluent used, and reported as percent total hemolysis (**Table 15**).

In each case, hemolytic activity was only observed at the highest concentration of amphiphile (well 1, 570 μg/mL); however, activity was not observed below 570 μg/mL. Dendritic macromonomers **MI**(OH) and **MIII**(OH) exhibited the lowest hemolytic activity, 0.1 and 0.2%, respectively. An increase in activity was observed for the copolymer series (0.3–0.6%). The dendronized homopolymers demonstrated the highest percent hemolysis; activity seemed to increase as a function of molecular weight. Based on IV data from SEC and MALDI-TOF MS, the dendronized homopolymer prepared with 10 mol% MMP, P**MIII**$(OH)_{10}$, is a low molecular weight polymer, while the dendronized homopolymer prepared without MMP, P**MIII**$(OH)_0$, is a high molecular weight polymer—at least relative to one another. P**MIII**$(OH)_0$ (1.9 %) exhibited a slightly higher percent hemolysis compared to P**MIII**$(OH)_{10}$ (1.4 %).

Based on these results, the dendritic macromonomers and dendronized homopolymers were not toxic below 570 μg/mL; therefore, monomers or polymers with antimicrobial or antiviral activity in this range would be effective in topical microbicide formulation.

	% Hemolysis
MI(OH)	0.1
MIII(OH)	0.2
$PMIII(OH)_0$[a]	1.9
$PMIII(OH)_{10}$[b]	1.4
MIII(OH)/MMA	
5:95	0.6
10:90	0.6
25:75	0.3
TEA	0.3

[a]Dendronized homopolymer prepared with 0 mol% MMP.
[b]Dendronized homopolymer prepared with 10 mol% MMP.

Table 15. Hemolytic activity.

Chapter 5: Summary

The need for a preventative agent to curtail the rampant spread of HIV, other STDs and mucosal pathogens is urgent. Topical microbicides based on amphiphilic compounds have been identified as an attractive means toward this goal. Additionally, polyanionic molecules are potent *in vitro* inhibitors of HIV replication and show promise as effective microbicides.[29] Antimicrobial activity of a homologous series of amphiphiles, as triethanolammonium salts, with hydrophobic tail lengths of 12–22 carbons and tri-functional hydrophilic headgroups have been reported by our group. [30, 31] Here we presented the synthesis of amphiphilic dendronized polymer analogues.

Novel dendritic methacrylate macromonomers were synthesized: Di-*tert*-butyl 4-(2-*tert*-Butoxycarbonyl-ethyl)-4-[3-(2-methacryoloxyethyl)ureido]heptandioate (**MI**) and di-*tert*-butyl 4-(2-*tert*-Butoxycarbonylethyl)-4-[3-methyl-3-(2-methacryoloxyethyl)ureido]heptanedioate (**MIII**). Characterization was achieved with ^{1}H and ^{13}C NMR, high resolution mass spectrometry (HRMS), FTIR, elemental analysis, and melting point analysis. Purification was achieved via flash column chromatography; macromonomer **MI** required multiple columns to separate it from the mixture of mono- and di-substituted methacrylates obtained. The formation of the di-substituted methacrylate and the need for multiple columns significantly reduced the **MI** yield (60 %) compared to **MIII** (80–90%). The synthesis and purification of macromonomer **MIII** proved to be more efficient; therefore, the majority of further research proceeded with **MIII**.

Dendronized homopolymers were achieved via conventional free radical polymerization of **MIII** in acetonitrile employing AIBN as an initiator; polymerization was only achieved at

critical monomer (≥30 wt%) and initiator (1.0 mol%) concentrations. Purification was achieved via precipitation of $CHCl_3$ or CH_2Cl_2 solutions in hexanes. The dendronized homopolymers (P**MIII**) were characterized with ^{1}H NMR, TGA, DSC, and SEC. Due to the significant tailing observed, reliable baselines could not be determined and molecular weight data could not be obtained via SEC. In DSC analysis, a range of glass transition temperatures, 52–66 °C, was observed for the **MIII** homopolymer replicates synthesized; the variation was attributed to fractionation during purification via precipitation.

The dendritic methacrylate macromonomer, **MIII**, was copolymerized with methyl methacrylate via conventional free radical polymerization in acetonitrile employing AIBN as an initiator; copolymer composition was varied in **MIII** (5–50 mol%). As determined by ^{1}H NMR, copolymer composition correlated well with the monomer feed. SEC analysis, in THF, proved successful in the analysis of the copolymer series; the data revealed an increase in number-average molecular weight as the copolymer composition was increased in **MIII**. The number-average molecular weights ranged from 15,000 to 65,000 g/mol with PDIs between 1.3 and 1.6. Glass transition temperatures ranged from 80 to 49 °C, decreasing as the copolymer composition was increased in **MIII**.

A chain transfer agent, methyl 3-mercaptopropionate (MMP), was employed to target low molecular weight (<10,000 g/mol) polymers. In a model study, the polymerization of methyl methacrylate in the presence of MMP, 0–10 mol%, resulted in a series of poly(methyl methacrylate) homopolymers (PMMA) with number-average molecular weights ranging from 4,300 to 15,400 g/mol; molecular weight decreased as a function of increasing MMP concentration. A series of dendronized homopolymers were prepared from **MIII** with varying MMP concentrations: 0, 0.5, 1.0, and 10 mol%; the homopolymer series was characterized by ^{1}H

NMR, TGA, DSC, and matrix-assisted laser/desorption ionization time of flight mass spectrometry (MALDI-TOF MS). Glass transition temperatures ranged from 55 to 65 °C, increasing with decreasing MMP concentration. Characterization by MALDI-TOF MS proved successful for the homopolymer prepared with the highest MMP concentration (10 mol%); a number-average molecular weight of 2,481 g/mol was determined. The MALDI-TOF data confirmed the polymerization of the novel dendritic methacrylate macromonomer and the presence MMP end-groups.

MIII was copolymerized, in the presence of MMP, with alkyl methacrylates of varying aliphatic chain length (methyl, ethyl, *n*-butyl). For each alkyl methacrylate, a series of copolymers was prepared via conventional free radical polymerization in acetonitrile employing AIBN as an initiator; the copolymer composition was varied in **MIII** from 5 to 25 mol%. The copolymers were characterized via ^{1}H NMR, TGA, DSC, and SEC. Copolymer composition, as determined by ^{1}H NMR, correlated well with monomer feed; number-average molecular weights between 3,000 and 10,000 g/mol were obtained by end-group analysis via ^{1}H NMR and SEC, in THF, employing the multi-angle laser light scattering (MALLS) detector. Glass transition temperatures were shown to be a function of copolymer composition (i.e. **MIII** content and choice of alkyl methacrylate).

The *tert*-butyl ester functional groups of the dendritic substituent were removed via acidolysis with trifluoroacetic acid to afford amphiphilic dendronized homo- and copolymers. In ^{1}H NMR, the disappearance of the large singlet at 1.43 ppm, attributed to the *tert*-butyl ester protons, served as evidence of a successful deprotection reaction. Deprotection of dendronized polymers yielded carboxylic acid functional polymers that may be ionized, polyelectrolytes. In the case of the copolymer series, a special class of polyelectrolytes results, ionomers—

copolymers that contain nonionic repeat units and less than ~20% ion-containing repeat units. The carboxylic acid functionality significantly increased intermolecular hydrogen bonding which was evident in the increase in T_g observed for the acid functional copolymers compared to their corresponding esters. After deprotection, the T_gs of the dendronized homopolymer series, prepared with various MMP concentrations, decreased as a function of decreasing MMP concentration. For the dendronized copolymers, the T_gs of the acids were shown to increase as the copolymer composition was increased in **MIII**.

In an effort to identify a biologically compatible medium in which biological efficacy could be studied, the solubilities of the deprotected dendritic macromonomer and dendronized homo- and copolymers were investigated in 5 w/v % aqueous triethanolamine (aq TEA), 1/10 aqueous dimethylsulfoxide (aq DMSO), and 0.05M phosphate buffer solution (0.05M PBS). In aq TEA, the deprotected dendritic macromonomer, **MIII**(OH), dendronized homopolymer, P**MIII**(OH), and dendronized copolymer series prepared from **MIII** and MMA, **MIII**(OH)/MMA, were all soluble at a concentration of 12.5 mg/mL. Solubility in aq TEA became an issue for copolymers prepared with ethyl methacrylate, **MIII**(OH)/EMA; in this case, solubility was not achieved below 10 mol% **MIII**. aq TEA solutions of copolymers prepared with *n*-butyl methacrylate, **MIII**(OH)/*n*BMA, were very turbid, even at 70 mol% **MIII**; turbidity was attributed to aggregation. In aq DMSO, **MIII**(OH) was partially soluble at 11 mg/mL and soluble at 6 mg/mL. The dendronized homopolymer, P**MIII**(OH), and **MIII**(OH)/MMA copolymer series were insoluble in aq DMSO at 12.5 mg/mL. Solubility investigations in 0.05M PBS revealed that the dendritic macromonomer, **MIII**(OH), and dendronized homopolymer, P**MIII**(OH), were soluble but the **MIII**(OH)/MMA copolymer series was insoluble at 12.5

mg/mL. Of the three solvents investigated, aq TEA proved the most effective by solubilizing the macromonomers, homopolymers, and a majority of the copolymers.

To compare solubility in aq TEA, model copolymers, containing one acid group per repeat unit, were prepared from *tert*-butyl methacrylate (***t*BMA**) and MMA (10, 25, and 50 mol% ***t*BMA**), and subsequently deprotected to achieve poly(methacrylic acid-co-methyl methacrylate) (**MAA**/MMA). Copolymer solubility, at 12.5 mg/mL, was investigated in aq TEA. The **MAA**/MMA copolymers were, at best, only partially soluble even at 50 mol% **MAA**.

The antimicrobial activity of dendritic macromonomer **MI**(OH), the **MI**(OH)/MMA copolymer series (5, 10, and 25 mol% **MI**), the **MIII**(OH)/MMA copolymer series (5, 10, and 25 mol% **MIII**), and the **MIII**(OH)/EMA copolymer series (10 and 25 mol% **MIII**) was investigated against *Mycobacterium smegmatis* (*M. smegmatis*), *Staphylococcus aureus* (*S. aureus*), and a methicillin-resistant isolate of *Staphylococcus aureus* (MRSA). In general, the dendritic macromonomer and dendronized amphiphilic copolymers effectively inhibited the growth of each microbe tested. Complete inhibition was achieved in each case; however, high concentrations were needed. The greatest activity was observed against *M. smegmatis* and exhibited by all of the compounds tested. A decrease in activity was observed against *S. aureus* and MRSA. The changes in activity observed for *S. aureus* and MRSA, Gram positive bacteria, compared to *M. smegmatis* suggested that the observed activity was species specific.

Lytic activity against mammalian red blood cells (hemolytic activity) was evaluated as a measure of toxicity. Hemolysis assays were performed with the dendritic macromonomers, **MI**(OH) and **MIII**(OH), dendronized homopolymers, P**MIII**$(OH)_0$ and P**MIII**$(OH)_{10}$, and the **MIII**(OH)/MMA dendronized copolymer series (5, 10, and 25 mol% **MIII**). In each case, hemolytic activity (0.3–1.9%) was only observed at the highest concentration of amphiphile

(well 1, 570 μg/mL); however, activity was not observed below 570 μg/mL. Therefore, macromonomers or polymers with antimicrobial or antiviral activity in this range would be suitable in topical microbicide formulation.

The amphiphilic dendronized copolymer series incorporates many features shown beneficial in the pursuit of effective antiviral and antimicrobial agents: amphiphilicity, multiple anionic functional groups, and a polymer backbone. The significant increase in functionality imparted by the dendritic side chains in the polymer analogues are expected to enhance biological activity compared to the small molecule amphiphiles. Additionally, selectivity (e.g. cytotoxicity) is expected to be tunable through the control of molecular weight, alkyl chain length, copolymer composition, and molecular architecture.

Chapter 6: Conclusions

Novel dendritic methacrylate macromonomers were prepared. Polymerization of the dendritic macromonomer proved feasible through conventional free radical polymerization; dendronized homopolymers were obtained. The dendritic macromonomer was successfully copolymerized with methyl, ethyl, and *n*-butyl methacrylate in the presence of a thiol chain transfer agent. As determined by end-group analysis in ^{1}H NMR and SEC-MALLS, low molecular weight polymers resulted. Multiple copolymer series were achieved by varying the feed ratio (ratio of dendritic to alkyl methacrylate comonomer) and the alkyl methacrylate comonomer (methyl, ethyl, *n*-butyl methacrylate). Copolymer composition was shown to have a significant effect on the polymer properties including T_g and solubility.

Molecular weight characterization of the dendronized homopolymers proved challenging. Due to the significant tailing observed, reliable baselines could not be determined and molecular weight data could not be obtained. Conversely, SEC analysis, in THF, employing the MALLS detector proved successful in the analysis of the copolymer series; the data revealed an increase in number-average molecular weight as the copolymer composition increased in **MIII**. As an alternative means, MALDI-TOF MS was investigated and proved successful in the characterization of the homopolymer prepared with the highest MMP concentration (10 mol%). MALDI-TOF MS confirmed the homopolymerization of the dendritic macromonomer, **MIII**, and the fact that low molecular weight oligomers, with MMP end-groups, were obtained. The presence of MMP afforded the determination of number-average molecular weight by end-group analysis via ^{1}H NMR. The data obtained from ^{1}H NMR was lower than that obtained from SEC.

The *tert*-butyl ester functional groups of the dendritic substituent were removed via acidolysis with TFA affording the targeted amphiphilic dendronized homo- and copolymers. Significant increases in T_g and changes in solubility were observed for the acid functional polymers compared to their ester functional precursors.

Use in biological applications necessitates solubility in a biologically compatible medium. The acid functional dendritic macromonomer and corresponding homopolymers were soluble in 0.05M PBS buffer solution. Amphiphilic dendronized copolymers, with MMA as a comonomer, were soluble in aq TEA, for copolymers with ≥5 mol% of the hydrophilic comonomer. However, solubility decreased upon the incorporation of more hydrophobic comonomers (ethyl and *n*-butyl methacrylate). The ethyl methacrylate copolymer series was insoluble for copolymer compositions with less than 10 mol% of the hydrophilic comonomer; the *n*-butyl series was "insoluble" at all compositions. In aq TEA, poly(methacrylic acid-co-methyl methacrylate) copolymers, a model copolymer with one acid group per repeat unit, were only partially soluble at comparable degrees of polymerization. The dendronized copolymer, with three acids per hydrophilic repeat unit, proved more effective in imparting solubility to the hydrophobic comonomer and polymer backbone compared to methacrylic acid copolymer, with one acid group per hydrophilic repeat unit. Biological analysis of the *n*-butyl copolymer series will require identification of suitable biologically compatible medium.

The antimicrobial activity of dendritic macromonomer **MI**(OH), the **MI**(OH)/MMA copolymer series (5, 10, and 25 mol% **MI**), the **MIII**(OH)/MMA copolymer series (5, 10, and 25 mol% **MIII**), and the **MIII**(OH)/EMA copolymer series (10 and 25 mol% **MIII**) (aq TEA solutions) was investigated against *Mycobacterium smegmatis* (*M. smegmatis*), *Staphylococcus aureus* (*S. aureus*), and a methicillin-resistant isolate of *Staphylococcus aureus* (MRSA). In

general, the dendritic macromonomer and dendronized amphiphilic copolymers effectively inhibited the growth of each microbe tested. Complete inhibition was achieved in each case; however, high concentrations were needed. The greatest activity was observed against *M. smegmatis* and exhibited by all of the compounds tested. A decrease in activity was observed against *S. aureus* and MRSA. The changes in activity observed for *S. aureus* and MRSA, Gram positive bacteria, compared to *M. smegmatis* suggested that the observed activity was species specific.

Lytic activity against mammalian red blood cells (hemolytic activity) was evaluated as a measure of toxicity. Hemolysis assays were performed with the dendritic macromonomers, **MI**(OH) and **MIII**(OH), dendronized homopolymers, P**MIII**$(OH)_0$ and P**MIII**$(OH)_{10}$, and the **MIII**(OH)/MMA dendronized copolymer series (5, 10, and 25 mol% **MIII**). In each case, hemolytic activity (0.3–1.9%) was only observed at the highest concentration of amphiphile (well 1, 570 μg/mL); however, activity was not observed below 570 μg/mL. Therefore, macromonomers or polymers with antimicrobial or antiviral activity in this range would be suitable in topical microbicide formulation.

This research contributes to the scientific community the synthesis and characterization of two novel dendritic macromonomers and the polymerization of these monomers to afford dendronized amphiphilic homo- and copolymers.

REFERENCES

1. The Global Fund to Fight AIDS, Tuberculosis and Malaria - HIV/AIDS Disease Report. http://www.theglobalfund.org/en/files/about/replenishment/disease_report_hiv_en.pdf (November),

2. Ickovics, J.; Rodin, J. *Health Psychology* **1992,** 11, 1-16.

3. Padian, N.; Marquis, L.; Francis, D.; Anderson, R.; Rutherford, G.; O'Malley, P. *JAMA* **1987,** 258, 788-90.

4. Quinn, T. C.; Overbaugh, J. *Science* **2005,** 308, 1582-1583.

5. Elias, C.; Coggins, C. *AIDS* **1996,** 10, (Supplement 3), s43-s51.

6. Rosenthal, S.; Cohen, S.; Stanberry, L. R. *Sexually Transmitted Diseases* **1998,** 25, 368-377.

7. Stein, Z. *American Journal of Public Health* **1990,** 80, 460-462.

8. Doncel, G. F. *Human Reproductive Update* **2006,** 12, (2), 103-117.

9. HIV gross. In *Wikimedia commons*, 2005; Vol. 2009.

10. Hitchcock, P., Topical microbicides. In *Sexually Transmitted Disease, Vaccines, Prevention and Control*, Stanberry, L.; Bernstein, D., Eds. Academic Press: San Diego, 2000; pp 149-166.

11. McCormack, S.; Hayes, R.; Lacey, C.; Johnson, A. *BMJ* **2001,** 322, 410-413.

12. Mauck, C.; Doncel, G. *Curr Infect Dis Rep* **2001,** 3, 561-568.

13. Dezzutti, C. S.; James, V. N.; Ramos, A.; Sullivan, S. T.; Siddig, A.; Bush, T. J.; Grohskopf, L. A.; Paxton, L.; Subbarao, S.; Hart, C. E. *Antimicrob Agents Chemother* **2004,** 48, (10), 3834-3844.

14. Ndesendo, V. M. K.; Pillay, V.; Choonara, Y. E.; Buchmann, E.; Bayever, D. N.; Meyer, L. C. R. *AAPS Pharm Sci Tech* **2008,** 9, (2), 505-520.

15. Gandour, R. D. *Current Pharmaceutical Design* **2005,** 11, (29), 3757-3767.

16. Fihn, S.; Boyko, E.; Chen, C.; Normand, E.; Yarbro, P.; Scholes, D. *Archives of Internal Medicine* **1998,** 158, (3), 281-287.

17. Fihn, S.; Boyko, E.; Normand, E.; Chen, C.; Grafton, J.; Hunt, M.; Yarbro, P.; Scholes, D.; Stergachis, A. *American Journal Epidemiology* **1996,** 144, (5), 512-520.

18. Geiger, A. M.; Foxman, B. *Epidemiology* **1996,** 7, (2), 182-187.

19. Feldblum, P. *Genitourin Med* **1996,** 72, (6), 451-452.

20. Stephenson, H. *JAMA* **2000,** 284, (8), 949.

21. Tashiro, T. *Macromolecular Material Engineering* **2001,** 286, (2), 63-87.

22. Tiller, J. C.; Liao, C.-J.; Lewis, K.; Klibanov, A. M. *Proceedings of the National Academy of Sciences USA* **2001,** 98, (11), 5981-5985.

23. Baudrion, F.; Perichaud, A.; Coen, S. *J Appl Polym Sci* **1998,** 70, (13), 2657-2666.

24. Kenaway, E.; Abdel-Hay, F.; El-Shanshoury, A.; El-Newehy, M.; Mohamed, H. *J Control Rel* **1998,** 50, (1-3), 145-152.

25. Kuroda, K.; DeGrado, W. F. *Journal of American Chemical Society* **2005,** 127, (12), 4128-4129.

26. Gelman, M.; Weisblum, B.; Lynn, D.; Gellman, S. *Org Lett* **2004,** 6, (4), 557-560.

27. CONRAD Multi-country Phase III clinical trials to test Microbicides to Prevent HIV Infection. http://www.medicalnewstoday.com/medicalnews.php?newsid=23804

28. Family Health International Microbicide Products Enter Human Trials. http://www.fhi.org/en/RH/Pubs/Network/v20_2/NWvol20-2micrbcides.htm

29. D'Cruz, O. J.; Uckun, F. M. *Current Pharmaceutical Design* **2004,** 10, (3), 315-336.

30. Sugandhi, E. W.; Macri, R. V.; Williams, A. A.; Kite, B. L.; Slebodnick, C.; Falkinham III, J. O.; Esker, A. R.; Gandour, R. D. *Journal of Medicinal Chemistry* **2007,** 50, (7), 1645 - 1650.

31. Williams, A. A.; Sugandhi, E. W.; Macri, R. V.; Falkinham III, J. O.; Gandour, R. D. *Journal of Antimicrobial Chemotherapy* **2007,** 59, 451-458.

32. Witvrouw, M.; De Clercq, E. *General Pharmacology* **1997,** 29, (4), 497-511.

33. Mitsuya, H.; Popovic, M.; Yarchoan, R.; Matsushita, S.; Gallo, R. *Science* **1984,** 226, (9), 172-174.

34. Luscher-Mattli, M. *Antiviral Chemistry & Chemotherapy* **2000,** 11, (4), 249-259.

35. Baba, M.; Pauwels, R.; Balzarini, J.; Arnout, J.; Desmyter, J.; De Clercq, E. In *Mechanism of inhibitory effect of dextran sulfate and heparin on replication of human immunodeficiency virus in vitro*, Proc Natl Acad Sci, USA, 1988; USA, 1988; pp 6132-6136.

36. Nakashima, H.; Yoshida, O.; Baba, M.; De Clercq, E.; Yamamoto, N. *Antiviral Research* **1989,** 11, 233-246.

37. Schols, D.; Pauwels, R.; Witvrouw, M.; Desmyter, J.; De Clercq, E. *Antiviral Chemistry and Chemotherapy* **1992,** 3, 23-29.

38. Witvrouw, M.; Este, J.; Quinones Mateu, M.; Reymen, D.; Andrei, G.; Snoeck, R.; Ikeda, S.; Pauwels, R.; Vittori Bianchini, N.; Desmyter, J.; De Clercq, E. *Antiviral Chemistry and Chemotherapy* **1994,** 5, 497-511.

39. Chan, D.; Kim, P. *Cell* **1998,** 93, 681-684.

40. O'hara, B.; Olson, W. *Curr Opin Pharmacol* **2002,** 2, 523-528.

41. Starr-Spires, L.; Collman, R. *Clin Lab Med* **2002,** 22, 681-701.

42. Flexner, C.; Barditch-Crovo, P.; Kornhauser, D.; Farzadegan, H.; Nerhood, L.; Chaisson, R.; Bell, K.; Lorentsen, K.; Hendrix, C.; Petty, B.; Lietman, P. *Antimicrob. Agents Chemother.* **1991,** 35, 2544-2550.

43. Ueno, R.; Kuno, S. *Lancet* **1987,** 1, 1379.

44. Mitsuya, H.; Looney, D. J.; Kuno, S.; Ueno, R.; Wong-Staal, F.; Broder, S. *Science* **1988,** 240, (4852), 646-649.

45. Ito, M.; Baba, M.; Pauwels, R.; De Clercq, E.; Shigeta, S. *Antiviral Research* **1987,** 7, 361-367.

46. Baba, M.; Nakajima, M.; Schols, D.; Pauwels, R.; Balzarini, J.; De Clercq, E. *Antiviral Research* **1988,** 9, 335-343.

47. Yoshida, O.; Nakashimma, H.; Toshida, T.; Kanedo, Y.; Matsuzaki, K.; Uryu, T.; Yamamoto, N. *Biochem Pharmacol* **1988,** 37, 2887-2889.

48. Pauwels, R.; De Clercq, E. *Journal of Acquired Immune Deficiency Syndrome & Human Retrovirology* **1996,** 11, (3), 211-221.

49. Neyts, J.; Reymen, D.; Letourneur, D.; Jozefonvicz, J.; Schols, D.; Este, J.; Andrei, G.; McKenna, P.; Witvrouw, M.; Ikeda, S.; Clement, J.; De Clercq, E. *Biochemical Pharmacology* **1995,** 50, (6), 743-751.

50. Neyts, J.; Snoeck, R.; Schols, D.; Balzarini, J.; Esko, J.; Van Schepdael, A.; De Clercq, E. *Virology* **1992,** 189, 48-58.

51. Vicenzi, E.; Gatti, A.; Ghezzi, S.; Oreste, P.; Zoppetti, G.; Poli, G. *AIDS* **2003,** 17, (2), 177-181.

52. Pacciarini, F.; Ghezzi, S.; Pinna, D.; Cima, S.; Zoppetti, G.; Oreste, P.; Poli, G.; Vicenzi, E. *Microbiologica* **2004,** 27, (2), 5-9.

53. Rusnati, M.; Oreste, P.; Zoppetti, G.; Presta, M. *Current Pharmaceutical Design* **2005,** 11, (19), 2489-2499.

54. Meylan, P.; Kornbluth, R.; Zbinden, I.; Richman, D. *Antimicrob. Agents Chemother.* **1994,** 38, 2910-2916.

55. Moulard, M.; Lortat-Jacob, H.; Mondor, I.; Roca, G.; Wyatt, R.; Sodroski, J. *J Virol* **2000,** 74, 1948-1960.

56. Ylisastigui, L.; Bakri, Y.; Amzazi, S.; Gluckman, J.; Benjouad, A. *Virology* **2000,** 278, 412-422.

57. Baba, M.; Schols, D.; De Clercq, E.; Pauwels, R.; Nagy, M.; Gyorgyi-Edelenyi, J.; Low, M.; gorog, S. *Antimicrobial Agents & Chemotherapy* **1990,** 34, 134-138.

58. Zaneveld, L. J. D.; Waller, D. P.; Anderson, R. A.; Chany Ii, C.; Rencher, W. F.; Feathergill, K.; Diao, X.-H.; Doncel, G. F.; Herold, B.; Cooper, M. *Biol Reprod* **2002,** 66, (4), 886-894.

59. Herold, B.; Bourne, N.; Marcellino, D.; Kirkpatrick, R.; Strauss, D.; Zaneveld, L.; Waller, D.; Anderson, R.; Chany, C.; Barham, B.; Stanberry, L.; Cooper, M. *Journal of Infectious Disease* **2000,** 181, (2), 770-773.

60. Christensen, N. D.; Reed, C. A.; Culp, T. D.; Hermonat, P. L.; Howett, M. K.; Anderson, R. A.; Zaneveld, L. J. D. *Antimicrob. Agents Chemother.* **2001,** 45, (12), 3427-3432.

61. Tan, G.; Wickramasinghe, A.; Verma, S.; Hughes, S.; Pezzutojm; Baba, M. *Biochim Biophys Acta* **1993,** 1181, 183-188.

62. Rusconi, S.; Moonis, M.; Merrill, D.; Pallai, P.; Neidhardt, E.; Singh, S. *Antimicrob. Agents Chemother.* **1996,** 40, 234-236.

63. Balzarini, J.; Mitsuya, H.; De Clercq, E.; Broder, S. *Biochemical Biophysical Research Communications* **1986,** 136, 64-71.

64. Cushman, M.; Wang, P.; Chang, S.; Wild, C.; De Clercq, E.; Schols, D.; Goldman, M.; Brown, J. *Journal of Medicinal Chemistry* **1991,** 34, 329-337.

65. Leydet, A.; Barthelemy, P.; Boyer, B.; Lamaty, G.; Roque, J.; Bousseau, A.; Evers, M.; Henin, Y.; Snoeck, R.; Andrei, G.; Ikeda, S.; Reymen, D.; De Clercq, E. *Journal of Medicinal Chemistry* **1995,** 38, (13), 2433-2440.

66. Leydet, A.; Barthelemy, P.; Boyer, B.; Lamaty, G.; Roque, J. P.; Witvrouw, M. C.; De Clercq, E. *Bioorganic & Medicinal Chemistry Letters* **1996,** 6, (4), 397-402.

67. Leydet, A.; Barragan, V.; Boyer, B.; Montero, J. L.; Roque, J. P.; Witvrouw, M.; Este, J.; Snoeck, R.; Andrei, G.; De Clercq, E. *J. Med. Chem.* **1997,** 40, (3), 342-349.

68. Leydet, A.; Moullet, C.; Roque, J. P.; Witvrouw, M.; Pannecouque, C.; Andrei, G.; Snoeck, R.; Neyts, J.; Schols, D.; De Clercq, E. *J. Med. Chem.* **1998,** 41, (25), 4927-4932.

69. Schols, D.; De Clercq, E.; Witvrouw, M.; Nakashima, H.; Snoeck, R.; Pauwels, R.; Van Schepdael, A.; Claes, P. *Antiviral Chemistry & Chemotherapy* **1991,** 2, 45-53.

70. Jansen, R.; Molema, G.; Pauwels, R.; Schols, D.; De Clercq, E.; Meijer, D. *Molecular Pharmacology* **1991,** 39, 818-823.

71. Jansen, R.; Schols, D.; Pauwels, R.; De Clercq, E.; Meijer, D. *Molecular Pharmacology* **1993,** 44, 1003-1007.

72. Swart, P.; Meijer, D. *International Antiviral News* **1994,** 2, 69-71.

73. Zacharopoulos, V. R.; Phillips, D. M. *Clinical and Diagnostic Laboratory Immunology* **1997,** 4, (4), 465-468.

74. Smit, A. J. *Journal of Applied Psychology* **2004,** 16, (4), 245-262.

75. Boskey, E. R.; Cone, R. A.; Whaley, K. J.; Moench, T. R. *Human Reproduction* **2001,** 16, (9), 1809-1813.

76. Kornberg, A. *J Bacteriol* **1995,** 177, (3), 491-496.

77. Kulaev, I., *The Biochemistry of Inorganic Polyphosphares*. John Wiley & Sons: New York, 1979.

78. Wood, H.; Clark, J. *Annu Rev Biochem* **1988,** 57, 235-260.

79. Tinsley, C.; Manjula, B.; Gotschlich, E. *Infect Immun* **1993,** 61, 3703-3710.

80. Noegel, A.; Gotschlich, E. *J Exp Med* **1983,** 157, 2049-2060.

81. Hsieh, P.; Shenoy, B.; Jentoft, J.; Phillips, H. *Protein Exp Purif* **1993,** 4, 76-84.

82. Matsuoka, A.; Tsutsumi, M.; Watanabe, T. *J Food Hyg Soc Jpn* **1995,** 36, 588-594.

83. Palumbo, S.; Call, J.; Cooke, P.; Williams, A. *Food Safety* **1995,** 15, 77-87.

84. Lorenz, B.; Leuck, J.; Kohl, D.; Muller, W.; Schroder, H. *Journal of Acquired Immune Deficiency Syndrome and Human Retrovirology* **1997,** 14, (2), 110-118.

85. Krust, B.; Callebaut, C.; Honavessian, A. *Aids Research and Human Retroviruses* **1993,** 9, 1087-1090.

86. Montefiori, D.; Mitchell, W. *Proceedings of the National Academy of Sciences USA* **1987,** 84, 2985-2989.

87. Veazey, R. *Nature* **2005,** 438, 99-102.

88. Liu, S.; Lu, H.; Neurath, A.; Jiang, S. *Antimicrob. Agents Chemother.* **2005,** 49, (5), 1830-1836.

89. Lederman, M. M.; Offord, R. E.; Hartley, O. *Nature Reviews* **2006,** 6, 371-382.

90. Justin-Temu, M.; Damian, F.; Kinget, R.; Van Den Mooter, G. *Journal of Women's Health* **2004,** 31, (7), 834-843.

91. Mammen, M.; Choi, S.-K.; Whitesides, G. M. *Agnew Chem Int Ed* **1998,** 37, 2754-2794.

92. Yuan, H. L.; Tazuke, S. *Polymer Journal* **1983,** 15, (2), 125-133.

93. Tomalia, D. A.; Dvornic, P. R., Dendritic Polymers, Divergent Synthesis (Starburst Polyamidoamine Dendrimers). In *Polymeric Materials*, Salamone, J. C., Ed. CRC Press: New York, 1996; Vol. 3, pp 1814-1829.

94. Buhleier, E.; Wehner, W.; Vogtle, F. *Synthesis* **1978**, 155-158.

95. Denkewalter, R. G.; Kolc, J.; Lukasavage, W. Macromolecular highly branched homogeneous compound based on lysine units. 4289872, 1981.

96. Denkewalter, R. G.; Kolc, J. F.; Lukasavage, W. Preparation of Lysine Based Macromolecular Highly Branched Homogeneous Compound. 4,360,646, 1979.

97. Tomalia, D.; Baker, H.; Dewald, J.; Hall, M.; Kallos, G.; Martin, S.; Roeck, J.; Ryder, J.; Smith, P. *Polymer J (Tokyo)* **1985,** 17, (1), 117-132.

98. Newkome, G.; Yao, Z.; Baker, G.; Gupta, V. *Journal of Organic Chemistry* **1985,** 50, (11), 2003-2004.

99. Newkome, G.; Yao, Z.; Baker, G.; Gupta, V.; Russo, P.; Saunders, M. *Journal of American Chemical Society* **1986,** 108, (4), 849-850.

100. Lee, C. C.; MacKay, J. A.; Frechet, J. M. J.; Szoka, F. C. *Nature Biotechnology* **2005,** 23, (12), 1517-1526.

101. Halford, B., Dendrimers Branch Out. *Chemical and Engineering News* June 13, 2005, 2005, pp 30-36.

102. Hawker, C.; Frechet, J. M. J. *J Chem Soc Chem Comm* **1990**, 1010-1013.

103. Frey, H. *Angew Chem Int Ed* **1998,** 37, (16), 2194-2197.

104. Balagurusamy, V.; Ungar, G.; Percec, V.; Johansson, G. *Journal of American Chemical Society* **1997,** 119, (7), 1539-1555.

105. Hudson, S.; Jung, H.-T.; Percec, V.; Cho, W.; Johansson, G.; Ungar, G.; Balagurusamy, V. *Science* **1997,** 278, (5337), 449-452.

106. Choi, S.-K., *Synthetic Multivalent Molecules: Concepts and Biomedical Applications*. Wiley: New York, 2004.

107. Andre, S.; Liu, B.; Gabius, H.; Roy, R. *Organic & Biomolecular Chemistry* **2003,** 1, 3909-3916.

108. Barnard, D.; Sidwell, R.; Gage, T.; Okleberry, K.; Matthews, B.; Holan, G. *Antiviral Research* **1997,** 34, A88.

109. Jiang, Y. H.; Emau, P.; Cairns, J. S.; Flanary, L.; Morton, W. R.; McCarthy, T. D.; Tsai, C.-C. *AIDS Research and Human Retroviruses* **2005,** 21, (3), 207-213.

110. Witvrouw, M. C.; Pannecouque, C.; Matthews, B.; Schols, D.; Andrei, G.; Snoeck, R.; Neyts, J.; Leyssen, P.; Desmyter, J.; Raff, J.; De Clercq, E.; Holan, G. *Antiviral Research* **1999,** 41, A25.

111. Bourne, N.; Stanberry, L. R.; Kern, E. R.; Holan, G.; Matthews, B.; Bernstein, D. I. *Antimicrob. Agents Chemother.* **2000,** 44, (9), 2471-2474.

112. McCarthy, T. D.; Karellas, P.; Henderson, S. A.; Giannis, M.; O'Keefe, D. F.; Heery, G.; Paull, J. R. A.; Matthews, B. R.; Holan, G. *Molecular Pharmaceutics* **2005,** 2, (4), 312-318.

113. Boas, U.; Christensen, J.; Heegaard, P., *Dendrimers in Medicine and Biotechnology: New Molecular Tools*. The Royal Society of Chemistry: Cambridge, UK, 2006.

114. Witvrouw, M.; Fikkert, V.; Pluymers, W.; Matthews, B.; Mardel, K.; Schols, D.; Raff, J.; Debyser, Z.; De Clercq, E.; Holan, G.; Pannecouque, C. *Molecular Pharmacology* **2000,** 58, (5), 1100-1108.

115. Gong, E.; Matthews, B.; McCarthy, T.; Chu, J.; Holan, G.; Raff, J.; Sacks, S. *Antiviral Research* **2005,** 68, (3), 139-146.

116. Gong, Y.; Matthews, B.; Cheung, D.; Tam, T.; Gadawski, I.; Leung, D.; Holan, G.; Raff, J.; Sacks, S. *Antiviral Research* **2002,** 55, (2), 319-329.

117. Bernstein, D. I.; Stanberry, L. R.; Sacks, S.; Ayisi, N. K.; Gong, Y. H.; Ireland, J.; Mumper, R. J.; Holan, G.; Matthews, B.; McCarthy, T.; Bourne, N. *Antimicrob. Agents Chemother.* **2003,** 47, (12), 3784-3788.

118. Kiefel, M. J.; Beisner, B.; Bennett, S.; Holmes, I. D.; von Itzstein, M. **1996,** 39, (6), 1314-1320.

119. Rojo, J.; Delgado, R. *Journal of Antimicrobial Chemotherapy* **2004,** 54, 579-581.

120. Weis, W.; Brown, J.; Cusack, S.; Paulson, J.; Skehel, J.; Wiley, D. *Nature* **1988,** 333, (6172), 426-431.

121. Turnbull, W. B.; Stoddart, J. F. *Reviews in Molecular Biotechnology* **2002,** 90, (3-4), 231-255.

122. Lee, R.; Lee, Y. *Glycoconjuate Journal* **2000,** 17, 543-551.

123. Lee, Y.; Lee, R. *Accounts of Chemical Research* **1995,** 28, 321-327.

124. Schengrund, C.-L. *Biochemical Pharmacology* **2003,** 65, (5), 699-707.

125. Toyokuni, T.; Dean, B.; Hakomori, S. *Tetrahedron Letters* **1990,** 31, 2673-2676.

126. Nagahori, N.; Lee, R.; Nishimura, S.-I. *ChemBioChem* **2002,** 3, 836-844.

127. Landers, J.; Cao, Z.; Lee, I.; al., e. *Journal of Infection Diseases* **2002,** 186, 1222-1230.

128. Reuter, J.; Myc, A.; Hayes, M.; Zhonghong, G.; Roy, R.; Qin, D.; Yin, R.; Piehler, L.; Esfand, R.; Tomalia, D.; Baker, J. *Bioconjuate Chemistry* **1999,** 10, (2), 271-278.

129. Roy, R. *Current Opinion in Structural Biology* **1996,** 6, (5), 692-702.

130. Frauenrath, H. *Progress in Polymer Science* **2005,** 30, (3-4), 325-384.

131. Percec, V.; Ahn, C. H.; Ungar, G.; Yeardley, D. J. P.; Moller, M.; Sheiko, S. S. *Nature* **1998,** 391, (6663), 161-164.

132. Tomalia, D. A.; Kirchhoff, P. Rod-shaped dendrimers. 4,694,064, 1987.

133. Yin, R.; Zhu, Y.; Tomalia, D. A.; Ibuki, H. *Journal of American Chemical Society* **1998,** 120, 2678-2679.

134. Freudenberger, R.; Claussen, W.; Schluter, A. D.; Wallmeier, H. *Polymer* **1994,** 35, (21), 4496-4501.

135. Schluter, A. D. *C.R. Chimie* **2003,** 6, 843-851.

136. Schluter, A. D.; Rabe, J. P. *Angew Chem Int Ed* **2000,** 39, 864-883.

137. Chen, Y.-M.; Chen, C.-F.; Chen, Y.-F.; Liu, W.-H.; Li, Y.-F.; Xi, F. *Macromol Rapid Commun* **1996,** 17, (6), 401-407.

138. Draheim, G.; Ritter, H. *Macromol Chem Phys* **1995,** 196, (7), 2211-2222.

139. Neubert, I.; Klopsch, R.; Claussen, W.; Schluter, A. D. *Acta Polymerica* **1996,** 47, (10), 455-459.

140. Percec, V.; Ahn, C.-H.; Barboiu, B. *Journal of American Chemical Society* **1997,** 119, (52), 12978-12979.

141. Hawker, C.; Wooley, K. L.; Lee, R.; Frechet, J. M. J. *Polymeric and Material Science Engineering* **1991,** 64, 73.

142. Hawker, C.; Frechet, J. M. J. *Polymer* **1992,** 33, 1507-1511.

143. Zhang, A.; Shu, L.; Zhishan, B.; Schluter, A. D. *Macromolecular Chemistry and Physics* **2003,** 204, 328-339.

144. Frechet, J. M. J.; Gitsov, I. *Macromol Symp* **1995,** 98, 441-465.

145. Gitsov, I.; Frechet, J. M. J. *Macromolecules* **1993,** 26, (24), 6536-6546.

146. Gitsov, I.; Wooley, K. L.; Hawker, C. J.; Ivanova, P. T.; Frechet, J. M. J. *Macromolecules* **1993,** 26, (21), 5621-5627.

147. Chapman, T. M.; Hillyer, G. L.; Mahan, E. J.; Shaffer, K. A. *Journal of American Chemical Society* **1994,** 116, (24), 11195-11196.

148. van Hest, J. C. M.; Baars, M. W. P. L.; Elissen-Roman, C.; van Genderen, M. H. P.; Meijer, E. W. *Macromolecules* **1995,** 28, (19), 6689-6691.

149. van Hest, J.; Delnoye, D.; Baars, M.; van Genderen, M.; Meijer, E. W. *Science* **1995,** 268, 1592-1595.

150. Hietala, S.; Nyström, A.; Tenhu, H.; Hult, A. *Journal of Polymer Science Part A: Polymer Chemistry* **2006,** 44, (11), 3674-3683.

151. Uppuluri, S.; Keinath, S.; Tomalia, D. A.; Dvornic, P. *Macromolecules* **1998,** 31, 4498-4510.

152. Zhang, Z.-B.; Teng, Y.-H.; Freas, W.; Mohanty, D. K. *Macromolecular Rapid Communication* **2006,** 27, (8), 626-630.

153. Zhang, Y.; Li, X.; Deng, G.; Chen, Y. *Macromolecular Chemistry and Physics* **2006,** 207, (15), 1394-1403.

154. Zhang, Y.; Huang, J.; Chen, Y. *Macromolecules* **2005,** 38, (12), 5069-5077.

155. Deng, G.; Chen, Y. *Macromolecules* **2004,** 37, (1), 18-26.

156. Yi, Z.; Zhang, Y.; Chen, Y.; Xi, F. *Macromolecular Rapid Communications* **2008,** 29, 757-762.

157. Hu, D. J.; Cheng, Z. P.; Wang, G.; Zhu, X. L. *Polymer* **2004,** 45, 6525.

158. Zhang, L. F.; Eisenberg, A. *Journal of American Chemical Society* **1996,** 118, 3168.

159. Xie, D.; Jiang, M.; Zhang, G.; Chen, D. *Chemistry An European Journal* **2007,** 13, (12), 3346-3353.

160. Cheng, C.-X.; Tang, R.-P.; Xi, F. *Journal of Polymer Science Part A: Polymer Chemistry* **2005,** 43, (11), 2291-2297.

161. Chen, C. X.; Tian, Y.; Shi, Y. Q.; Tang, R. P.; Xi, F. *Langmuir* **2005,** 21, 6576-6581.

162. Voyer, N.; Robitaille, M. *Journal of American Chemical Society* **1995,** 117, (24), 6599-6600.

163. Bo, Z.; Rabe, J. P.; Schluter, A. D. *Angew Chem Int Ed* **1999,** 111, 2540-2542.

164. Bo, Z.; Zhang, C.; Severin, N.; Rabe, J. P.; Schluter, A. D. *Macromolecules* **2000,** 33, (7), 2688-2694.

165. Albrecht, M.; van Koten, G. *Angewandte Chemie International Edition* **2001,** 40, (20), 3750-3781.

166. Liang, C. O.; Helms, B.; Hawker, C. J.; Frechet, J. M. J. *Chem Comm* **2003**, (20), 2524.

167. Bart, M.; Suijkerbuijk, J. M.; Shu, L.; Gebbink, R. J. M. K.; Schluter, A. D.; van Koten, G. *Organomet* **2003,** 22, 4175.

168. Shu, L.; Goossl, I.; Rabe, J. P.; Schluter, A. D. *Macromolecular Chemistry and Physics* **2002,** 203, (18), 2540-2550.

169. Bao, Z.; Amundson, K. R.; Lovinger, A. J. *Macromolecules* **1998,** 31, (24), 8647-8650.

170. Jakubiak, R.; Bao, Z.; Rothberg, L. *Synthetic Metals* **2000,** 114, (1), 61-64.

171. Malenfant, P. R. L.; Frechet, J. M. J. *Macromolecules* **2000,** 33, (10), 3634-3640.

172. Pogantsch, A.; Wenzl, F. P.; List, E. J. W.; Leising, G.; Grimsdale, A. C.; Mullen, K. *Advanced Materials* **2002,** 14, (15), 1061-1064.

173. Sato, T.; Jiang, D.-L.; Aida, T. *Journal of American Chemical Society* **1999,** 121, (45), 10658-10659.

174. Setayesh, S.; Grimsdale, A. C.; Weil, T.; Enkelmann, V.; Mullen, K.; Meghdadi, F.; List, E. J. W. L.; Leising, G. *Journal of American Chemical Society* **2001,** 123, (5), 946-953.

175. Barner, J.; Mallwitz, F.; Shu, L.; Schluter, A. D.; Rabe, J. P. *Angew Chem Int Ed* **2003**.

176. Stocker, W.; Karakaya, B.; Schurmann, B. L.; Rabe, J. P.; Schluter, A.-D. *Journal of American Chemical Society* **1998,** 120, (31), 7691-7695.

177. Stocker, W.; Schurmann, B. L.; Rabe, J. P.; Forster, S.; Lindner, P.; Neubert, I.; Schluter, A.-D. *Advanced Materials* **1998,** 10, (10), 793-797.

178. Gossl, I.; Shu, L.; Schluter, A.-D.; Rabe, J. P. *Journal of American Chemical Society* **2002,** 124, (24), 6860-6865.

179. Roy, R.; Zanini, D.; Meunier, S.; Romanowska, A. *J Chem Soc Chem Comm* **1993**, 1869-1872.

180. Spaltenstein, A.; Whitesides, G. M. *Journal of American Chemical Society* **1991,** 113, 686-687.

181. Sashiwa, H.; Shigemasa, Y.; Roy, R. *Macromolecules* **2001,** 34, 3905-3909.

182. Sashiwa, H.; Yajima, H.; Aiba, S. I. *Biomacromolecules* **2003,** 4, (5), 1244-1249.

183. Sashiwa, H.; Aiba, S.-I. *Progress in Polymer Science* **2004,** 29, (9), 887-908.

184. Hassan, M. L.; Moorefield, C. N.; Kotta, K.; Newkome, G. R. *Polymer* **2005,** 46, (21), 8947-8955.

185. Hassan, M. L.; Moorefield, C. N.; Newkome, G. R. *Macromolecular Rapid Communications* **2004,** 25, 1999-2002.

186. Zhang, C.; Price, L. M.; Daly, W. H. *Biomacromolecules* **2006,** 7, (1), 139-145.

187. Lee, C. C.; Yoshida, M.; Frechet, J. M. J.; Dy, E. E.; Szoka, F. C. *Bioconjuate Chemistry* **2005,** 16, (3), 535-541.

188. Barratt, G. *Cell Mol Life Sci* **2003,** 60, 21-37.

189. Kasemi, E.; Zhuang, W.; Rabe, J. P.; Fischer, K.; Schmidt, M.; Colussi, M.; Keul, H.; Yi, D.; Colfen, H.; Schluter, A. D. *Journal of American Chemical Society* **2006,** 128, (15), 5091-5099.

190. *CrysAlis*, v1.171; Oxford Diffraction: Wroclaw, Poland, 2004.

191. Sheldrick, G. M. *SHELXTL NT*, 6.12; Bruker Analytical X-ray Systems, Inc: Madison, WI, 2001.

192. Stevens, M. P., *Polymer Chemistry: An Introduction*. 3re ed.; Oxford Universtiy Press: New York, 1999.

193. Mitsuoka, T.; Torikai, A.; Fueki, K. *Journal of Applied Polymer Science* **1993,** 47, (6), 1027-1032.

194. Donth, E.; Beiner, M.; Reissig, S.; Korus, J.; Garwe, F.; Vieweg, S.; Kahle, S.; Hempel, E.; Schroter, K. *Macromolecules* **1996,** 29, (20), 6589-6600.

195. Cao, C.; Lin, Y. *Journal of Chemical Information and Computer Science* **2002,** 43, 643-650.

196. Thompson, E. *Journal of Polymer Science; Part A-2: Polymer Physics* **1966,** 4, (2), 199-208.

197. Biros, J.; Larina, T.; Trekoval, J.; Pouchly, J. *Colloid and Polymer Science* **1982,** 260, 27-30.

198. Swadesh, J. K., Gel Permeation Chromatography: update 2000. In *HPLC Practical and Industrial Applications*, 2nd ed.; Swadesh, J. K., Ed. CRC Press: Boca Raton, 2001.

199. Hindenlang, D. M.; Sedgwick, R. D., In *Comprehensive Polymer Science*, Allen, G.; Berington, J. C., Eds. Pergamon: Oxford, 1989; Vol. 1, p 573.

200. Xie, T.; Penelle, J.; Verraver, M. *Polymer* **2002,** 43, 3973-3977.

201. Saito, T.; Lusenkova, M. A.; Matsuyama, S.; Shimada, K.; Itakura, M.; Kishine, K.; Sato, K.; Kinugasa, S. *Polymer* **2004,** 45, 8355-8365.

202. Forster, S.; Neubert, I.; Schluter, A. D.; Lindner, P. *Macromolecules* **1999,** 32, (13), 4043-4049.

203. Eisenberg, A.; Rinaudo, M. *Polymer Bulletin* **1990,** 24, (6).